Differential Requirement for Homologous Recombination Repair and Non-Homologous End Joining after High-Energy Proton and Photon Irradiation

---

Dissertation

zur

Erlangung der naturwissenschaftlichen Doktorwürde

(Dr. sc. nat.)

vorgelegt der

Mathematisch-naturwissenschaftlichen Fakultät

der

Universität Zürich

von

Andrea Orlando Fontana

aus

Novazzano (TI)

Promotionskomitee

Prof. Dr. Martin Pruschy (Leitung der Dissertation und Vorsitz)
Prof. Dr. Alessandro Sartori
Prof. Dr. Anthony Lomax
PD Dr. med. Oliver Riesterer

Zürich, 2015

Abstract

Nowadays, the most common form of radiotherapy used in clinics employs high energy linear accelerators (LINACs) to generate and precisely target a photon beam to the tumor mass. Each year, thousands of patients are routinely treated with photon-based radiotherapy alone and in combination with chemotherapy and surgery for curative or palliative purposes. On the other hand, particle beam therapy, especially proton and carbon ions have evolved in the past decades from a niche treatment to a valid option. Currently, several centers worldwide employ high energy protons for the treatment of cancer. Protons display special particle kinetics, with strong deceleration after tissue penetration leading to a differential dose distribution, which is called the *Bragg peak*, allowing highly selective dose deposition in the tumor, while sparing the surrounding normal tissue from damage. This localized dose delivery of radiation to the tumor site allows treatment of selected tumors, like uveal melanomas and chondrosarcomas that are seated near critical organs and for which protons represent a valid and safe treatment option.

The physical and technological knowledge of proton radiotherapy steadily increased during the last decade. However, radiobiological research of proton irradiation is minimal. Several *preclinical* (*in vitro*) experiments have pointed out an enhanced efficacy for proton radiation, compared to conventional photon radiation. Currently, there are still a lot of uncertainties regarding the biological and mechanistic basis of protons, thus limiting further expansion of this powerful technology from the radiobiological point-of-view. DNA is the key target for ionizing radiation, and it has been speculated that proton radiation-induced DNA damage might be quantitatively or qualitatively different from photon-induced damage, but only a few studies have been performed to elucidate this issue.

The aim of the present PhD work is to elucidate the molecular and cellular effects of high-energy, low-LET proton radiation in defined human cancer cellular systems, compared to photon radiation.

We initially have shown that exponentially growing mutant Chinese hamster ovary cells (CHO cells) deficient in homologous recombination repair (HRR) were significantly more sensitive to proton irradiation than photon irradiation, compared to cells with intact HRR (relative biological effectiveness, RBE_{10} of 1.44±0.06 vs. 1.24±0.03). When these HRR-deficient cells were irradiated in plateau (growth arrested) phase, there was no longer a difference in the RBE of the two cell lines (RBE_{10} of 1.29±0.03 vs. 1.27±0.03), indicating a more critical role of HRR after proton vs. photon irradiation in exponentially growing cells, as HRR is only active in S/G_2 phase. In contrast, exponentially growing non-homologous end joining (NHEJ)-deficient cells did not show a specifically enhanced sensitivity to proton irradiation (RBE_{10} of 1.2±0.05, vs. 1.09±0.10). Analysis of initially induced γH2AX and 53BP1 foci revealed no difference in response to the two types of radiation. The repair kinetics of DNA damage in wild type cells were the same after both types of radiation (γH2AX, Rad51, and 53BP1 foci), even though proton irradiation resulted in more residual chromosomal DNA fragments and lethal chromosome aberrations. Interestingly, the repair kinetics in HRR-deficient cells was significantly delayed after proton irradiation, leading to an elevated amount of residual γH2AX-foci 24 h after irradiation. These data demonstrated

that photon and proton radiation induce the same amount of initial DNA DSBs but most of a differential quality of the DNA damage.

In the second part of this work, we have investigated several end points in human cancer cells with a particular focus on DNA damage and its repair by the two major pathways, homologous recombination repair and non-homologous end joining. We used a panel of different human cell lines with defined mutations or downregulated selected genes by the small interfering RNA approach. Our work revealed a differential sensitivity of cells to proton versus photon radiation, which depends on the specific cellular repair capacity linked to the genetic background of the cell.

We primarily focused on the non-small cell lung cancer cell line A549. A549 cells represent a good model for *in vitro* and *in vivo* studies. They are p53 wild-type, but harbor a mutation in the KRAS oncogene. Irradiation of A549 cells with high-energy proton radiation (136 MeV) in the middle of the spread out *Bragg* peak led to an RBE_{10} of 1±0.04 over photon radiation (200 KeV). Treatment of A549 cells with 1Gy of both photon and proton radiation induced the same amount of initial γH2AX and 53BP1-foci. Likewise, removal of these foci over time was similar in response to both types of irradiation. This was coupled with an identical cell cycle profile after both proton and photon radiation, with approximatively 50% of cells in G_2-phase after 24 hours. Thus, proton-induced damages in wild-type A549 cells are repaired in a similar fashion than photon-induced damages.

To further investigate the involvement of the two main DSB repair pathways in response to proton and photon irradiation in detail, we analyzed repair kinetics for DNA-PKcs phosphorylation at both Ser-2056 and Thr-2609 loci along with RAD51 and RPA32-foci formation. We observed a time-dependent increase of RAD51 and RPA32-foci formation in these cells 1 hour and 4 hours after photon ionizing radiation. Proton irradiation induced a similar amount of foci, suggesting that HRR is activated in a similar way after both types of radiation. In contrast, DNA-PKcs activation was strongly hampered after proton radiation in comparison to photon radiation, with a reduction of about 40% after 1 hour for both phosphorylation clusters analyzed. Therefore, even if the cell killing in A549 cells appears to be equal after both types of irradiation, there is a differential activation of the DNA repair pathways, especially for the DNA-PKcs-dependent NHEJ in response to the two types of irradiation.

We therefore investigated the role of DNA-PKcs and NHEJ in more detail by selectively inhibiting the catalytic subunit with the novel compound NU7026, which interferes with the capacity of the enzyme to autophosphorylate at Ser-2056, thereby blocking the synaptic resolution process.

We observed a potent sensitization toward photon radiation, but to much a smaller extent toward proton radiation (DMF_{10} of 1.91±0.05 versus 1.49±0.06) by cellular pretreatment with DNA-PKcs inhibitor. As expected, γH2AX-and 53BP1-foci removal was strongly delayed in cells pretreated with NU7026 after photon radiation, but was surprisingly only minimally affected in NU7026-pretreated cells after proton radiation. Analysis of pDNA-PK (Thr-2609) foci revealed a strong delay in cells pretreated with NU7026 after photon radiation, but again only minimally affected in NU7026-pretreated cells after proton radiation, therefore suggesting that NU7026 directly blocks the catalytic subunit to the damage site, avoiding its release.

Analysis of RPA32-foci formation, a known marker for HRR, revealed that DNA-PKcs inhibition by NU7026 strongly reduced RPA32-foci formation after photon irradiation, with only about 35% of foci detectable 4 hour after irradiation in comparison to cell not treated with the DNA-PKcs inhibitor. In cells

irradiated with protons, almost no reduction in RPA32-foci formation was observed after pretreatment with NU7026.

We then investigated the effect of NHEJ deficiency by downregulating the NHEJ-factor DNA-PKcs in A549 cells. Although significantly more radiosensitive than siLuc-transfected cells, siDNA-PKcs-transfected cells were equally sensitive to both types of irradiation (RBE_{10}=0.94±0.07 versus 1±0.04 in wild-type cells). The repair kinetics of DNA damage (γH2AX foci) was comparable after both types of radiation in DNA-PKcs-knockdown cells, although strongly delayed compared to siLuc-treated cells. RPA32-foci resolution analysis showed that siDNA-PKcs-transfected cells had a much slower activation of HRR, compared to control cells.

To validate the importance of HRR for the repair of proton irradiation-induced DNA damages in a human system, we have downregulated the key HRR-recombinase RAD51 by siRNA treatment. SiRAD51-treated A549 cells were markedly hypersensitive toward proton than photon radiation.

To confirm a differential sensitivity to proton and photon irradiation in NU7026-pretreated, thus DNA-PKcs-inhibited cells in comparison to DNA-PKcs-knockdown cells, we have investigated cell survival and γH2AX-focus repair in the DNA-PKcs-deficient M059J cells and their proficient, isogenic counterpart M059K cells. Similarly to siDNA-PKcs-treated A549 cells, we observed no difference between photon and proton radiation at the level of clonogenic survival and γH2AX-foci repair (RBE_{10}=0.88±0.05 versus 1.02±0.11 for wild-type). Similarly to A549 cells, pretreatment of the proficient M059K cells with NU7026 resulted in a stronger radiosensitizing effect toward photon radiation than toward proton radiation (DMF_{10} of 1.49±0.02 versus 1.2±0.1).

To additionally validate the importance of HRR for the repair of proton-induced DNA damage, we took advantage of the BRCA2-deficient ovarian cancer cells PEO1 and their wild-type, isogenic counterpart the ovarian cancer cells PEO4. As expected, BRCA2-deficient PEO1 cells were in general much more sensitive towards irradiation than BRCA2-proficient PEO4 cells. But again, exponentially growing cells deficient in BRCA2 were significantly more sensitive to proton irradiation than wild-type PEO4 cells, with have an intact HRR (RBE_{10} of 1.2±0.02 versus 1.08±0.06).

To test the effect of direct pharmacological targeting of the HRR pathway, we exposed cells to SAHA (Vorinostat), a broad-range histone deacetylase inhibitor known to downregulate RAD51 protein. Pretreatment of A549 cells sensitized cells only mildly to photon irradiation, whereas sensitization to proton irradiation was much stronger (DMF_{10} of 1.11±0.07 vs. 1.45±0.15).

This work demonstrates that the cellular background strongly determine a differential sensitivity toward proton or radiation, respectively. We first demonstrated in a defined system using CHO cells that there is a differential quality of DNA damage by proton- versus photon irradiation with a specific requirement for homologous recombination for DNA repair and enhanced cell survival. In the second part of the work we have validated these results in human tumor cell lines. These results suggest an essential role for HRR to properly repair a certain percentage of proton-induced DNA damages, which cannot be properly recognized and repaired by NHEJ. Furthermore, we demonstrate for the first time that selective inhibition of the catalytic subunit of DNA-PKcs by NU7026 can strongly impair photon-induced but not proton-induced DNA damage repair, further indicating that damage complexity is a key factor determining which pathway will actively repair damage, with HRR being more important for the repair of

proton-induced DSBs. These data provide a new, biology-based rationale for further stratification of patients in a clinical setting, where proton therapy may become relevant for patients carrying specific mutations in the DNA damage repair pathways. Likewise, our research provides the biological background for novel combined treatment modalities to be defined for a specific type of ionizing radiation.

Zusammenfassung

Die Strahlentherapie gehört mit der Chemotherapie und Chirurgie zu den wichtigsten Behandlungsoptionen bei soliden Tumoren. Jedes Jahr profitieren Tausende von Patienten von einer Strahlentherapie allein oder in Kombination mit einer weiteren Modalität in einem kurativen oder palliativen Ansatz. Meist wird mittels hochenergetischen Linearbeschleunigern ein Photonenstrahl erzeugt, der präzise gegen das Tumorgewebe gerichtet wird. Weitere Strahlenarten, die in der Strahlentherapie verwendet werden, sind Partikelstrahlen wie Elektronen, Neutronen, Pi-Mesonen, Protonen und schwere, geladene Ionen wie Carbon-Ionen (12C). Von diesen ist die Protonentherapie die bekannteste Form und erlangt immer mehr an Bedeutung. Protonen haben spezielle physikalische Eigenschaften, welche eine exaktere Bestrahlung des Tumors möglich machen als dies mit Photonen-basierter Strahlentherapie möglich ist.

Während Photonen das Gewebe gleichmäßig durchdringen, zeigen Protonen eine besondere Partikel-Kinetik, mit einer starken Abbremsung und Verzögerung nach Eindringen in das Gewebe, welche zu einer Differentialdosisverteilung führt, dem sogenannten Bragg-Peak. So findet eine hochselektive Dosisdeposition im Tumor statt, wobei das umliegende Gewebe weitgehend geschont werden kann. Diese lokalisierte Dosisabgabe von Strahlung im Tumor ermöglicht auch die Behandlung von ausgewählten (mit Photonen schwierig zu behandelnden) Tumoren wie Aderhautmelanomen und Chondrosarcomas, die in der Nähe von kritischen Organen liegen. Für diese Tumorentitäten stellt die Protonentherapie bereits heute eine akzeptierte und sichere Behandlungsoption dar. In den letzten Jahrzehnten haben sich die physikalischen und technologischen Kenntnisse in der Protonen-Strahlentherapie stetig weiterentwickelt, so dass immer mehr Patienten mit weiteren klinischen Indikationen von der Protonenbestrahlung profitieren konnten. Auf der biologischen Ebene ist das Feld aber weitgehend unerforscht geblieben. Einige präklinische (in vitro) Experimente haben eine bessere Wirksamkeit für die Protonenbestrahlung im Vergleich zur herkömmlichen Photonenbestrahlung gezeigt. Derzeit gibt es aber noch eine Menge Unsicherheiten bezüglich der biologischen und mechanistischen Wirkung von Protonen, was die Verbreitung und Etablierung dieser Technologie noch verzögert.

DNA ist die kritische Zielstruktur für ionisierende Strahlung, und es wird spekuliert, dass sich protonen-induzierte DNA-Schäden möglicherweise quantitativ oder qualitativ von Photonen-induzierten DNA-Schäden unterscheiden. Es gibt nur wenige Studien, welche diese Frage bisher untersuchten.

Das Ziel der vorliegenden PhD-Dissertation ist es, die molekularen und zellulären Wirkungen der Protonenbestrahlung in definierten humanen Zell-Systemen aufzuklären und mit der Photonenstrahlung zu vergleichen. Das Augenmerk wird dabei vor allem auf verschiedene DNA-Reparatursysteme gerichtet. Wir haben bereits gezeigt, dass exponentiell wachsende HRR (Homologe Rekombination Reparatur)-defiziente CHO-Zellen signifikant sensitiver sind gegenüber Protonenbestrahlung als Zellen mit intakter HRR (relative biologische Effektivität, RBE_{10} von 1.44±0.06 vs. 1.24±0.03). Wurden diese HRR-defiziente Zellen in der Plateauphase (wachstumsarretiert) bestrahlt, war der Unterschied im RBE_{10} zwischen den beiden Zelllinien nicht mehr vorhanden (RBE10 von 1.29±0.03 vs.1.27±0.03). Dies zeigt, dass HRR eine wichtigere Rolle in exponentiell wachsende Zellen nach Protonen als nach

Photonenbestrahlung spielt, da HRR nur in der S/G_2 Phase aktiv ist. Andererseits waren exponentiell wachsende NHEJ (non-homologous end joining)-defiziente Zellen nicht signifikant sensitiver gegenüber Protonenbestrahlung verglichen mit Photonenbestrahlung (RBE10 von 1.2±0.05 vs. 1.09±0.10). Dieselben Zellen waren nach Bestrahlung in der Plateauphase viel radiosensitiver und signifikant sensitiver gegenüber Protonenbestrahlung als der Wildtyp (RBE10 von 1.32±0.05 vs. 1.25±0.03).
In den wildtyp-Zellen wurde kein Unterschied in der Anzahl von initialen DNA-Schäden (γH2AX und 53BP1 Foci) nach Bestrahlung mit den beiden Strahlentypen festgestellt. Auch die DNA Reparaturkinetiken waren in den wildtyp-Zellen gleich (γH2AX, RAD51 und 53BP1-Foci), obwohl die Protonenbestrahlung zu mehr verbleibenden Chromosomenfragmenten und letalen Chromosomenaberrationen führte. Interessanterweise war die Reparaturkinetik in HRR-defizienten Zellen nach Protonenbestrahlung signifikant langsamer, was sich 24 Stunden nach Bestrahlung in einer erhöhten Anzahl an nicht aufgelösten γH2AX-Foci zeigte. Folglich zeigen die Daten gleich viele DNA DSB (Doppelstrangbrüche) (Quantität) nach beiden Bestrahlungsarten und deuten eher auf eine unterschiedliche Struktur (Qualität) des Schadens hin.

Im zweiten Teil dieser Arbeit wurden verschiedene Endpunkte in humanen Krebszelllinien untersucht, im Speziellen die Beteiligung von DNA Doppelstrangbruch Reparatur Systemen, namentlich der Homologen Rekombination Reparatur und dem Nicht-Homologen End Joining nach Photonen- und Protonenbestrahlung. Dafür wurden verschiedene humane Zelllinien mit definierten Mutationen verwendet, oder spezifische Gene wurden mit Hilfe von small-interfering RNA (siRNA) runterreguliert, um Unterschiede in der Strahlenempfindlichkeit (Protonen vs Photonen) aufgrund der Reparaturkapaziät (genetischer Background) zu zeigen.
Die vorliegende Arbeit hat sich hauptsächlich auf die nicht-kleinzellige Lungenkrebszelllinie A549 fokussiert. A549 Zellen sind ein gutes Modell für in-vitro- und in vivo-Studien. Sie sind p53-wildtyp, tragen jedoch eine Mutation im KRAS-Onkogen. Die Zellen wurden in der Mitte des Spread-Out Bragg-Peaks mit Hoch-Energie Protonen bestrahlt, was zu einer RBE_{10} von 1 ± 0,04 führte. Es wurden keine Unterschiede in der Anzahl von initialen γH2AX und 53BP1-Foci nach Bestrahlung mit beiden Strahlentypen festgestellt. Dies zeigte sich in einem identischen Zellzyklus-Profil sowohl nach Protonen- als auch nach Photonenstrahlung, mit etwa 50% G_2-Phase Zellen nach 24 Stunden. Diese Daten zeigen, dass Protonen-induzierte Schäden in A549-Zellen in ähnlicher Weise wie Photonen-induzierte Schäden repariert werden können. Die beiden DSB-Reparaturwege wurden nach Protonen- und Photonenbestrahlung im Detail untersucht: DNA-PKcs an beiden Ser-2056 und Thr-2609 Phosphorylierungsstellen für NHEJ und RAD51 und RPA32 für HRR.
Wir beobachteten eine zeitabhängige Zunahme der RAD51 und RPA32-Foci-Bildung in den Zellen 1 Stunde und 4 Stunden nach Photonen- und Protonenbestrahlung. Die DNA Reparaturkinetik war in den A549 Wildtypzellen gleich (ähnlich wie bei γH2AX und 53BP1), was darauf hindeutet, dass die HRR auf ähnliche Weise nach beiden Arten von Strahlung aktiviert wird. Die DNA-PKcs-Aktivierung war hingegen stark beeinträchtig nach Protonenstrahlung verglichen mit Photonenstrahlung, mit einer Reduktion von etwa 40% nach 1 h an beiden Phosphorylierungsstellen.
Die Rolle von DNA-PKcs und NHEJ wurde detaillierter untersucht durch die selektive Hemmung der katalytischen Einheit von DNA-PKcs mit dem neuartigen, hochselektiven Inhibitor NU7026, der die

Autophosphorylierung von Ser-2056 des Enzyms hemmt und damit eine Blockierung des synaptischen Auflösungsprozesses induziert. NU7026-Behandlung führt zu einer starken Sensibilisierung in Kombination mit Photonenstrahlung, in viel geringerem Maße jedoch mit Protonenstrahlung (DMF_{10} von 1,91±0,05 gegenüber 1,49±0,06).

Wie erwartet, verzögert sich die γH2AX-und 53BP1-Foci Ablösung stark in NU7026 vorbehandelten Zellen nach Photonenstrahlung, aber nur minimal nach Protonenstrahlung. Das gleiche Muster wurde bei pDNA-PKcs-Foci (Thr-2609) beobachtet, was darauf hindeutet, dass NU7026 direkt die katalytische Untereinheit blockiert.

Die RPA32-Foci Analyse, ein bekannter Marker für HRR, zeigte, dass in mit NU7026 vorbehandelten A549 Zellen, die DNA-PKcs Inhibition zu einer stark reduzierten RPA32-Foci-Bildung nach Photonenbestrahlung führt, mit nur noch ca. 35% der Foci nachweisbar nach 4 Stunden, im Vergleich zu unbehandelten Zellen. Nach Protonenbestrahlung wurde nahezu keine Abnahme nach Vorbehandlung mit NU7026 beobachtet.

Um die erhöhte Empfindlichkeit der HRR-mutierten Zellen gegenüber Protonenstrahlung in menschlichen Krebszellen zu bestätigen, wurde die HRR-Rekombinase RAD51 in A549-Zellen runterreguliert. A549-Zellen mit niedrigem RAD51 waren deutlich empfindlicher auf Protonenstrahlung, im Vergleich zu Kontrollzellen, welche nur einen minimalen Unterschied in der Strahlenempfindlichkeit zeigten (DMF_{10} von 1.49±0.02 versus 1.2±0.1).

Der Einfluss von NHEJ wurde durch die Runterregulierung der NHEJ-Faktor-DNA-PKcs mittels siDNA-PKcs in A549-Zellen untersucht. Obwohl deutlich strahlenempfindlicher als siLuc-transfizierte Zellen, waren exponentiell wachsende NHEJ-defiziente Zellen nicht sensitiver gegenüber Protonen- (RBE_{10} = 0,94 ± 0,07 vs. 1± 0,04 für Wildtyp) als Photonenbestrahlung. Die γH2AX-Foci Reparaturkinetik war in den siDNA-PKcs-behandelten Zellen nach Photonen- und Protonenbestrahlung gleich, wenn auch im Vergleich zu siLuc behandelten Zellen stark verzögert. Die RPA32-Foci Analyse zeigte, dass siDNA-PKcs-transfizierte Zellen eine viel langsamere Aktivierung der HRR hatten, im Vergleich zu Kontrollzellen. Um eine differentielle Empfindlichkeit gegenüber Protonen und Photonen in NU7026-behandelten DNA-PKcs-gehemmten Zellen im Vergleich zu genetisch runterregulierte siDNA-PKcs Zellen zu bestätigen, wurde das Überleben und die γH2AX-Foci Reparatur von DNA-PKcs-defizienten M059J Zellen und ihren kompetenten, isogenen M059K Zellen untersucht. Wie erwartet, waren M059J Zellen deutlich strahlenempfindlich als M059 Zellen, zeigten jedoch wieder auf dem klonogenen Überleben (RBE_{10} = 0,88±0,05 vs. 1.02± 0,11 für Wildtyp) und der γH2AX-Foci Reparatur keinen Unterschied zwischen Photonen- und Protonenstrahlung. Ähnlich zu den A549-Zellen, führte die Vorbehandlung von kompetenten M059K Zellen mit NU7026 zu einer stärkeren radiosensibilisierenden Wirkung nach Photonenstrahlung im Vergleich zu Protonenstrahlung (DMF_{10} von 1,49±0,02 gegenüber 1,2±0,1).

Um zusätzlich die Bedeutung der HRR für die Reparatur von Protonen-induzierten DNA-Schäden zu validieren, wurden BRCA2-defiziente Eierstockkrebs Zelllinie PEO1 Zellen und BRCA2-profizienze Eierstockkrebs Zelllinie PEO4 untersucht. PEO4 und PEO1 Zellen waren im klonogenen Überleben generell sensitiver gegenüber Protonen- als Photonenbestrahlung. Interessanterweise waren aber

exponentiell wachsende BRCA2-defiziente Zellen signifikant sensitiver gegenüber Protonenbestrahlung verglichen mit den BRCA2-profizienten Zellen (RBE_{10} von 1,2 ± 0,02 gegenüber 1,08 ± 0,06).
Zusätzlich wurde die Wirkung von SAHA (Vorinostat), ein Histone-deacetylase Inhibitor untersucht, welcher ebenfalls RAD51 runterreguliert. Vorbehandlung von A549-Zellen mit SAHA konnte die Zellen nur leicht für die Photonenbestrahlung sensibilisieren, wohingegen die Strahlensensibilisierung für Protonenbestrahlung deutlich stärker war (DMF_{10} von 1,11±0,07 vs. 1,45±0,15).

In dieser Arbeit wird zum ersten Mal gezeigt, dass die genetischen Voraussetzungen der Zellen die Zellantwort gegenüber Protonenbestrahlung stark beeinflusst. Fehlt HRR in schnell proliferierenden Zellen, ist deren Sensitivität gegenüber Protonenbestrahlung (im Vergleich zu Wildtypzellen) signifikant erhöht. Dies zeigt, dass HRR für die korrekte Reparatur eines bestimmten Anteils von vermutlich hoch-komplexen Protonen-induzierten DNA-Schäden essentiell ist. Weiterhin zeigt die Arbeit zum ersten Mal, dass eine selektive Inhibition der katalytischen Untereinheit von DNA-PKcs durch NU7026 die Reparatur von photoneninduzierten, aber nicht von protoneninduzierten DNA-Schäden stark beeinträchtigen kann. Diese Daten stellen eine neue, Biologie-basierte Rationale für die weitere Stratifizierung von Patienten in der Klinik dar und weisen darauf hin, dass Patienten mit aggressiven, schnell wachsenden Tumoren, denen HRR und deren Zellzykluskontrollmechanismen fehlen, von einer Protonentherapie profitieren können. Ebenso bietet unsere Forschung die biologisch fundierte Grundlage für neuartige, kombinierte Behandlungsmethoden mit verschiedenen Bestrahlungsarten.

Contents

List of Abbreviations

2DXRT	2 dimensional x-ray therapy
3DXRT	3 dimensional x-ray therapy
4DCRT	4 dimensional conformational radiation therapy
53BP1	p53 binding protein 1
Ab	antibody
A-EJ	alternative end joining
APE	AP endonuclease 1
ATM	ataxia telangiectasia mutated
ATR	ataxia telangiectasia and Rad3-related protein
ATR-IP	ATR interacting protein
BER	base excision repair
BRCA1/2	breast cancer susceptibility gene 1/2
CDK	cyclin-dependent kinase
CHK	checkpoint kinase
CHO	Chinese hamster ovary
CNS	central nervous system
CSC	cancer stem cells
CT	computer tomography
CTV	clinical target volume
DDR	DNA damage response
DNA	deoxyribonucleic acid
DNA-PK	DNA protein kinase
DNA-PKcs	DNA protein kinase catalytic subunit
DSB	double strand break
DSBR	double strand break repair
Gy	gray
H2AX	histone variant 2AX
HBV	hepatitis B virus
HCV	hepatitis C virus

HDAC	histone deacetylase
HDACi	histone deacetylase inhibitor
HPV	human Papilloma Virus
HRR	homologous recombination repair
ICL	inter-strand crosslink repair
IMPT	intensity modulated proton therapy
IMRT	intensity modulated radiation therapy
IR	ionizing radiation
IRIF	ionizing radiation induced foci
KeV	kilo electron volt
LET	linear energy transfer
Lig	ligase
LINAC	linear accelerator
MDM2	mouse double minute 2 homolog
MDR	multidrug resistance
MeV	mega electron volt
MMEJ	microhomology-mediated end joining
MRI	magnetic resonance imaging
MRN	Mre11-Rad50-Nbs1
NER	nucleotide excision repair
NHEJ	non-homologous end joining
NSCLC	non-small cell lung cancer
OCL	oxidative cluster lesions
OER	oxygen enhancement ratio
PARP	poly (ADP-ribose) polymerase
PCC	premature chromosome condensation
PET	positron emission tomography
PSI	Paul Scherrer Institute
PTV	planning target volume
RNA	ribonucleic acid
Rb	retinoblastoma

ROS	reactive oxygen species
RPA	replication protein A
SAHA	Suberanilohydroxamic acid
SDSA	strand displacement annealing
siRNA	small interfering RNA
SOBP	spread out Bragg peak
SSA	single strand annealing
SSB	single strand break
SSBR	single strand break repair
TNBC	triple negative breast cancer
US	united states (of America)
USZ	university hospital Zurich
UV	ultra violet
VEGF	Vascular endothelial growth factor
WHO	world health organization
WT	wild-type
XRCC	x-ray complementing defective repair in Chinese hamster cells

1 Introduction

1.1. Cancer and Cancer treatment

1.1.1. What is cancer?

A neoplasm (from Ancient Greek, meaning “new formation”) commonly referred to as a tumor, is a new abnormal growth of tissue, which usually do not respond to external and internal stimuli and have lost a clear structural and functional organization. Typically, neoplasms form a distinct, solid mass that can either be benign or malign. The malignant, invasive and disruptive form of a neoplasm is called cancer.

Cancer cells are typically defined by two heritable properties: they reproduce in defiance of the normal restraints on the controlled cell division, and so do their progeny, and have the ability to invade and colonize tissues and organs normally reserved for other cells [1].

As long as the neoplastic entity remains clustered in a single mass, it is defined as a benign tumor and it can usually be removed by surgery, leading to full recovery. When tumor growth leads to organ invasion and its disruption and in case of an essential organ, the disease becomes lethal.

Often, cancer cells acquire the ability to leave their primary site trough bloodstream or lymphatic vessels. This invasive, exaggerated and uncontrolled ability of the cancerous mass to spread and invade distant parts of the body is called the metastatic process, which makes cancer usually very difficult to be eradicated and thus often lethal.

Nowadays, more than 100 different types of cancer have been described [2]. Cells from almost every tissue of the body can give rise to cancer. Cancers of the different types are classified according to the site of origin: carcinomas are cancer of epithelial origin; sarcomas typically originate from mesenchymal tissue. Leukemias are derived from hematopoietic cells, and cancers from the nervous system.

1.1.2. Cancer Epidemiology

Cancer is the leading cause of death in the economically developed countries (“first world”) and stands only behind cardiovascular diseases [3]. Incidence of cancer is constantly rising due to several factors. People are getting older, thus increasing the probability of developing cancer. Diagnostic methodologies, especially for some cancer types like breast or colon cancer are also steadily improving. Cancer-promoting behaviors, like tobacco smoking, alcohol consumption or unhealthy eating styles coupled with sedentary lifestyles are also vastly spread, especially in developed countries.

Worldwide, the incidence of cancer rate was estimated to be at almost 12.7 million new cases in 2008 (Figure 1.1), with a trend toward increasing of about 100-150% in the next 15 years [4].

The annual number and cancer type distribution of newly diagnosed cancers strongly varies among geographical regions. The most common cancer is breast cancer in women and lung and prostate cancer in men, followed by colorectal cancer. These four types of cancer account altogether for about half of the newly diagnosed cancers worldwide, with a major prevalence in Europe and the US. Cervix and stomach cancers, whose etiology is strongly dependent on factors like viral infections (HPV and the

different hepatitis strains among them), are much more common in developing countries like Russia and West Africa.

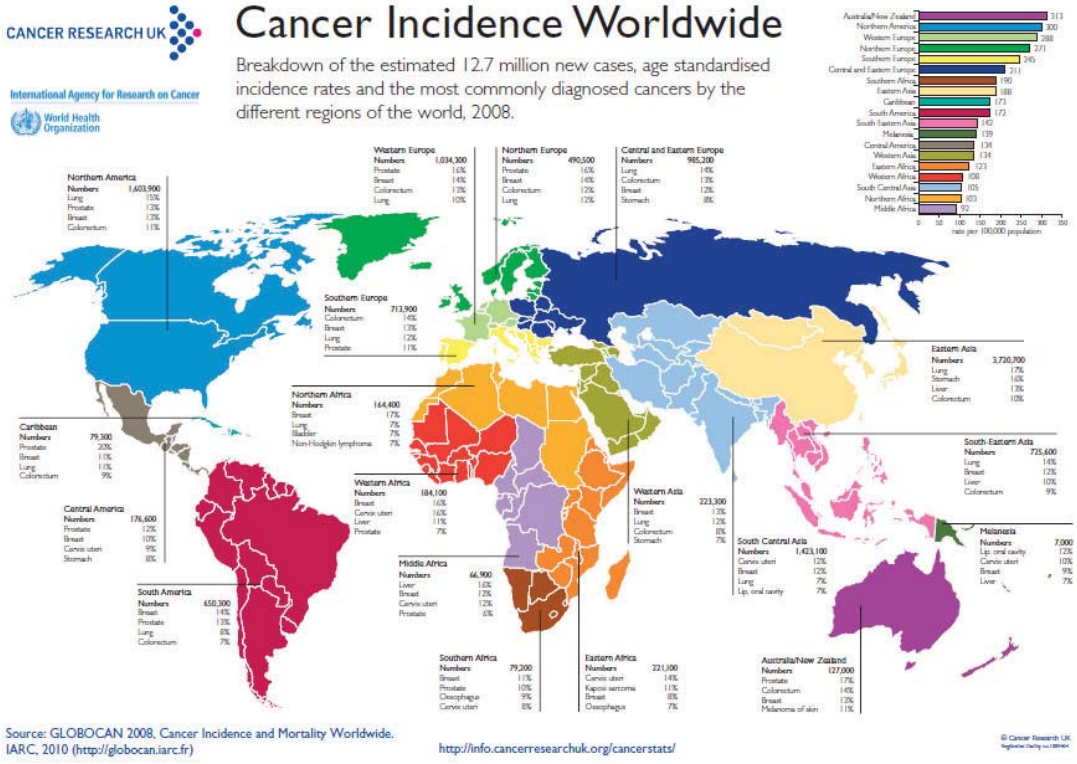

Figure 1.1 Cancer Incidence worldwide (2008) classified by world regions. First-world regions (Australia, US and Europe) have the highest registered rate of cancer per 100'000 population, compared to second and third world regions (Africa and South America). As the world's population continues to grow and age, the burden of cancer is predicted to inevitably increase, even if current incidence rates will remain the same (due to increasing cancer prevention). Currently, more than half of all cancers worldwide are already diagnosed in the developing countries, and without intervention this proportion is predicted to rise in the coming decades. It is estimated there will be almost 22.2 million new cases diagnosed annually worldwide by 2030.
From: Cancer Research UK. Sources: kch.illinois.edu and thecancerian.org

The causes of cancer are numerous and can partly explain the diversity in distribution and prevalence observed. Cancer arises primarily from somatic DNA lesions, acquired serially, which if left unrepaired or misrepaired, lead to alterations of the genetic material and finally to malignancies. Often, a key factor in the development of cancer are also germline (inherited) mutations, which often associate with specific tumors, like $BRCA_1$ and $BRCA_2$ mutations in breast and ovarian cancer [5]. However, cancer distribution varies among geographical and cultural regions, with men living in different countries or adopting different habits often lead to the risk of developing cancer. This supports the theory that inherited mutations renders people prone to developing some types of cancer, and environmental factors promote their development. One of the most known causative agents of cancer is tobacco consumption, which causes lung or head and neck cancer. Viral infections from the hepatitis B virus (HBV) and hepatitis C virus (HCV) are typically associated with uterine cancers among women. Continuous exposure to sun or UV radiation is a primary cause of melanoma, a highly invasive cancer if left untreated.

The immune system plays a key role in the control and development of neoplasms, as it has become evident from immunocompromised patients, which typically displays much higher rates of cancer compared to the normal population [6]. Chronic inflammation, for example due to exposure to asbestos or other environmental agents, is associated with certain, otherwise rare, types of cancers.
In summary, cancer is a multifactorial and multifaceted disease with both inherited and acquired contributing factors. Some are preventable, like social behavior or exposure to environmental agents, whereas others, for example genetic predisposition, may be evaded.

1.1.3. Tumor biology: The hallmarks of cancer

Cancer is rarely a single entity, but rather more an *ensemble* of different diseases. Hanahan and Weinberg suggested that the astonishing complexity of cancer can be reduced to six different traits, further extended to ten (figure 1.2), which together govern and promote the development of cancer [7-8]. Cancer is a multistep process and the hallmarks are factors that may intervene during this process in different order and combinations to promote its growth. Typically, one of the first steps for cells to evolve toward malignancy is by acquiring self-sufficiency in proliferation through growth factor receptor up-regulation or altered autocrine signaling loops. This step is usually accompanied by an increased insensitivity towards growth-arrest signals, allowing them to divide independent of the environment. The increased activation of proto-oncogenes to oncogenes, which are mostly responsible for the proliferation-prone behavior, accompanied to increased DNA damage normally leads to increased cell death. Bypassing apoptosis or acquiring the capacity of limitless reproduction, thus rendering the cell immortal, are important aspects toward malignant development. Nutrient supply and energetic or metabolic control is a key aspect for a cell to be able to growth without any restrain. Cancer cells adapt their energetic metabolism by switching from the relatively slow process of oxidative phosphorylation to fast glycolysis followed by lactic acid fermentation. Furthermore, these malignant growing tumor mass can induce secretion of pro-angiogenic factors, like VEGF leading to neovascularization into the tumor site, which in turn allows better nutrient delivery [9]. Neovascularization and the increased nutrient and growth factor supply is a key step in promoting detachment from the primary site and invasion of new areas. In order to be able to survive and proliferate in new environments, cancer cells need to create a niche by promoting vascularization, but also need to acquire the capacity to avoid immune cell destruction, a very effective mechanism of tumor control. Identification of these keystone steps in the development of malignancies not only allows a better understanding the etiology of the disease, but also to improve efficacy of treatment by selectively targeting the tumor cells.

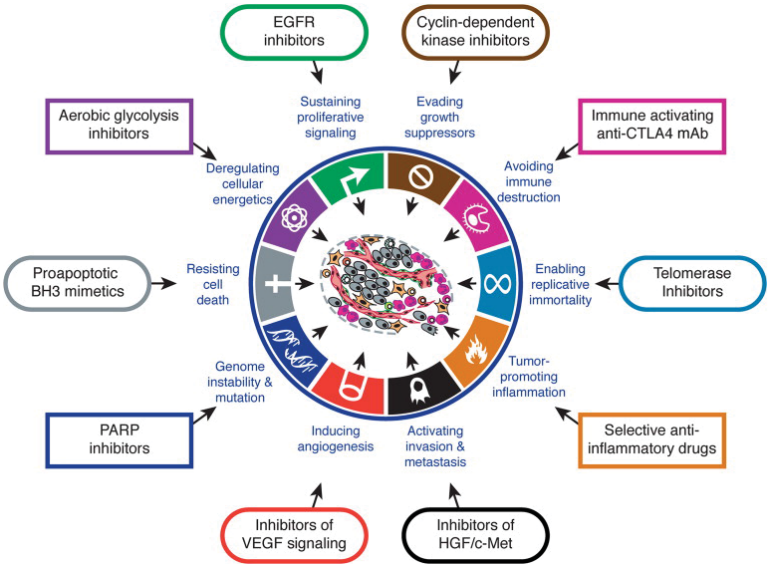

Figure 1.2 The hallmarks and enabling characteristic of cancer. In order to survive and proliferate, the cancer cells needs to be able to acquire certain characteristics, first described by Hanahan and Weinberg in 2001. Research in the past years led to the identification and description of new hallmarks of cancer in 2011: avoidance of immune destruction and deregulation of cellular energetics. Enabling characteristics include tumor promoting inflammation and genome instability. Adapted from [7-8].

1.1.4. Modalities of cancer therapy

Standard cancer treatment mainly consists of three different approaches, which are often combined with each other: surgery, chemotherapy and radiotherapy (Figure 1.3). Usually, local, early-stage diagnosed cancer can be easily treated with high success, typically by surgery alone. The most important aim for curative purposes is to completely eradicate all the tumor cells, in order to avoid recurrence. Therefore, surgery is often coupled with either chemotherapy or radiotherapy, and sometimes with both of them. Chemotherapy is a treatment modality which has remarkably developed during the last decades, from unspecific cytotoxic compounds like mustard gas (Iprit) to highly specific targeted biodrugs, which are able to specifically recognize and kill tumor cells. Chemotherapy is based on the use of toxic compounds which acts on highly proliferating cells, as is the case for most tumor cells, but also other healthy cells, e.g. hair follicles, gut mucosa or nails. Therefore often very strong side effects are observed with this systemic treatment modality, which on the other side allows treating not only the primary site of the tumor, but also eventual metastatic sites. As for chemotherapy, radiation treatment is based on the use of ionizing radiation to damage DNA and induce cell death. But differently from chemotherapy, radiation treatment can be designed to cover the whole tumor area, sparing healthy tissue, and is therefore often used if a particular tumor cannot be excised due to the same being situated close to or within a critical organ (e.g. brain tumors). Usually, the use of radiotherapy allows a good tumor control over long period of time. Furthermore, often the combination of chemotherapeutic agents with radiation results in a synergistic (supraadditive) effect, increasing the probability of tumor control.

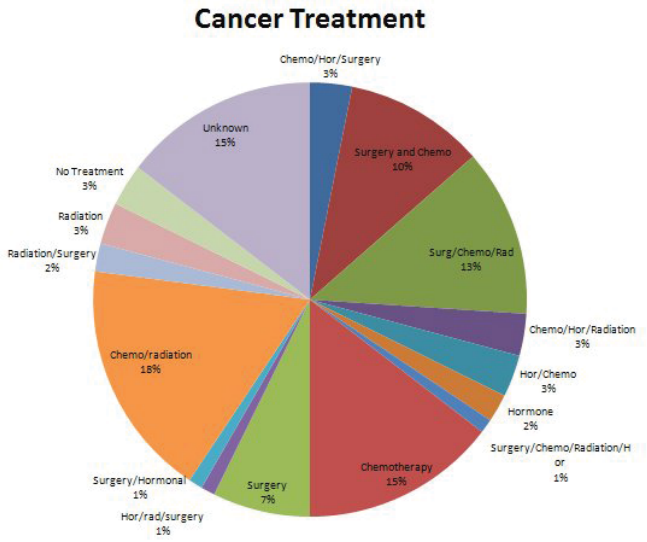

Figure 1.3 Cancer treatment options. Therapy of cancer is based primarily on surgery, chemotherapy and radiotherapy, often in combination together to allow better efficacy of treatment (by exploiting additive effects). Source: radiationtherapytumor.blogspot.org

1.1.5. Five R's of radiotherapy

The five R´s determine the final response of the tumor entity and surrounding normal tissue after irradiation. By modulating these four main biological response mechanisms to radiation, tumor control can be improved while normal-tissue toxicity can be minimized.

Recovery (or *Repair*) is a very fast process, usually taking place within the first 4-6 hours after the radiation dose has been delivered. Typically, radiation fractions are usually given in an interval of 24 hours. Because normal cells have a better capacity to fix the damages (in form of sublethal and potentially lethal damages) compared to tumor cells, the healthy tissue can be mostly spared [10].

Repopulation is the proliferation of cells to fill the gap left by cells died because of radiation treatment. It usually takes place in the days or even weeks following treatment. Ionizing radiation causes cells to die through well-defined mechanisms of programmed cell death. Healthy, surrounding cells then starts to proliferate and repopulate the area left by death cells, in order to keep the tissue intact. Repopulation is not elusive of healthy tissue, but it also occurs in the tumor. Rapid, uncontrolled repopulation of the cancer cells over normal cells can lead to tumor growth and bad outcomes.

Redistribution of cells within the cell cycle is the rapid, usually happening within few hours, return toward an even cell cycle distribution. Cells which happen to be in the radiosensitive, M/G_1/early-S phase of the cell cycle will die, whereas cells in late-S/G2 phase, which are more radioresistant, will continue to proliferate and redistribute throughout the cell cycle. Healthy tissue toxicity is usually the limiting factor in radiotherapy, and it is not sensitized by redistribution. Therefore, by using small and frequent doses the greatest effect can be obtained. However, prolonged treatment may not be positive because of regenerative response in the tumor. Therefore, giving one or eventually two fractions a day typically allows cell to redistribute and increase the probability of irradiating cycling cells in the sensitive phases.

Reoxygenation of the tumor is a major determinant of the effectiveness of radiotherapy. It is the process in which hypoxic (radioresistant) tumor cells become more exposed to oxygen by coming into closer proximity to the vasculature after cellular death and loss of other tumor cells due to previous irradiation treatment. Oxygenated cells are more radiosensitive, because oxygen takes part in the radical reactions, therefore leading to better damage fixation and more efficient cell killing, a phenomenon called the oxygen enhancement ratio (OER) [11]. Typically, Radiation with higher linear energy transfer (LET) tends to have a lower OER, because it causes mainly direct damages to the DNA, which do not require oxygen. After treatment with ionizing radiation, reoxygenation appears to precede rapidly, its rate and extent depending upon the treatment scheduling applied. Therefore, long treatment breaks (e.g. over week end) are helpful with regard to tumor tissue reoxygenation.

Intrinsic radiosensitivity is the inherent radiosensitivity of cells to ionizing radiation. It is the sum of several different genetic and molecular factors (DNA repair ability, cell-cycle checkpoints, cell death mechanisms and signal transduction or the hypoxic status) which influence the cellular response to ionizing radiation. The cell survival curves are mathematically described and compared by their shape using the parameters D_0 and N (Figure 1.4). D_0 describes the slope of the exponential portion of the curve after the initial shoulder, and it is the dose required to reduce the surviving fraction to a value of 1/e, which equals 0.37. Therefore, D_0 is the mean lethal dose for that cell population (extra dose required to reduce survival level from 10% to 3.7% or 1% to 0.37%).The initial size of the shoulder of a cell survival curve is described by extrapolating the exponential portion upwards to the vertical axis of the graph. This point on the graph is called the extrapolation number, *N*. The D_0 value can be seen as a measure of the intrinsic radiosensitivity of a cell population.

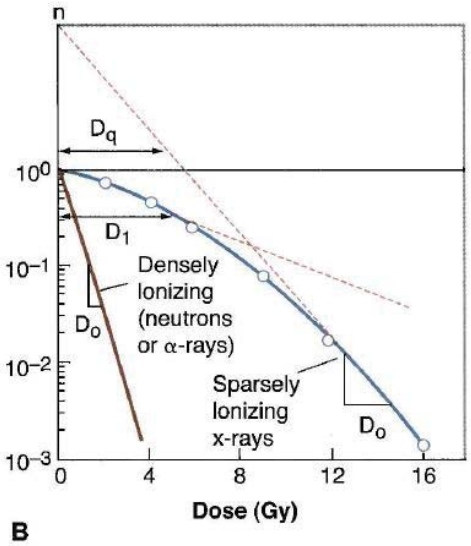

Figure 1.4 Parameters of cell survival curve in response to single doses of X-rays radiation. After an initial *shoulder* region, the larger the dose on a *linear* scale, the smaller the surviving fraction on a logarithmic scale. Source: quizlet.com.

1.2. Radiotherapy and cancer management

Treatment of cancer has greatly evolved during the last decades. For several years, surgery has been preferred treatment for almost every tumor, and for most cancers it remains as such [12]. Radiation treatment has experienced constant development since the discovery of X-rays by Wilhelm Roentgen in 1895 and it has been used for cancer treatment since [13]. To begin with, X-rays were developed and used with diagnostic purposes, but soon their potential in altering healthy tissue was reported, and soon they were employed in the treatment of several conditions.

Nowadays, Radiotherapy has consistently remained one of the most effective treatments for cancer, with almost half of the cancer patients receiving radiotherapy with curative or palliative intents [14]. One of the main advantages in using radiation for cancer is the ability to spare as much healthy tissue as possible, which is also possible thank to the fractionation approach: instead of delivering the whole dose (usually around 60Gy) in one single shot, which would be deadly for the patient, it is delivered in single 2Gy-fractions over 5-6 days a week over several weeks. This is carried out for several important reasons which led to the development e refinements of the 4 R's of radiobiology.

1.2.1. Physics and biological aspects of ionizing radiation

Modern, photon-based radiation therapy is usually given by linear accelerators producing X-rays with energy of 4-25 MeV, which employs higher energies than for diagnostic purposes [15]. X-rays, as γ–rays, are uncharged electromagnetic radiations with a very short wavelength (around 10^{-12} m) and enough energy to penetrate tissues and ionize the molecules they encounter. Ionization is the process by which a molecule acquires a negative or positive charge by gaining or losing electrons to form ions [16]. It is exactly this ionization process within the cell that results in the biological effects observed with radiotherapy. This can be achieved in two different ways, namely a *direct* effect on the DNA molecule and in *indirect* effect, primarily on the surrounding water molecules (Figure 2.1).

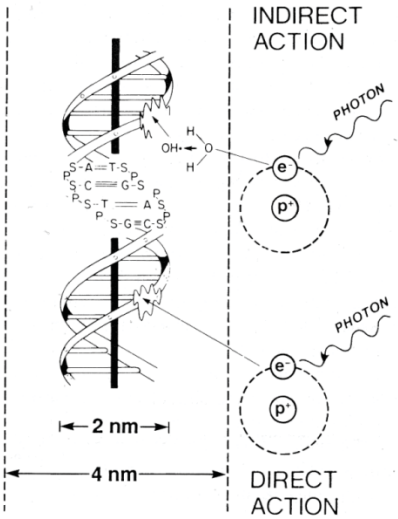

Figure 2.1 Direct and indirect actions of ionizing radiations on the cell. IR can act by directly damaging the DNA (direct action) or by ionizing surrounding water molecules, initiating a cascade of event which leads to DNA damage (indirect action). In this respect, oxygen and water molecules surrounding the DNA play a key role in the generation of active reactive oxygen species (ROS). Adapted from [20].

Typically, high energetic photon beams work by indirect ionization. By passing through the cell, they interact with electrons of atoms or molecules and give energy to these electrons, which can now leave the atom, becoming ionized. This step can be further repeated if the photon possesses enough initial energy, and it will stop as soon it is exhausted. Typically, about 1000 of these sparse tracks are produced per gray of absorbed dose. The predominant interaction takes place with water molecules, which compose the most abundant medium in the cell. Ionized water molecules are very reactive, and can annex hydrogen atoms or electrons from other surrounding molecules which, by diffusing within the cell can damage almost any component of the cell, including the DNA, proteins and lipids. If oxygen is present, even more damage can be created through the creation of reactive oxygen species (ROS) [17-18] by fixing the oxygen radicals with DNA, which renders the DNA molecule very difficult or even impossible to be correctly repaired, therefore inducing cell death by different mechanisms [19].

LET is used to describe the density of the ionizing radiation in particle tracks. It is the average energy (expressed in keV) given up by a charged particle traversing a distance of 1µm. typically, LET varies among a range between 0.3 keV/µm and 150 keV/µm for heavy ions, and it is strongly dependent on the particles type (molecular weight), its charge and the beam energy used (figure 2.2) [21-24].

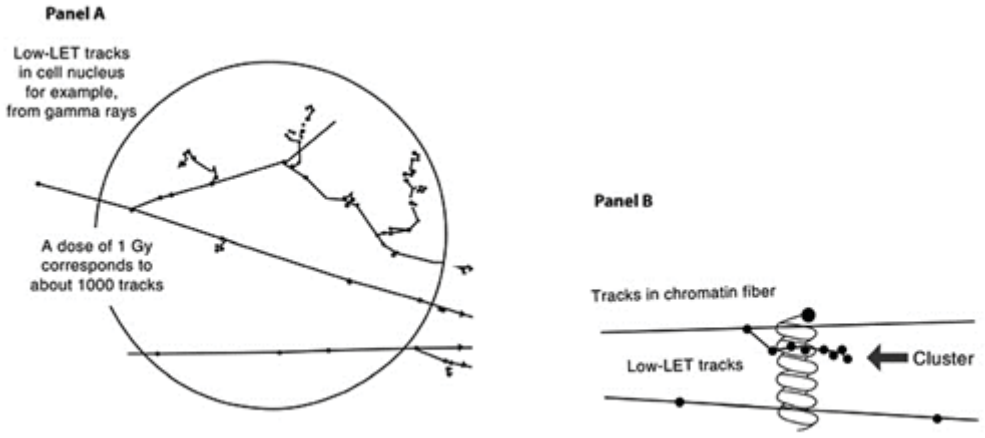

Figure 2.2 Primary and secondary electron tracks producing clusters of ionization events (Panel A) and of clustered damage (Panel B). Due to the electron cascade, ionization events produces by photon radiation are usually dispersed within a large volume, therefore show a low LET. On the other side, cluster damage is usually generated by energy deposition within a very narrow volume, rendering it very difficult to be repaired. Adapted from [21].

1.2.2. Conventional photon radiotherapy

Radiation therapy developed in the course of the last century out of simple X-rays machines. Treatment planning was based on a two-dimensional X-ray image and calculated by hand so that often other than tumor, healthy tissue could also be irradiated. With the introduction of high-resolution methodologies like CT, MRI or PET and the application of computer algorithms to create 3D plans, the field of radiation oncology quickly improved to its current status.

Historically, Radiation therapy has been divided in three main fields: External beam radiation therapy (EBRT or XRT), brachytherapy and systemic radioisotope therapy. XRT is the main field of application of radiation therapy.

Conventional external beam radiation therapy is delivered via two-dimensional beams using linear accelerator machines from several directions, usually front and back of the patient. To shape the beam in order to achieve the best coverage of the tumor, high energy electrons become abruptly stopped by a metal target usually made of tungsten or other high Z materials. This process allows the "design" of treatments fields similar to boxes, which cannot completely spare healthy tissue (Figure 2.3). The conformation of these boxes (fields) is due to depth-dose distribution of X-rays, which deposit most of its energy just under the skin and some residual dose to the tissue behind the tumor, with the depth of maximum energy deposition depending on beam energy (Figure 2.4). Thanks to 3D planning techniques as the beam's eye view [25], a more accurate dose delivery around the target mass can be delivered [26].

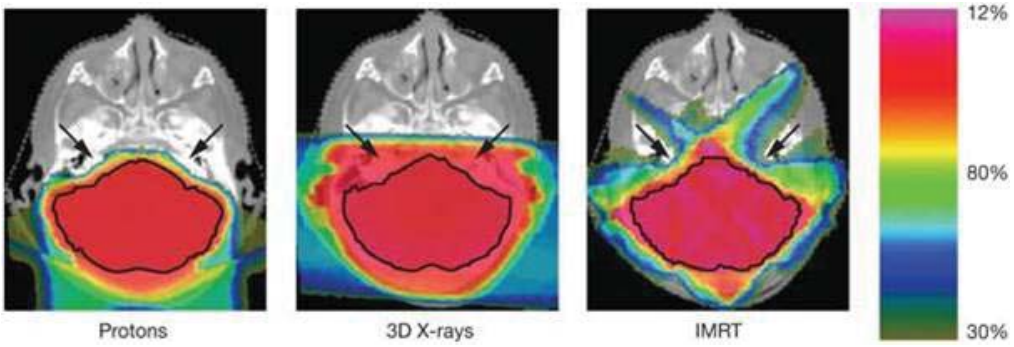

Figure 2.3 Difference in dose conformality using conventional 3D planned photons, IMRT or protons. For the posterior cranial fossa boost (circled area), the proton beam is able to spare both the cochlea and dose to the rest of the brain compared with conventional 3D photons, and IMRT, due to better dose homogeneity. The arrows depict the cochlea. Adapted from [27].

A further improvement from 3DCRT is the intensity-modulated radiation therapy (IMRT) technique. IMRT allows for the radiation dose to conform more precisely to the three-dimensional (3-D) shape of the tumor by modulating the intensity of the radiation beam in multiple small volumes using collimators, a device that narrows a beam of particles or waves. IMRT also allows higher radiation doses to be focused to regions within the tumor while minimizing the dose to surrounding normal critical structures. Therefore, despite being very time-consuming in planning, IMRT is growing as the treatment option of choice for many tumor sites as CNS tumors. An important issue in radiation therapy regards tumors located in or near organs naturally moving due to breathing motions, such as lung or colon tumors. The Four-dimensional conformal radiation therapy (4DCRT) measures the motion of tumors, usually by sensors applied on the patient's body, and includes this in the treatment formula configurations. This ensures sparing as much healthy tissue as possible for those tumors which are usually very difficult to be targeted.

Brachytherapy consists on placing the radiation source directly inside or very next to the patient. It allows usage of high dose with minimal side effects, which make it useful for the treatment of cervix and prostate cancer [28-29]. A whole course of brachytherapy is completed in a shorter period of time compared to XRT, reducing chances of tumor relapse during treatment.

Systemic radioisotope therapy is based on the use of soluble radioactive substances, given orally or intravenously to the patient. These substances have typically very similar properties as their physiological, non-radioactive form, and are therefore usually indistinguishable from the body. A typical example is the use of iodine-131 isotope for the treatment of thyroid diseases. Iodine is physiologically necessary for the thyroid to properly synthesize thyroid hormones; therefore the radioactive form concentrates within the organ where it emits beta and gamma radiation directly at the site of interest. Nowadays, systemic radioisotope therapy profits from the development of tumor-specific antibodies, which can target the tumor with high specificity. These antibody-conjugated Radioisotopes, for example Tositumomab/iodine-131 (Bexxar®) for Non-Hodgkin's lymphoma, are the main agents used in radioimmunotherapy [30].

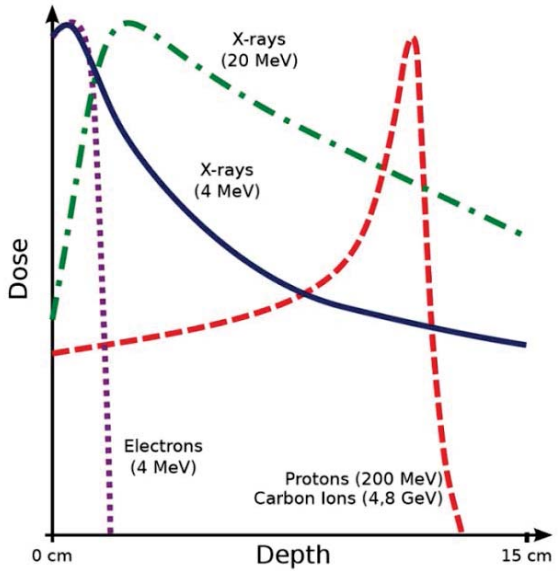

Figure 2.4 Dose-depth distributions for X-rays of different energies, electrons, high-energy protons (low-LET) and carbon ions (high-LET). X-rays and electrons show the highest dose deposition near the entry site, the depth being directly proportional to the energy, to then steadily decrease. In contrast, particle radiation deposits its energy at a specific depth (called the *Bragg peak*), to fall abruptly off after the peak with almost no dose deposition. Adapted from: Dreebit Ltd.

1.2.3. Proton Radiotherapy

Proton and in general hadron therapy has experienced a steep development over the last decades, from a niche treatment option for selected cancers to a broadly used alternative. Interestingly, even though particle therapy currently has a fixed place in radiation oncology and has become the preferred treatment for several tumors, much is still unknown, especially regarding the biological and physical aspects of proton radiation.

1.2.3.1. History and rationale of proton radiotherapy

The existence of proton was first demonstrated in 1908 by Ernst Rutherford [31-32]. It was Robert Wilson in 1940 who suggested using accelerated protons for medical purposes [33]. The idea behind it was that the dose versus depth curve is nearly up to about 1 cm flat of the final proton range, then increasing steeply to yield a localized, high-dose region, to fall abruptly off so that virtually no dose is delivered at

the distal end. This peak at the end of the dose range is called *Bragg peak* (figure 2.4) [34]. This particular pattern of dose delivery allowed the treatment of tumors with very difficult localization, for example brain tumors which are rather close to the brain stem or nerves.

The first cyclotron, the machine used to generate and accelerate the energetic particles like protons, was built shortly after the Second World War by E. Lawrence, in order to conduct the first experiments on animals [35]. The first center using protons was in Harvard, where in 1949 the 160 MeV Harvard Cyclotron was commissioned for physics research purposes. Due to a decrease in research interest, by 1961 it was increasingly used for medical purposes and the first cancer patients would be treated (figure 2.5) [36]. Proton therapy commenced in Europe around 1957 in Sweden, where small groups of patients were treated employing single doses or small fractions. Tumor control rates with proton radiation are reported to be around 95% for chondrosarcomas and for uveal melanomas, two types of cancer which are typically very harsh to treat with conventional photon therapy [37].

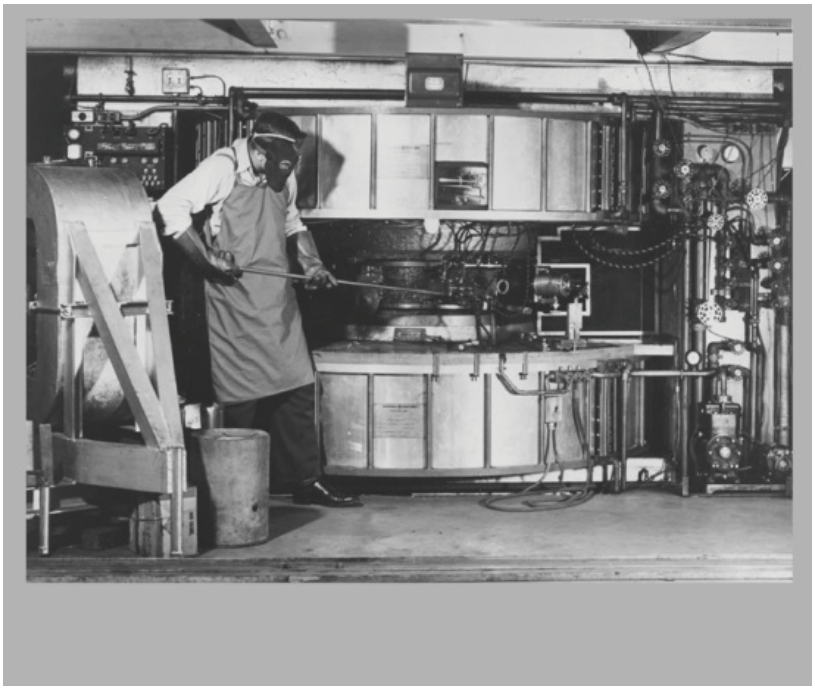

Figure 2.5 The first Harvard high-energy cyclotrone (1961) used primarily for physics experiments, followed by medical experiments due to reduced interest in high-energy physics. Adapted from: The story of the Harvard University cyclotrons. Source: physics.harvard.edu

1.2.3.2. Physics and biological aspects of hadron therapy

Protons are sub-atomical particles that, with neutrons and electrons, are the principal constituents of an atom. Theoretical analyses reports that protons have a finite half-life of about 10^{32} years, decading in a neutron, positron and a neutrino. Protons have per definition a unit mass and a unit charge, and are 1836 times heavier than electrons. Because of their mass and positive charge they attract electrons, resulting in the ionization of atoms upon interaction and following formation of loose secondary electrons. Protons lose little energy during each ionization process and are, because of their mass, only minimally deflected from nuclei, mostly due to Columbus interactions with the positively charged nuclei.

The proton can strike a nucleus along its path, thus losing a big fraction of its energy and being deflected. During this process, secondary neutrons are produced, which may contribute to the increased LET of proton radiation. The rate of energy deposition is inversely proportional to the proton's mean velocity squared, which is in turn directly proportional to its initial energy. High- energy protons are thus traveling very fast and can penetrate tissue deeply, but have a reduced dose deposition because do not experience strong interaction with matter. Upon reaching a certain velocity, a proton experience stronger interactions until it slows down depositing its energy due to the maximal interactions with the surrounding electrons, creating the *Bragg peak* [38]. A single, mono-energetic Bragg peak is not enough to cover the size of a tumor, as a single photon beam is not. Therefore, several mono-energetic beams of different energies are overlaid to result in a beam able to cover all the desired volume, with the most energetic beams covering the distal part and the less energetic beams the proximal portion. The resulting *ensemble* of beams is called the spread-out Bragg peak (SOBP). Normally, the most distal portion of the SOBP contains Bragg peak high-LET particles, whereas the proximal portion of the beam consists mainly of higher-energy, lower-LET particles. This may cause a variation in the RBE along the beam track. The broader the SOBP, the bigger is the entrance dose at the plateau region due to overlapping of the single mono-energetic beams, which can be a major issue with protons, as skin can get injured severely. To prevent this side effect, typically several beams are used from multiple sides to cover the tumor volume by minimizing the damage to the health tissue [39]. The number of ionized biomolecules produced per unit dose of charged particles or photons is very similar, but the resulting biological effect is very different among the radiation type and the particle energy. When comparing particle radiation with conventional photon radiation, the fraction of cells surviving a particular dose of x-radiation is larger than the fraction of cells surviving a particle radiation fraction. This ratio of the dose of standard 250 keV X-rays to produce a specific effect and the dose a specific radiation is called relative biological effectiveness (RBE). Typically, cell survival is selected as an end-point (typically 10% or 1%), but it may also be mutation rate or tissue damage. Virtually all types of radiations show an RBE>1, meaning the type of radiation is biologically more effective because a lower dose is needed to result in the same biological effect. The LET for mono-energetic beams increases to a maximum as the velocity of the particles slow near the end of their range (*plateau*), the region of maximum energy deposition, the Bragg peak. Usually, a relation is observed between the change in LET and the RBE. In the case of low LET radiation (< 10 keV/μm) secondary electrons produced by collisions are the biggest contributor to the RBE, whereas as LET increases (> 10 keV/μm) their contribution become only minor to the total yield of complex lesions, whereas the direct effect (direct DNA damage) plays a key role for high-LET particles (> 40 keV/μm) [40]. In order to effectively kill the cell, damage to the DNA molecules is the primary causative lesion. Because these types of lesions are generated by direct energy deposition to the DNA molecules, densely ionizing tracks (high LET) can induce damages which are more difficult to be repaired, leading to a higher RBE. Indirect damage by ionization of the surrounding water molecules can also cause DNA damage by the generated electron splash, but less efficiently than densely ionizing radiation. Therefore, low-LET radiation has typically a lower RBE.

Radiation	Low-LET	Electron track-ends	High-LET
Tracks in nucleus	1000	1100	2
Ionization in nucleus	100 000	100 000	100 000
Ionization in DNA	1500	1500	1500
Excitation in DNA	1500	1500	1500
Base damage	10^4	10^4	10^4
DNA ssb	850	500	450
8-Hydroxyadenine	700	–	–
Hydrogen peroxide	5×10^5	–	–
RBE for DNA dsb	~1	~1	~1
PCC breaks: initial	6	–	12
8 h:	<1	–	4
DNA protein crosslink	150	–	–
Chromosome aberration	0·3	–	2·5
Dicentric	0·1	–	0·8
Complex aberration	10%	20%	45%
Chromosome instability	<10%	50%	40%
HPRT mutation	10^{-6}	10^{-5}	10^{-5}
Lethal lesions	0·5	1·1	2·6
Cell inactivation	30%	60%	85%

Table 1 Approximate number of events (DNA damages) in a single mammalian cell after 1Gy low- and high-LET ionizing radiation. Both radiations produce approximately 100'000 ionization in the nucleus and 1'500 ionization in DNA, resulting from about 1'000 diffuse low-LET tracts and two tracts of densely ionizing α-particles. SSB: single-strand breaks; DSB: double-strand breaks; PCC: premature chromosome condensation. Adapted from [41].

Table 1 shows the events after low- and high-LET ionizing radiation. Both radiation types produce the same amount of nuclear and DNA ionizations, but they results from a very different number of tracks (due to the track pattern of sparsely versus densely ionizing radiation). Even though the initial number of DSBs is very similar, the residual (after 8 hours) notably differs, meaning a differential type of damage is induced, with significant effects on cell survival. It is important to note that even if the particle radiation yield is the same, the *distribution* varies greatly [42]. This is resulting from a differential energy distribution between low and high-LET radiation, with almost all energy deposited in a very narrow volume for high-LET radiation, leading to a more severe damage and an increase in RBE.

1.2.3.3. Technical aspects of proton therapy and the *Gantry 1* at PSI

Protons are positively charged nuclei of hydrogen atoms, which are composed of a positively charged proton and a negatively charged electron, resulting in a neutral atom. The primary source of protons is hydrogen gas. Typically the most frequently used accelerators contain an external ion source (Electron Cyclotron Resonance (ECR) ion source from IBA), which is a so-called hot-plasma ion source to extract the particles. At the Paul Scherrer Institute, protons are extracted using an internal "cold cathode" ion source (Varian/Accel). In general electrons are accelerated and ionize the plasma. Special extraction geometry of the source helps to extract the positively charged protons, which otherwise would tend to rejoin the negatively charged electrons to keep the plasma neutral. After extraction protons need to be accelerated to clinically relevant desired energies of 70 - 250 MeV for high-energy protons. There are two different types of circular accelerators (LINAC), the devices that control an electric field in such a way as to efficiently accelerate the charged particle, namely cyclotrons and synchrotrons (Figure 2.6). In a *cyclotron*, which is a vertically divided pillbox, an electric field is applied across the gap between the two *dees* (for the resemblance with the alphabet letter), or halves, and a magnetic dipole field cover both dees. Protons are injected perpendicular to the magnetic field and travel along the semicircular

path getting accelerated by crossing the electric field. When the beam leaves the electric field, it enters the magnetic field regions and it gets bent by 180 degrees, reentering the electric field to be accelerated in the opposite direction. Polarity of the electric field is switched at the exact time when the beam reaches the gap to ensure acceleration of the beam. Protons have now gained energy and therefore speed, and since the magnetic field is constant, the radius of the trajectory increases with the energy, assuming the form of a spiral. The particle is then extracted at the desired energy from the edge of the cyclotron.

Synchrotrons is a narrow vacuum tube ring (or some closed shape) contained with magnets. The beam is injected from outside the synchrotron by typically a LINAC with energy of 3 to 7 MeV. The beam circulates within the ring repeatedly through the accelerating structure (ring). In order to keep the beam within the closed ring, the magnetic field of the magnet must increase in strength in synchrony with the beam energy. Thus, the beam is contained within the ring as the magnetic field increases, in contrast to the cyclotron, where the magnetic field remains constant. After reaching the desired energy, the beam is extracted and delivered.

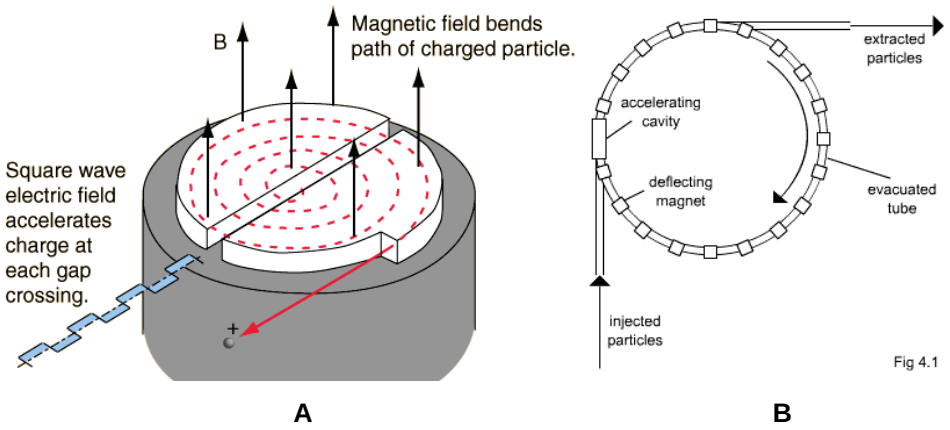

Figure 2.6 Beam line and electric and magnetic fields in a cyclotron (A) and a synchrotron (B). In a cyclotron, the particles are held to a spiral trajectory by a static magnetic field and accelerated by a rapidly varying electric field (space-dependent). In a synchrotron, the direct descendent of the cyclotron, the guiding magnetic field (bending the particles into a closed path) is time-dependent, being synchronized to a particle beam of increasing kinetic energy.

Once the accelerated beam has been extracted, it must be directed to the patient in the appropriated direction. The most commonly used mechanism is a fully rotating *gantry*, which allows the beam to be directed to the patient in every desired angle. A typical Gantry for proton is very large, covering up to a diameter of about 10 meters (Figure 2.7). The beam is spread out to cover the field cross section and extend in depth of the planning target volume (PTV) in a section of the beam called the *nozzle* (beam delivery system, analogous to the treatment head in photon LINACs). This can be achieved in two ways, namely passive beam scattering and pencil beam scanning. The passive beam scattering uses arrangements of scatters, usually lead foils, and degraders to spread out the beam. For larger fields the energy loss and reduction in beam quality is usually huge and therefore a double-scattering technique is applied.

Figure 2.7 Gantry 1 at Paul Scherrer Institute, characterized by a compact rotational gantry combined with an off-axis couch. The spot scanning beam moves along the longitudinal axis only, the other dimensions being achieved by couch movement. Source: Protonzentrum.psi.ch

To ensure greater dose delivery in depth, a range modulator is used to spread out the SOBP. Because of all these material arrangements, passive scattering has some technical limitations, for example using lead foils as scatters cause energy loss up to 10% [43]. Therefore, passive scattering technique can only achieve certain combinations of radius, depth and modulation for a given beam energy. The pencil beam scanning technique is based on the characteristic that protons are positively charged and therefore enables magnetic scanning of narrow pencil beams. The pencil beam scanning delivers the dose inside the patient trough the sequential superimposition of many elementary physical pencil beams (size σ) of small size (varying among tumor type, usually 3 mm ≤ σ ≤ 5 mm), allowing very fine dose distribution, almost close to the physical limits [44]. Beam scanning delivers a true three-dimensional dose distribution, which is of advantage for very complex targets. Furthermore, with the scanning technique the need for field-specific devices is strongly reduced or even absent, therefore reducing the chance of secondary neutron productions, which is of great advantage for pediatric patients [45]. Proton beam scanning inherently promotes the delivery of IMPT fields (Figure 2.3). In IMPT, or intensity-modulated proton therapy, a number of individually inhomogeneous (in-dose) fields are calculated in such a way that, when combined, these fields deliver a homogenous and conformal dose to the target volume while simultaneously reducing the dose to selected normal tissues [46]. A critical issue in radiation therapy is the management of intrafraction organ motion. If one spot is delivered to the wrong position it can have quite a huge impact, especially for tumors seated near sensible organs [47]. This problem is solved by rescanning the volume a second time, with each scan delivering half of the dose. Thus, by using IMPT it would be possible to track organ motion, a major issue in dosimetry. At PSI, the scanning method was implemented on a proton gantry to meet available space constrains [48]. The first veterinary patients were treated in 1994 and in 1996 the first human patient could be treated [49]. IMPT has been implemented since 2000 and it is now the standard technique at PSI.

1.2.4. Combined treatment modalities

Both chemo- and radiotherapy target fast proliferating cell populations, which is the main difference between normal tissue and cancer cells. In contrast, molecular targeted therapy is based on highly specific drugs, which are able to discriminate between cancer and normal cells based on molecular characteristic (e.g. surface receptors) and not on growth kinetics.

The main quantitative difference between chemotherapy and radiotherapy is that radiation treatment is designed to cover the whole tumor homogeneously, whereas with pharmacological treatment the dose of active drug form is variable within the tumor cells and it depends on several physiological factors. These issues are even more relevant in the typical multi-drug regimens adopted in cancer therapy.

In most clinical situations, chemotherapy augments the radiation-induced cell kill within the irradiated volume, but often treatment optimization (e.g. schedule of drug and radiation delivery) is necessary. For example, it has been shown that continuous infusion of 5-Fluorouracile (5-FU) is better than bolus administration in radiation enhancement [50]. An important issue regards cancer stem cells (CSC), which are slow-cycling cells and often express multi-drug resistance proteins (MDR) [51]. Often, chemotherapy alone fails to kill them, thus giving origin to tumor relapses. New, highly selective chemotherapy drugs or combination approaches are therefore needed to eradicate CSC and cure the patient.

Interaction between chemo- and radiotherapy takes place on several levels (figure 2.8) [52].

Spatial cooperation describes the use of chemotherapy and radiotherapy to target diseases in different anatomical sites, resulting in a net gain in tumor control. *Independent cell killing* implies that if two effective therapeutic modalities can both be given at full doses then, even in absence of direct interactive processes, the tumor response (in term of total cell kill) should be greater than that achieved with either agent alone. *Repopulation* plays also a key role, particularly in fractionated regimens. Cell loss due to chemotherapy may trigger accelerated cell repopulation, so that a certain radiation dose is wasted in counteracting this effect. Therefore, in such a setting the effect of combined treatment is not superior compared to radiation alone, but with toxicity resulting from both. Therefore, an accurate and rationale treatment planning is fundamental to ensure proper tumor control.

Enhanced DNA damage and repair is an important molecular aspect of the efficacy of the combination of radiation and chemotherapy. Several chemotherapeutic agents have been shown to inhibit the DNA repair of radiation damage, thus enhancing the effect of radiation. Several substances used are directly inhibiting cell division and thus proliferation, they become potentially lethal in some cell cycle phase. As a consequence of this *cell-cycle synchronization*, delivering radiation during the most sensible cell phases (e.g. S- and M-phase) increases the efficacy of radiation therapy. *Re-oxygenation* is usually associated with poor response to radiotherapy, because functionally insufficient tumor vascular network does not permit adequate oxygen diffusion throughout the tumor mass. Therefore, chemotherapy, by inducing some degree of tumor shrinkage, might facilitate a more even diffusion of oxygen and increase overall tumor oxygenation, which in turn would increase tumor radiosensitivity.

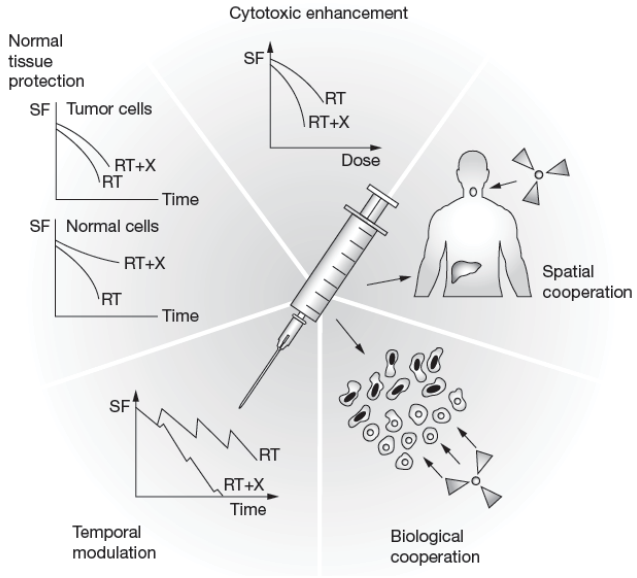

Figure 2.8 Schematic representation of the interplay between spatial cooperation, cytotoxic enhancement, biological cooperation, temporal modulation and normal tissue protection.
RT, radiotherapy; SF, surviving fraction; X, drug. Adapted from [52].

1.3. Molecular biology of ionizing radiation

1.3.1. Molecular aspects of photon versus particle radiation

The principal damaging effect of ionizing radiation arises from its ability to ionize, or eject electrons from molecules within cells. Most of the biological damage, however, is done by the ejected electrons themselves, which go on to cause further ionizations in molecules they collide with, progressively slowing down [53]. At the end of electron tracks, interactions with other molecules become more frequent, giving rise to cluster of ionizations. Normally, clusters are such that several ionizations can occur within a few base pairs of the DNA [54]. After photon irradiation, typically only few percent of the damage is clustered. The cell has particular difficulty to cope with complex damage, particularly when the DNA, which is present in only two copies, is severely damaged [55]. Even if the number of ionized biomolecules produced by both photon and particle radiation is very similar, the resulting, biological effect is substantially different.

High-LET particle radiation is characterized by deposition of large quantities of energy within a very limited space, usually few nanometers. This clustering of energy deposition results in multiple DSBs along with single-strand breaks, DNA crosslinks and other types of damage [56-58]. Therefore, the major difference between low- and high-LET radiation and high-energy protons versus protons near their densely ionizing track ends is the deposition of energy in localized regions of the DNA, nucleosome, or chromatin fiber. Although the average macroscopic number of events does not differ, the clustering of strand breaks and associated damage is believed to render the lesions less amenable to competent repair. Analysis of relative biological effectiveness showed little variation *in vivo* but rather a huge variation *in vitro* (figure 3.1) [59]. One of the reasons behind these differences may be due to the different particle energies used, where typically low energy protons (<30 MeV, LET=20 keV/µm) show greater RBE variations, probably due to increased apoptosis or radical formations, compared to high-energy

protons [60]. The genetic background of the cells may also play a key role in the determining the radiation sensitivity, and thus the RBE of the cells.

Several reports published in the past years suggest that there are differences in the radiation response between low-LET proton and photon irradiation [61-64]. Analysis of the response of mutant cell lines deficient in various component of the DNA repair machinery, compared to their repair-proficient cells showed that DSBs produced by low-LET radiation are more amenable to repair than DSBs produced by high-LET radiation [65]. Furthermore, despite the clear evidence for DNA being the crucial site for radiation insult leading to radiation-induced cell killing, some cells have been shown to activate different pathway of cell death in response to high-LET radiation [66]. These studies point out a differential molecular response of cells after proton irradiation compared to the conventional, low-LET photon radiation. For normal treatment planning a RBE value of 1.1 is generally used, but the response of single tumors may be different based on its genetic background, giving very variable clinical responses. Other unknown parameters could influence the RBE, increasing clinical uncertainty. Furthermore, combining chemotherapeutic agents with proton therapy may give completely unexpected results.

1.3.2. DNA damage

As discussed above, the primary critical site for radiation-induced cellular effects is the DNA. Depending on LET, ionizing radiation can induce different types of events (Figure 2.6). Certain types of damage are structurally more complex, their resolution by the cellular repair machinery may thus be impaired leading to the differential biological effectiveness (cluster lesions).

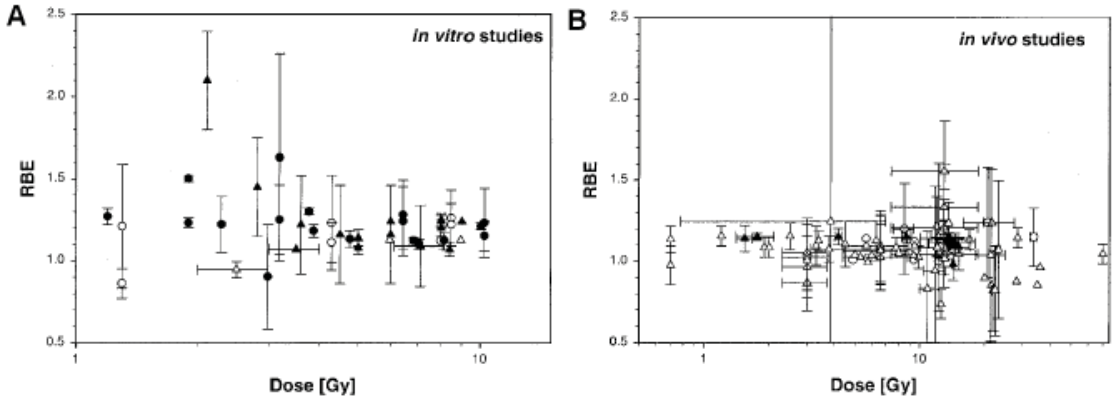

Figure 3.1 Experimental proton RBE values (relative to $_{60}$Co) over dose/fraction for (A) cell inactivation *in vitro* and (B) measured *in vivo* in the center of a SOBP. Circles represent RBEs for beam energies less than 100 MeV, triangles for beam energies of more than 100 MeV. Adapted from [56].

1.3.2.1. Single strand breaks

Single-strand breaks (SSBs) are discontinuities in one strand of the DNA double helix and are usually accompanied by loss of a single nucleotide and by damaged 5'- and/or 3'-termini at the site of the break [67]. SSBs are the most common damage generated after metabolic stress, UV-light or ionizing radiation. One of the most common sources of SSBs is oxidative damage by both endogenous and exogenous (IR-induced) reactive oxygen species (ROS).

DNA single strand breaks and base damages are up to 3-5 times more frequent than DSBs, and after radiation exposure can be up to 50 times more frequent than DSBs. DSBs are typically the most severe damage when not repaired because they can causes loss of complete chromosomal regions [68, 71].SSBs can occur directly by disintegration of the oxidized DNA sugar but also indirectly during the DNA base-excision repair (BER) of oxidized bases or abasic sites, priorly damaged [69-70]. Furthermore, SSBs can arise as the result of erroneous activity of cellular enzymatic activity such DNA polymerases.

The most likely consequence of unrepaired SSBs in proliferating cells is the blockage or collapse of DNA replication forks during the S phase of the cell cycle, possibly leading to the formation of DSBs, which are then repaired by the Homologous Recombination (HRR) pathway [72]. Typically, SSBs are repaired by the single strand break repair pathway (SSBR). End-processing is achieved by specific AP endonucleases, and polynucleotide kinase-phosphatase (PNKP), or tyrosyl-DNA phosphodiesterase (Tdp1) [73]. To ensure proper resynthesis and end ligation a 3'-hydroxyl end and a phosphate-5'-end is needed and are prepared by the AP endonuclease. Then poly-ADP-ribosylation by poly-(ADP-ribose) polymerase 1 ($PARP_1$) is thought to promote the sequestration of other DNA repair proteins, like XRCC1 and ligase III. If the concentration of SSBs is elevated, prolonged activation of $PARP_1$ leads to depletion of cellular NAD^+ and ATP and/or release of apoptosis-inducing factor (AIF) from mitochondria, causing cell death.

1.3.2.2. Double strand breaks

DNA double strand breaks (DSBs) are generated by different means, typically during replication in case the replication fork meets a DNA SSB, during the process of V(D)J recombination or through direct effects of ionizing radiation. These types of break are very toxic for the cell, and a single, unrepaired DSB can lead to cell death. Usually, after exposure to 1 Gy of IR about 20 DSBs are generated, and can be located in both the heterochromatic or euchromatic regions of the genome. DSBs provoke an extensive reaction in neighboring chromatin, characterized by phosphorylation of histone H2AX on serine 139 of its C-terminal tail (to form "γH2AX") [74] and chromatin relaxation to allow proper repair. Two main pathways are involved in repairing DSBs, homologous recombination (HRR) and non-homologous end joining (NHEJ) [75-76].Both pathways are completely different from each other in respect of the set of proteins/enzymes they use, the speed and the accuracy, and activity pattern during the cell cycle. Both pathways will be discussed in detail (see below).

1.3.2.3. Oxidative base damages

Oxidative base damages (OBD) are a common form of cellular damage, which can be induced endogenously through normal metabolic processes, or exogenously by ionizing radiation. There are several types of oxidative base damages, the most common and dangerous type of OBD is 7,8-dihydro-8-oxo-guanine (8-OHgua) as a major IR-product with a clear mutagenic potential [77]. Every subtype of OBD is detected and removed by specialized proteins called glycosylases. Several of these enzymes are present within the cell, every one specific for a particular subclass of oxidative base damage. Glycosylases work by hydrolyzation of the N-glycosidic bond to generate abasic sites (Aps). The DNA backbone is then cut by the 5'-AP endonuclease 1 (APE1), a specialized enzyme which then leaves a

3'-hydroxyl adjacent to a 5' deoxyribosephosphate, which in turn generates a SSB. These are repaired by the SSBR or the BER pathways.

1.3.3. The DNA damage response

Cells suffer from continuous stress from both endogenous (e.g. metabolic stress or replication) and exogenous (e.g. naturally occurring UV-radiation or ionizing radiation) origin. Therefore, the cell has evolved mechanisms to sense the damage (*sensors*), to transduce this signal in order to coordinate the cellular response (*transducers*), to promote their repair (*effectors*). The ensemble of these processes is called the DNA damage response (DDR) [78-79]. The DDR is not a single pathway, but a group of highly interrelated pathways, each controlling different effects on the cell and its activation depending upon the type of insult induced (Figure 3.2).

There is compelling evidence that the DDR reacts differently to low- and high-LET radiation. Because of the differential nature and composition of the damage (both DSBs and OCDLs) induced by the two types of radiation [80], both HRR and NHEJ have been shown to be differentially involved in the recognition, transduction and repair of the DNA damage [81-83].

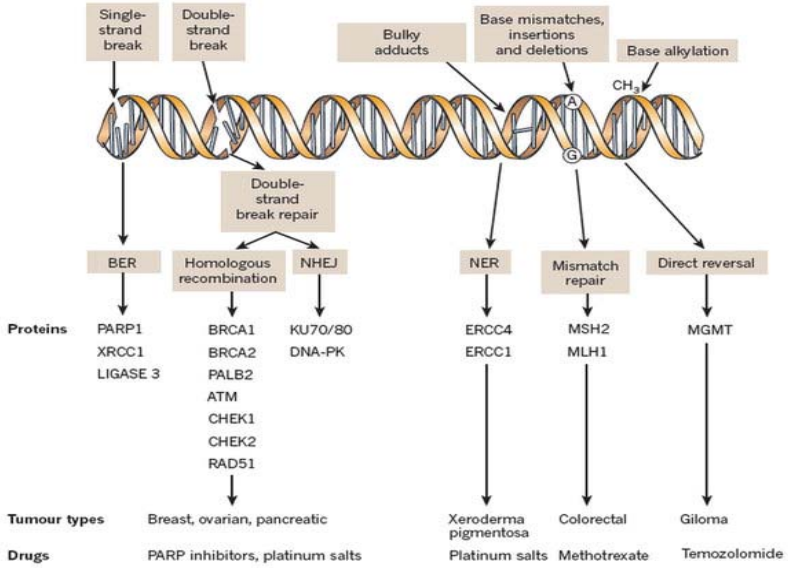

Figure 3.2 The DNA damage response (DDR). Depending on the type of damage induced (SSBs, DSBs, base alterations or mismatches) different proteins are required to sense and repair the damage. DDR components are typically subdivided in sensor, transducer and effector proteins. Deficiency in one or more of the DDR components leads to tumor development and other syndromes. Adapted from [84].

1.3.4. Sensing of the DNA damage

The initial cellular response to DSBs is characterized by the recruitment of a large number of different proteins to the site of DNA damage. It is well established that the following three PI3-like kinases: ataxia telangiectasia mutated (ATM), ATM and Rad3-related (ATR), and catalytic subunit of DNA-dependent protein kinase (DNA-PK_{cs}) are the conductors of the DSB damage/checkpoint orchestra. ATM is the main protein activated upon DNA damage, and cells with impaired ATM functions are typically unable to promote DDR through (ATM-dependent) γH2AX foci formation [85].

These three kinases are not able to recognize the DSB by themselves, but require at least one additional protein or protein complex. Recruitment of ATM to the break requires the Mre11-Rad50-Nbs1 protein complex (MRN). Rad50 binds directly to DNA breaks and the adaptor protein NBS1 recruits ATM to the break. Mre11 is an endonuclease responsible for the production of short single-strand oligonucleotides, a process called *end resection*, which further allows DNA processing and ligation [86]. Notably, MRN assembles at DSB sites faster than any other protein and does not depend on any other protein to induce repair foci formation [87]. Upon reaching the DSB, ATM undergoes autophosphorylation at Ser-1981 and changes from an inactive dimer to an active monomer leading to H2AX phosphorylation of relatively large chromatin regions and to alterations in the chromatin structure [88]. DNA Protein Kinase catalytic subunit (DNA-PKcs) is a kinase structurally similar to ATM and which plays a key role in NHEJ repair. In absence of ATM, DNA-PKcs can also phosphorylate H2AX, but only ATM promotes γH2AX formation to maximal distance and maintains γH2AX densities at DSBs [89]. As for the ATM kinase, DNA-PKcs is unable to sense the DNA damage by itself. The sensor function is carried out by the Ku70-Ku80 complex which senses DSBs, binds directly to them, and recruits DNA-PKcs (forming the DNA-PK complex, also called the synaptic complex). The third kinase capable of phosphorylating H2AX is ATR together with ATRIP (ATR interacting protein), which recruits ATR to damage sites. ATR does not seem to play a substantial role in DBS recognition, but instead is involved in phosphorylation of γH2AX at single-stranded DNA and at stalled or broken replication forks. Because DSBs processing can create stretches of single-stranded DNA, ATR will be activated [90]. This activation down-stream of ATM is needed to fully activate all components of the DDR effector pathways as ATM and ATR phosphorylate not only H2AX but a distinct set of proteins that translate the signal to the DDR effectors.

Activation of ATM, ATR and DNA-PKcs leads to the phosphorylation not only of γH2AX, but also of many other cellular proteins. Recent studies have shown that as many as 700 proteins are direct or indirect substrates for the three kinases in response to DNA damage [91]. Phosphorylation of these other proteins act as the 'signals' to activate the various different downstream effectors of the DDR, namely apoptosis induction, cell cycle arrest through checkpoint activation and DNA repair.

ATM protein plays most probably the most important role in transmitting these signals in response to IR-induced DSBs and is thus considered to be a master regulator of the DDR, with ATR and DNA-PK playing more a "support" role [92].

1.3.5. Cell cycle regulation

A major effector pathway of the DDR is the activation of cell-cycle checkpoints. Treatment of cells with ionizing radiation causes delays in the movement of cells through the G1, S and G2 phases of the cell cycle [93]. This provides more time to the cell-cycle arrested cells to repair the DNA damage.

Checkpoints are specific points in the cell cycle at which progression of the cell into the next phase can be blocked. 4 major checkpoints are activated by DDR in response to irradiation that takes place at different points within the cell cycle, namely G_1, S, early-G_2 and late-G_2 checkpoints.

All movements through the cell cycle are driven by cyclin-dependent kinases (CDKs). CDK activity is affected by the binding of its specific cyclins, which are differentially expressed during the cell cycle, by

its phosphorylation status, and through special CDK inhibitors (CDKIs). CDK inhibition triggers checkpoint activation, and therefore cell cycle arrest.

Transition from G_1 to S phase is primarily controlled by activation of the E2F transcription factor, which is kept inactive during G_1 by the Retinoblastoma protein (Rb), a tumor suppressor gene. As cells progress through the cell cycle, Rb gets phosphorylated by cyclin-CDKs, causing its release from E2F, allowing E2F to function as a transcription factor and initiate to S-phase.

The G_1-checkpoint lies at the transition between G_1 and S-phases that play an important normal role in the decision of the cell to initiate cell division. Irradiation leads to an ATM-dependent stabilization and activation of p53. One of its target genes which get upregulated is CDKI p21 (CDK1A). p21 in turn inhibits the G_1 cyclin-CDK complexes thereby preventing Rb phosphorylation and entry into the S-phase. As a result, cells irradiated while in the G_1-phase will delay their progression into S-phase [94].

The intra S-phase checkpoint, together with G_2-checkpoint is controlled by highly related proteins, the checkpoint kinases 1 and 2 (Chk1 and Chk2) [95]. Both are phosphorylated and activated by ATM and ATR kinase in response to ionizing radiation. Normally, cells which were irradiated react with a fast but reversible decrease in DNA synthesis by reducing the rate of origin firing and strand elongation, thus increasing time needed for replicate their DNA. The molecular target is the CDK2 kinase, which is dephosphorylated by Cdc25A and Cdc25C, upon activation of Chk1 and Chk2 by ATM and ATR they phosphorylate Cdc25A/C leading to their inactivation. As a result, CDK2 levels increase and the progression through S-phase slows down. Although ATM-Chk2 and ATR-Chk1 activation is the main mechanism for initiation of the S-phase checkpoint, several other proteins of DDR are involved. Among them, BRCA1 and BRCA2 proteins, two key players of the HRR pathway of DNA repair.

Two additional checkpoints are present in the G_2 phase, the early and the late G_2 checkpoint. The early-G2 checkpoint is again dependent on the ATM-Chk2-Cdc25A/C axis, and applies to all cells irradiated while in the G_2-phase. Target of the ATM-Chk2-Cdc25A/C complex is cyclinB-CDK1 complex [90], which must be phosphorylated to be active. Thus, all cells irradiated while in their G_2-phase are arrested and their entry into the M-phase (mitosis) is prevented [96]. The late-G2 checkpoint is observed after irradiation of cells which are in the G_1 or S-phase at the time of irradiation. After a transient cell arrest with attempts of DNA damage repair, cells progress to the G_2-phase where they reach hours later and could experience a second, usually very long delay, lasting several hours depending on the dose applied. Furthermore, this checkpoint is independent of ATM. Instead, the principal signaling axis occurs from ATR/ATRIP. ATR kinase activates Chk1, which in turn leads to the degradation of Cdc25A/Cdc25C. The late G_2 checkpoint is mechanistically very similar to the G_1 and S-phase checkpoints, but instead of being directly activated by DSBs, it reflects a type of damage that has been induced throughout the cell cycle but still persists after the other DNA repair processes have occurred but failed to properly activate ATR.

1.3.6. DNA damage repair mechanisms

As discussed above, DSBs are the most relevant type of damage a cell has to repair in order to survive. Already a single, unrepaired or misrepaired DSB is enough to cause cell death. Typically, 1Gy of ionizing radiation can generate around 20 DSBs. Therefore, the cells need to have highly specialized protein machineries to tackle these damages. Specialized proteins can sense DSBs, thereby initiating

the DDR, which focuses the cell on repairing these damages by primarily stopping cell proliferation (through activation of the checkpoints), properly marking the damage (trough γH2AX accumulation) and initiating repair. For DSBs, mammalian cells have two major pathways, HRR and NHEJ. These pathways are quite different with regards to a) proteins involved, b) their kinetics, c) phase of the cell cycle in which they get activated and d) the accuracy of repair. New evidences suggest that the HRR and NHEJ pathways are strongly interconnected to each other through shared gene (e.g. ATM, 53BP1, BRCA1 and XRRC4) and they are can mutually regulate after radiation-induced DNA damage.
Furthermore, alternative (back-up) pathways have been reported to kick in if HRR and/or NHEJ are not properly functional. However, they are error-prone repair mechanism and their exact mechanism of action has not been clearly elucidated yet [97].

1.3.6.1. Homologous recombination repair

HRR uses homologous undamaged DNA (sister chromatid produced while progressing through the S-phase) as the template to repair the damaged DNA [98]. Because HRR uses DNA with the same sequence as the basis for repair, the whole process is usually slow but error-free (Figure 3.3).
The first step is activation of ATM kinase and recruitment of the MRN complex to the damage site, therefore initiating HRR. Single-strand regions are then generated around each side of DNA by nucleolytic degradation [100], followed by their coating with specialized proteins like SMC5/6, which have the primary function of keeping chromatids together [101]. The two proteins involved in the initiation process are Mre11 and CtIP. After initiation by Mre11 and/or CtIP, the processive single-strand exonuclease Exo1 carries out extensive 5'-3' resection [102]. When the single stranded DNA is formed, it is immediately stabilized and protected by binding of the single strand binding protein replication protein A (RPA), a heterotrimeric protein with very high affinity for single-stranded DNA [103]. The RPA protein complex is then displaced by RAD51, a central protein in HRR, resulting in the formation of a nucleoprotein filament of DNA coated with RAD51. Because RPA has a greater affinity than RAD51 for single-stranded DNA, protein mediators are needed for this step, including BRCA2, which directly interact with RAD51 promoting its binding to DNA [104]. At this point, the nucleoprotein filaments undergoes the search for homologous DNA in the form of the sister chromatid. Several proteins, called RAD51 paralogues, help with these processes including RAD51B, RAD51C, RAD51D, XRCC2 and XRCC3. From this stage, there are two possible types to complete repair. In synthesis-dependent strand annealing (SDSA) the genetic information is copied from the intact strand and afterwards the newly synthesized strand reverts to its original position. Alternatively, two sister chromatids exchange strands and built a so-called Holliday junction. Helicases, including BLM and other members RecQ family with the help of RAD54, an ATP-dependent chromatin remodeler, enlarge the subsequent 'bubble' structure and help untangle the DNA to allow branch migration (called DSBR pathway) [105]. Correct pairing of the two strands occurs with the help of RAD52.
The following DNA synthesis is carried out by DNA polymerases, the identity of which is still uncertain but several studies have identified polymerases δ, ε and η to promote repair synthesis [106].
Finally, the open gaps are sealed by Ligase I. To properly function, HRR requires several highly specific proteins and many specific steps have to be completed in an ordered fashion. Homology directed repair can take up to 6-8 hours but it is very accurate.

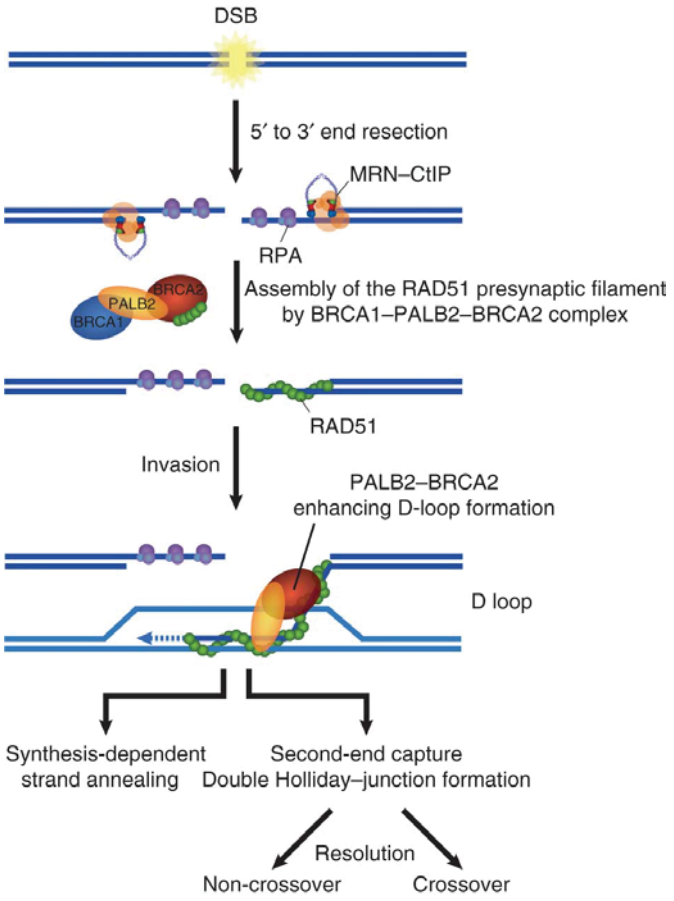

Figure 3.3 HRR is a slow but accurate process. Damage recognition by the Mre_{11}-RAD_{50}-NBS_1 (MRN) complex initiate CtIP-dependent DNA end resection. The single-strand DNA is first bound by RPA, thus preventing the ssDNA from forming secondary structures. Later, the nucleoprotein binds to RAD_{51} and its accessories factors and search for homologous sequence in sister chromatids to form Holliday Junctions. Finally, resolution of the heteroduplex by several helicases takes place. Adapted from [99].

The single strand annealing (SSA) pathway repairs DSBs between two repeat sequences (patterns of nucleic acids that occur in multiple copies throughout the genome) [107]. Opposite to the SDSA or DSBR pathways, SSA does not require a separate similar or identical molecule of DNA. In this pathway, the two 3'-overhangs are aligned and annealed within the region of the repeated sequences. Overhanging single-stranded DNA will be digested, and gaps will be filled and sealed. Furthermore, this process does not require RAD51 but involves other HRR proteins like RPA, RAD52 and RAD50. Therefore, SSA may play a key role in cells with corrupted RAD51 function [108].

1.3.7.1.1 The nuclease Mre11

Mre11 is a component of the MRN protein complex (Mre11-Rad50-Nbs1) [109]. A stable MRN complex is critical to guarantee chromosome stability because of its repairing role in both broken replication forks and two-ended DSBs [110]. The MRE11 plays a fundamental role in DSB repair complex, by acting as a sensor of DSBs together with RAD50 and NBS1, and governs the activation and activity of the central transducing kinases Ataxia telangiectasia mutated (ATM) and ATM and RAD3 related (ATR). Upon irradiation, a strong hyperphosphorylation of Mre11 is induced [111].

The MRN complex functions as DNA end-binding dimer, being able to bind two separate molecules through long-range tethering. The Mre11, which possesses both single-strand DNA endonuclease and 3'-5' exonuclease activities [112], can bind one or two-ended DSBs together with Rad50, which induces an ATP-mediated conformation change upon binding, so that the Mre11-Rad50 complex acts like a transient molecular clamp around the damage site [113] to promote DNA end resection. New evidences suggest that the Mre11-dimer ($Mre11_2$) is able to bind DNA fragments independent of their size and structure [83,114]. Therefore, the HRR pathway can be activated in response to both low- and high-LET radiations, with Mre11 playing a key role in the activation step.

1.3.7.1.2 The DNA repair protein RAD51

The mammalian protein Rad51 is a recombinase which plays a pivotal role in the process of gene conversion and its regulation [115]. Maintenance of proper chromosomal stability relies on the high fidelity of the HRR repair, which allows DSB repair with virtually no mistakes. Typically, cells harbouring mutations in the key components of HRR (RAD51, the BRCA genes, RAD paralogues and XRRC3) show very high levels of genetic instability [116]. Similarly, non-physiological pathway overactivation, observed in several tumors, can also contribute to genetic instability, other than chemo- and radioresistance [117]. RAD51 mRNA and protein levels are elevated by approximately 4–6-fold in cancer cells due to extreme activation of the RAD51 promoter and with activity increased at least 840-fold compared to normal cells [118]. For this reason HR repair has to be tightly regulated in order to prevent inaccurate repair leading to genetic instability and tumor formation. For this purpose the essential HRR protein Rad51 is regulated carefully at both the expression and activity level. During cell cycle, RAD51 levels fluctuate, with an increase of gene expression at the beginning of the S-phase, rising until G_2, to decrease again during G_1 [119] thus reflecting the profile of HRR activity. An important regulator of RAD51 is p53. Binding of p53 to the Rad51 promoter leads to a suppression of Rad51 mRNA transcription and to reduced Rad51 protein levels [120]. RAD51 is also controlled by the Bcr/Abl fusion kinase [121], which is overexpressed in CML. Activity of RAD51 is also strictly regulated, likely through is binding with RAD paralogues and by $BRCA_2$, which plays a supportive role in RPA displacement from the single-stranded filaments to promote RAD51 loading.

Recently, it has been shown that RAD51 plays an important role in the progression of malignancy in addition to its HRR involvement [122], by regulating metastatic gene expression in concert with c/EBPβ, possibly acting as a transcriptional co-factor. Overexpression of the RAD51 recombinase activates c/EBPβ transcription and the subsequent upregulation of metastatic genes that control cell mobility, proliferation, adhesion and extra-cellular matrix, promoting tumor progression and dissemination.

1.3.7.1.3 The cancer susceptibility genes $BRCA_1$ and $BRCA_2$

BRCA genes 1 and 2, together with the Fanconi Anemia family [123] are two classes of genes involved in HRR. Mutations in one of those genes compromise the correct execution of HRR, although in a different fashion, depending on the non-functional gene. The primary role of BRCA2 is to promote RAD51 loading on single-stranded DNA. Therefore, cells deficient in BRCA2 have an impaired RAD51 foci formation [124] which causes radio and chemosensitivity.

The role of BRCA1 gene is broader, as it is tightly involved in cell cycle regulation and apoptosis other than DNA repair [125]. $BRCA_1$ interacts with its partner BARD1 and it can ubiquitinylate other proteins, therefore strongly regulating their activity. Furthermore, BRCA1 can interact with the MRN complex to modulate the NHEJ pathway. As a result, new evidence suggests is role in being a modulator which promotes either HRR or NHEJ, depending on the cellular context [126].

1.3.6.2. Non-homologous end joining

The fastest and most straight forward way to repair a DSB is simply to rejoin the broken ends. NHEJ does effectively join two DNA DSB ends together without requiring any homologous DNA sequence [127]. NHEJ repair is extremely efficient in a quantitative sense, but the fidelity and accuracy of repair usually decreases as soon as the pathway gets saturated by excessive DSBs, resulting in chromosomal translocations and other rearrangements [128]. Ionizing radiation usually causes the formation of non-blunt end, which need to be processed before being ligated. Therefore, NHEJ repair often results in small deletions at the breakage site. Even if the process *per se* is error-prone and can cause loss of genetic material, it is still able to allow cell to survive without losing genetic material, as it would be the case by unrepaired DSBs. NHEJ is active throughout the cell cycle. It is responsible for the repair not only for most of the IR-induced DSB in eukaryotic cells, but it is also strongly involved in V(D)J recombination [129]. Notably, patients with deficient components of the NHEJ pathway, like DNA-PK_{cs} or XRCC4 are radiosensitive and often immunocompromised. NHEJ starts with the binding of the Ku heterodimer (Ku70/Ku80) to the blunt DNA ends, which usually occurs within seconds after break formation because of the high abundance of the Ku dimer and its high affinity for DNA ends (figure 3.4.) [130-131]. The binding serves both to protect ends from exonucleases degradation and to recruit the principal mediator of NHEJ, namely DNA-PK_{cs}. Activation of the kinase activity of DNA-PKcs occurs only when it is bound to the Ku complex at a break site, forming the DNA-PK complex, also called the synaptic complex [132]. This can only take place after the Ku70/Ku80 heterodimer undergoes a conformational change upon DNA binding. The association with Ku bound to DNA activates its serine/threonine kinase activity, which promotes its own autophosphorylation at several sites, the two more important being Serine-2056 (called the PQR cluster) and Threonine-2609 (called the ABCDE cluster) [133] and other targets, including the histone H2AX. Autophosphorylation stimulates dissociation of the protein from DNA and the Ku70/Ku80 unit through a conformational change, allowing the next repair factors to access to the site [109]. DNA-PK_{cs} exists in complex with Artemis, an endonuclease responsible for cleavage of 3'-overhangs, 5'-overhangs, hairpins, flaps, and gaps induced by ionizing radiation, making them suitable for ligation [134]. This step is followed by the recruitment of polynucleotide kinase (PNK), which is responsible for generating ligatable ends using its 5'-kinase and 3'-phosphatase activities.

Now that ends are suitable for ligation, Ku70/Ku80 recruits two main polymerases, namely pol λ and pol μ, which can fill single-stranded gaps (overhang, or non-blunt ends) produced by radiation. The final step is ligation of adjoining ends, which is carried out by the DNA ligase IV-XRCC4-XLF complex [135].

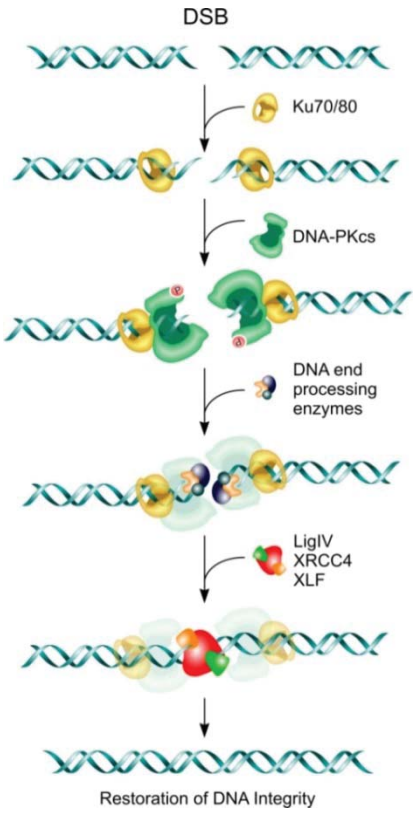

Figure 3.4 NHEJ consists primarily on three steps: first, DNA break recognition by the ku70/ku80 heterodimer, which in turn recruits DNA-PKcs to form the DNA-PK complex. This binding step is followed by DNA processing to remove non-ligatable ends by several enzymes, including Artemis, MRN and several DNA polymerases. End processing promotes the kinase activity of DNA-PKcs, leading to its autophosphorylation and release of the autophosphorylated catalytic subunit from the synaptic complex. Finally, the XRCC4-DNA-Ligase IV complex will relegate the two broken ends. Adapted from [136].

1.3.7.2.1 The Ku70/Ku80 heterodimer

The Ku70/Ku80 heterodimer is an abundant nuclear protein (about $4x10^5$ molecules per cell) that binds avidly to DNA ends as a ring structure (figure 3.5.) [136]. Ku binding to the DNA ends can occur in absence of the DNA-PKcs kinase [138]. Similarly to the Mre11 nuclease in MRN complex, which promote end processing and HRR, Ku contributes to DNA end processing as a 5'-dRP/AP lyase, which can remove abasic sites near breaks [139]. After initial binding to the end and its procession, the Ku70/Ku80 complex translocate inward about one to two helical turns upon binding with the DNA-PKcs unit. Then, in a DNA-dependent fashion, DNA-PKcs binds to the DNA ends [140] and promotes the recruitment of other NHEJ factors, including XRCC4 and LIG4. Electron crystallography studies have shown that DNA-PKcs molecules promotes the synapsis of the two DNA ends, the Ku70/Ku80 heterodimers promoting this process by acting as adaptors proteins to DNA to allow synapsis [141-142]. The Ku70/Ku80 binding properties have been recently shown to play a key role in the ability to distinguish between DNA of different sizes, thus directly affecting the binding and activation after low- and high LET radiation [83]. Due to its very dense and concentrated energy deposition profile, high-LET causes much more fragments of smaller size, compared to low-LET photon radiation. The Ku70/Ku80 heterodimer cannot bind these fragments due to structural hindrance of the ring structure, therefore 'positively selecting' for

the low-LET radiation-type of damage. This in turns have consequences for the activation of DNA-PKcs and generally NHEJ followed by high-LET radiation, usually promoting HRR [82,143].

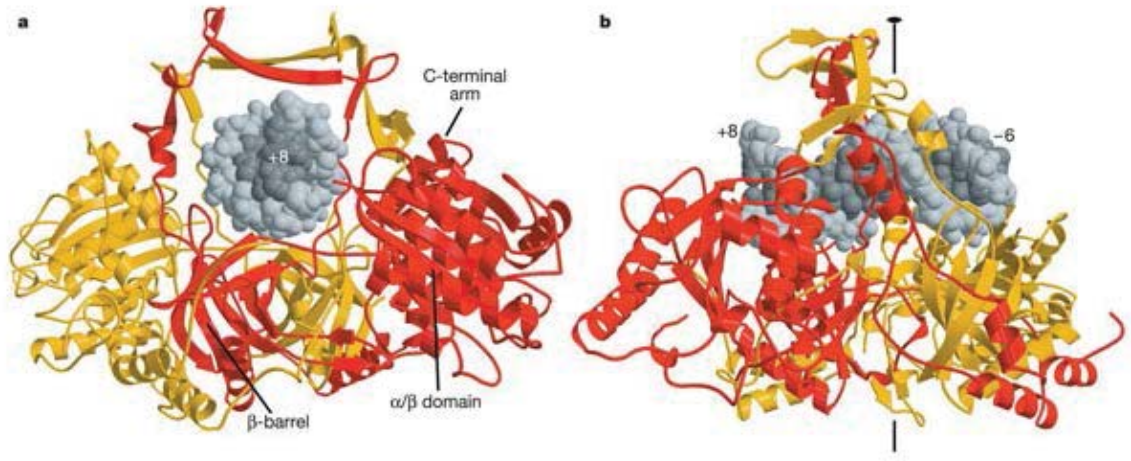

Figure 3.5 Crystallographic representation of the Ku70/Ku80 heterodimer bound to DNA (Ku70 is colored red and Ku80 orange, DNA in gray). Ku70/Ku80 can form a ring structure with a cavity able to accommodate the DNA. Adapted from [137].

1.3.7.2.2 The role of DNA-PK$_{cs}$ in double strand break repair

DNA-dependent protein kinase, catalytic subunit (DNA-PK$_{cs}$) is the largest cellular kinase known with a size of about 470 kDa, and for being fundamental player in the NHEJ pathway [76]. As previously described, the kinase is activated by binding to DNA ends together with the Ku70/Ku80 complex, forming the synaptic complex. Upon activation by Ku70/Ku80 and DNA, DNA-PKcs undergoes autophosphorylation and conformational changes to create a platform for the binding of subsequent factors.

Ku70/Ku80 bound to DNA-PKcs is forming a channel where the DNA fits in and differs from the conformation of unbound DNA-PKcs [144]. The interaction of DNA-PK complex with next, adjacent complex in *trans*-position at the other break end causes *trans*-autophosphorylation at both Ser-2056 and Thr-2609 cluster regions [145]. Several other sites are phosphorylated upon DNA binding, but their functional relevance is often not known. Notably, it has been shown that the kinase-death version of the enzyme (e.g. with mutations in one of those clusters) or treatment with small molecule inhibitors that inactivate DNA- PKcs kinase activity result in radiation sensitivity and defects in DSB repair, even stronger than in case of protein absence [146]. This is due to total blockade of end accessibility for not only NHEJ, but also end resection by MRN and subsequent HRR [147]. Thus, correct activation of the kinase is essential for complete NHEJ.

DNA-PKcs has been shown to play an important role in the process of V(D)J recombination. Recently the first human mutation in the DNA-PKcs gene has been identified leading to a radiosensitive and immunocompromised T-B-SCID patient [148], whereas before only mutations in the Artemis gene were known to be causative of severe SCID syndromes [149].

1.3.6.3. Alternative end joining

The Alternative end joining (Alternative EJ) is a DNA-PK independent repair mechanism which relies primarily on MRN, PARP1 and LIG III for break recognition, processing and repair of DNA damage. It can take place in absence of DNA-PKcs but also LIG IV and XRCC4 [150-151]. Alternative EJ is a very slow and error-prone process, and often involves increased usage of microhomology-mediated end joining (MMEJ) [152]. MMEJ results in the deletion of DNA sequences between short repeats of few nucleotides, typically 5-20, flanking the break. Components of NHEJ and HR like MRN, Ku dimers, LIG IV, CtIP and Rad52) are all involved in this step and seem to be used when the two classical pathways, NHEJ and HRR, have failed to repair the damage. MMEJ is not elusive of cells absent of DNA-PKcs, but can also be performed by cells proficient in DNA-PKcs [126]. Notably, in the absence of Ku70/Ku80 or the LIG IV-XRCC4 complexes, alternative EJ can result in an elevated rate of chromosomal translocations, due to the ligase properties of LIG III, which is strongly associated with high chromosomal translocations [153]. PARP-1 plays a key role in a-EJ by transient binding to both single- and double-strand breaks to activate ribosylation [154]. The affinity for DNA ends is much lower compared to Ku, which is also much more abundant in the nucleus. Thus, PARP-1 serves as a 'sensor' for DNA ends only when Ku70/Ku80 function is impaired.

1.3.6.4. Choice and hierarchy of double strand break repair

Several factors can determine which pathway will predominantly be used to repair DNA damages induced by ionizing radiation, like the cell type, chromatin status (euchromatic or heterochromatic DNA), complexity of the DNA damage and the degree of DNA damage burden [155]. The first step after DNA damage is end resection by nuclease, either Mre11 promoting HRR or Ku70/Ku80 promoting NHEJ, and additionally PARP-1 promoting a-EJ. Both Ku and Mre11 have very high affinity for DNA, therefore they will compete for binding to determine which pathway is subsequently used. This is called passive competition [156]. Another important factor is the template availability. NHEJ is the only repair pathway operating in G_1-phase, where HRR rarely can occur because no sister chromatid is present, and usually RAD51 protein levels are kept very low through active regulation by cyclin-dependent kinases (CDKs) [119]. Therefore, choice of the repair pathway is also an active process. In S- and G_2-cells, phosphorylation of CtIP by CDKs promotes end resection and thus HRR over NHEJ. These specific CDKs are mostly active only from the late G_1-phase on, thus favoring NHEJ in G_1. The damage complexity strongly influence which pathway will actively repair damage, because of the different affinity of Ku70/Ku80 and $(Mre11)_2$ for damaged DNA ends. In G_2 cells usually about 20% of low-LET-induced DSBs (simple breaks) are repaired by HRR. In contrast, almost every DSB produced by high-LET radiation is processed by HRR [157-158].

53BP1 together with BRCA1 play an important role in pathway choice, as they are reported to promote NHEJ other than HRR [159]. 53BP1 is known to associate with DSBs in G_1 to promote NHEJ by suppressing the inappropriate 5'-resection of DSBs [160]. As cells enter S-phase, the 53BP1-mediated barrier to DSB is alleviated by the action of CtIP-mediated BRCA1, which drives the removal of 53BP1 from DSBs in S/G_2, thus allowing resection and error-free repair by HRR [161].

The spectrum of functions of BRCA1 has become more and more complex and interconnected with other proteins. It plays multiple roles repair pathway choice, sustaining DSB repair as a scaffold protein

for HRR or to promote precise joining (ensuring high-fidelity of repair) in NHEJ [162], and checkpoint activation trough ATM-mediated phosphorylation on several residues. Therefore, ATM protein can be seen as a ‘molecular switch’ to promote either HRR or NHEJ.

2 Aim of the study

Currently, proton and particle therapy is widely used in the clinical practice for several tumor entities, but there is a wide gap between the clinical implementation and the radiobiological data supporting it. The first patients were treated with proton therapy almost fifty years ago, and typically today the rationale for new indications is rather more physics and technology-based than biology-based. A more in-depth knowledge on radiobiology of proton irradiation is necessary to allow further implementation of this potent treatment technique.

Several radiobiological experiments conducted in the last decades revealed approximately 10% higher biological efficacy (RBE) of proton compared to conventional photon radiation. This implies a dose adjustment in the clinical set-up when planning treatment with protons [163-164]. However, *in vitro* and *in vivo* studies highlighted how the effectiveness of protons can strongly vary among cell lines and tissues and in general the biological end-point employed [59, 165]. Therefore, using an RBE value of 1.1 in the clinical set-up is still reasonable, but a more accurate molecular-biological understanding is fundamental, especially to allow expansion of new clinical indications and particularly to implement radiochemotherapeutic approaches.

The issue regarding the biological differences between high-energy proton and photon is still far from being cleared. High energy protons (classified as low-LET radiation) show the same oxygen enhancement ratio compared to photon, which is strongly correlated with the LET [166]. On the other hand, it has been demonstrated that apoptosis and micronuclei formation is different [167]. Nevertheless, several studies highlighted the importance of genetic background on the cellular response to proton radiation, and in particular, the role of HRR and NHEJ has been outlined [168-169]. We have previously shown that there is a specific requirement for homologous recombination repair for DNA repair after proton irradiation, which may be due to a differential quality of DNA damage [170]. This has potential relevance for clinical stratification of patients carrying mutations in the DNA damage response pathways (e.g. BRCA genes in breast and ovarian cancer, or Ku in bladder carcinoma) and in the development for combined radiochemotherapy approaches.

The most important target for ionizing radiation is the DNA. Repair pathways play a key role in the response of proton radiation. The main goal of our research project was to investigate, in genetically-defined human cell systems, the effects of proton radiation in respect to DNA damage and repair and whether it differs from conventional, photon radiation.

We thus asked the following question, if:

1) Does the quality and quantity of the damage caused by proton irradiation differ from photon irradiation?
2) Which roles do the major DNA repair pathway, Homologous recombination repair and Non-homologous end joining after proton radiation play?
3) Can we exploit eventual differences as part of a combined treatment approach?

We investigated these issues by 1) using human cancer cells with defined genetic defects or by downregulation of selected genes using small interfering RNA approaches, 2) quantification of the initial DNA damage and the repair kinetics of selected proteins involved in DSB repair, 3) exploiting these differences by combining pharmacologically active substances with the two types of ionizing radiation.

References

1. Alberts B, Johnson A, Lewis J, Raff M, Roberts K, Walter P (2002). *Molecular Biology of the cell*. Garland Science publishing (New York). p. 1314-1315.
2. Kleihues P. and Sobin LH, World Health Organization classification of tumors. *Cancer.* 2000; **88**:2887.
3. Global cancer atlas, Facts and Figures, 2011.
4. Khatib O, Aljurf M. Cancer prevention and control in the Eastern Mediterranean region: the need for a public health approach. *Hematol. Oncol .Stem Cell Ther.* 2008; **1**(1):44–52.
5. Friedenson B. The BRCA1/2 pathway prevents hematologic cancers in addition to breast and ovarian cancers. *BMC Cancer* 2007; **7**:152.
6. Starzl TE. Immunosuppression and Cancer. Transplant Proc. 1973; 5(1):943–947.
7. Hanahan D, Weinberg RA. The Hallmarks of Cancer. *Cell* 2000; **100**(1):57–70.
8. Hanahan D, Weinberg, RA. Hallmarks of Cancer: The Next Generation. *Cell* 2011 **144**(5):646–674.
9. Karkkainen MJ, Petrova TV. Vascular endothelial growth factor receptors in the regulation of angiogenesis and lymphangiogenesis. *Oncogene* 2000; **19**(49):5598–5605.
10. Elkind MM, Swain RW, *et al.* Radiation response of mammalian cells grown in culture. V. Temperature dependence of the repair of X-Ray damage in surviving cells (aerobic and hypoxic). *Radiat. Res.* 1965; **25**:359-376.
11. Railton R, Hannan WJ, *et al.* The Oxygen enhancement ratio and relative biological effectiveness for combined irradiations of Chinese hamster cells by neutron and y-rays. *Int. J. Radiat. Biol.* 1974; **25**(2):121-127.
12. Rettig RA (2005). *Cancer Crusade: the history of the national cancer act of 1971*. Princeton University Press (Lincoln, NE). 4th edition.
13. Novelline R (1997). *Squire's Fundamentals of Radiology*. Harvard University Press. 5th edition.
14. Delaney G, Featherstone C, et al. The role of radiotherapy in cancer treatment: estimating optimal utilization from a review of evidence-based clinical guidelines. Cancer 2005: 104(6); 1129-1137.
15. Brenner DJ, Hall EJ. Computed tomography - an increasing source of radiation exposure.
    5.15.1.1. *N. Engl. J. Med.* 2007; **357**(22):2277–84.
16. *IUPAC: Compendium of Chemical Terminology.* (1997) 2nd edition.
17. Mishra KP, Fluorescence studies on radiation oxidative damage to membranes with implications to cellular radiosensitivity. *P Indian as-Chem Sci* 2002*;* **114**:705-711.
18. Stadtman ER. Oxidation of Free Amino-Acids and Amino-Acid-Residues in Proteins by Radiolysis and by Metal-Catalyzed Reactions. *Annu Rev Biochem* 1993; **62**:797-821.
19. Azzam EI, Jay-Gerin J, Pain D. Ionizing radiation-induced metabolic oxidative stress and prolonged cell injury. *Cancer Lett*. 2012: **327**(1):48-60.
20. Hall EJ, Radiobiology for the Radiologist. *Lippincott Williams and Wilkins Publishing* 6th edition, p. 656 (2006).

21. Health risk from exposure to low levels of ionizing radiations. BEIR VII Phase 2. National research council (2006).
22. Barendsen GW. Responses of cultured cells, tumors and normal tissues to radiations of different linear energy transfer. *Curr. Topics Radiat. Res. Q.* 1968; **4**:293-356.
23. Goodhead DT. Spatial and temporal distribution of energy. *Health Phys.* 1998; **55**:231-240.
24. Goodhead DT. The initial physical damage produced by ionizing radiation. *Int. J. Radiat. Biol.* 1989; **56**:623-634.
25. Van Dyk J. *The Modern Technology of Radiation Oncology*. Medical Physics Publishing. (1999).
26. Camphausen KA, Lawrence RC. Principles of Radiation Therapy. 2008.
27. Torunn IY, Tarbell NJ. Technology Insight: proton beam radiotherapy for treatment in pediatric brain tumos*. Nature Clinical Practice Oncology* 2004; **1**:97-103
28. Gerbaulet A, *et al.* General aspects of brachytherapy. In Gerbaulet A, Pötter R, Mazeron J, Limbergen EV. *The GEC ESTRO handbook of brachytherapy*. 2005.
29. Stewart AJ, *et al.* Radiobiological concepts for brachytherapy. In Devlin P. *Brachytherapy. Applications and Techniques*. 2007.
30. Milenic DE, Brady ED and Brechbiel MW. Antibody-targeted radiation cancer therapy. *Nature Rev Drug Discovery* 2004; **3**:488-98.
31. Rutherford E. Collisions of alpha particles with light atoms. III. Nitrogen and oxygen atoms. *Phil. Mag. VI.* 1919; **37**:571-580.
32. Rutherford E. Collisions of alpha particles with light atoms. IV. An anomalous effect in nitrogen. *Phil. Mag. VI.* 1919; **37**:581-587.
33. Wilson RR. Radiological use of fast protons. *Radiology.* 1946; **47**:487-491.
34. Bragg WH, Kleeman R. On the ionization curves of radium. *Phil. Mag. VI.* 1904; **8**:726-738.
35. Tobias AO, Lawrence JH. Radiological use of high energy deuterons and alpha particles. *Am. J. Roentgenol. Radium Ther. Nucl. Med.* 1952; **67**:1-21.
36. Kjellberg RN, Shintani A, Frantz AG. Proton-beam therapy in acromegaly. *New England Journal of Medicine* 1968; **278**:689-695.
37. Munzenrieder J, Liebsch N. Proton therapy for tumors of the skull base. *Strahlenther. Onkol.* 1999; **175(Supll.2)**:57-63.
38. M. Goitein, Ed., *Radiation Oncology: A Physicist´s-Eye View. Springer Editions (2008).*
39. Koehler AM, Preston WM. Protons in radiation therapy. Comparative dose distributions for protons, photons, and electrons. *Radiology* 1972; 104:191-195.
40. Ottolenghi A, Merzagora M, and Paretzke HG. DNA complex lesions induced by protons and alpha-particles: track structure characteristics determining linear energy transfer and particle type dependence. *Radiat Environ Biophys* 1997; **36**:97-103.
41. Nikjoo H, Wilson WE, *et al.* Track structure in radiation biology: Theory and application. *Int. J. Radiat. Biol.* 1998; 73:355-364.
42. Ryberg B. Clusers of DNA damage induced by ionizing radiation: Formation of shorts DNA fragments. II. Experimental detection. *Radiat. Res.* 1996; **145**:200-209.

43. Bortfeld T, Paganetti H, and Kooy H. Proton beam radiotherapy - The state of the art. *Medical Physics* 2005; **32**:2048-2049.
44. Widesott L, Lomax T, Schwarz M. Is there a single spot size and grid for intensity modulated proton therapy? Simulation of head and neck, prostate and mesothelioma cases. *Med Phys.* 2012; **39**(3):1298-1308.
45. Schneider U, Pedroni E. Secondary neutron dose during proton therapy using spot scanning. *Int. J. Radiation Oncology Biol. Phys*. 2002; **53**(1):244-251.
46. Lomax AJ. Intensity-modulated methods for proton therapy. *Phys Med Biol.* 1999; **44**:185-205.
47. Lomax AJ, Casiraghi M*, et al.* Advantages and limitations of the 'worst case scenario' approach in IMPT treatment planning. *Phys Med Biol.* 2013; 58(5):1323-1339.
48. Pedroni E, Blattmann H, *et al.* the 200-MeV proton therapy project at the Paul Scherrer Institute. Conceptual design and practical realization. *Med. Phys.* 1995; **22**:37-53.
49. Pedroni E, Schaffner B, *et al.* Initial experience of using an active beam delivery technique at PSI. *Strahlentherapie Und Onkologie* 1999; **175**, 18-20.
50. Gerard CR, Bonnetain F, *et al.* Preoperative chemotherapy (CT-RT) improves local control in T3-4 rectal cancers: results of the FFCD 9203 randomized trial. *Int. J. Radiation Oncology Biol. Phys*. 2005; **63**(Suppl.1) s2-s3.
51. Miller SJ, Sun TT, *et al.* Interpreting epithelial cancer biology in the context of stem cells: tumor properties and therapeutic implications. Biochem. Phys. Acta. 2005. 1756:25-52.
52. Bentzen S, Harari PM, Bernier J. Exploitable mechanisms for combining drugs with radiation: concepts, achievements and future directions. *Nature Clinical Practice*. 2006; **4**(3): 172-180.
53. Goodhead DT. Energy deposition stochastics and track structure: what about the target? *Radiat. Prot. Dosimetry.* 2006; **122**:3-15.
54. Chapman JD, Gillespie CJ. Radiation-induced events and their time-scale in mammalian cells. *Adv. Radiat. Biol.* 1981; **9**:143-198.
55. Warters RL, Hofer KG. Radionuclide toxicity in cultured mammalian cells. Elucidation of the primary site for radiation damage. *Curr. Top. Radiat. Res.* 1997; **12**:389-407.
56. Goodhead DT. Radiation effects in living cells. *Can. J. Phys*. 1989; **68**:872-886.
57. Ryberg B. Clusters of DNA damage induced by ionizing radiation: Formation of shorts DNA fragments. II. Experimental detection. *Radiat. Res*. 1996: **145**:200-209
58. Ward JF. The complexity of DNA damage: relevance to biological consequences. *Int. J. Radiat. Biol.* 1994; **66**:427-432.
59. Paganetti H, Suit SD. Relative biological effectiveness (RBE) values for proton beam therapy. *Int J Radiat Oncol Biol Phys* 2002*;* **53:**407-421.
60. Di Pietro C, Consoli U, et al., Cellular and molecular effects of protons: Apoptosis induction and potential implications for cancer therapy. *Apoptosis* 2006*;* **11**, 57-66.
61. Green ML, Tran DT, *et al.* Response of thyroid follicular cells to gamma irradiation compared to proton irradiation. I. Initial characterization of DNA damage, micronucleus formation, apoptosis, cell survival, and cell cycle phase redistribution. *Radiat Res* 2001: **155**:32-42.
62. Giedzinski E, Limoli CL,*et al.* Efficient production of reactive oxygen species in neural precursor cells after exposure to 250 MeV protons. *Radiat Res* 2005**; 164:**540-544.

63. Baluchamy S, Ramesh GT, *et al.* Differential oxidative stress gene expression profile in mouse brain after proton exposure. *In Vitro Cell Dev Biol Anim 2010:* **46**:718- 725.
64. Stisova V, Sutherland BM, *et al.* Response of Primary Human Fibroblasts Exposed to Solar Particle Event Protons. *Radiat. Res*. 2011.
65. Hill MA, Herdman MT, Steven DL, *et al.* Relative sensitivities of repair-deficient mammalian cells for clonogenic survival after α-particle irradiation. *Radiat. Res.* 2004: **162**:667-676.
66. Takashi A, Yuke K, et al. High-LET radiation enhanced apoptosis but not necrosis regardless of p53 status. *Int J Radiat Oncol Biol Phys* 2004*;* **60:**591-597.
67. Kaldecott KW. Single-strand break repair and genetic disease. *Nature Reviews Genetics* 2008; **9**:619-631.
68. Neijenhuis S, Vens C, *et al.* Mechanism of cell killing after ionizing radiation by a dominant negative DNA polymerase beta. *DNA Repair (Amst) 2009;* **8**:336-346.
69. Bradley MO, Kohn KW. X-ray induced DNA double strand break production and repair in mammalian cells as measured by neutral filter elution. *Nucleic Acids Res.* 1979; **7**:793–804.
70. Demple B, DeMott MS. Dynamics and diversions in base excision DNA repair of oxidized abasic lesions. *Oncogene* 2002; **21**:8926–8934.
71. Hegde M. L., Mitra S, *et al.* Early steps in the DNA base excision/single-strand interruption repair pathway in mammalian cells. *Cell Res.* 2008; **18**:27–47.
72. Kuzminov A. Single-strand interruptions in replicating chromosomes cause double-strand breaks. *Proc. Natl Acad. Sci. USA* 2001; **98**:8241–8246.
73. C. Vens C, Begg AC. Targeting base excision repair as a sensitization strategy in radiotherapy. *Semin Radiat Oncol.* 2010: **20**:241-249.
74. Scully R, Xie A. Double strand break repair functions of histone H2AX. *Mutation Research* 2013; 750(1):5-14.
75. Paques F, Haber JE. Multiple pathways of recombination induced by double- strand breaks in Saccharomyces cerevisiae. *Microbiol. Mol. Biol. Rev.* 1999; 63:349–404.
76. Lieber MR. The mechanism of double-strand DNA break repair by the non-homologous DNA end-joining pathway. *Annu. Rev. Biochem.* 2010; 79:181–211.
77. Stetina R, *et al.* Oxidative Damage to DNA: Do We Have a Reliable Biomarker? *Environmental health perspective.* 1996; **104**:465-469.
78. Harper JW, Elledge SJ. The DNA damage response: ten years after. *Mol Cell* 2007; **28**:739-745.
79. Jackson SP, Bartek J. The DNA-damage response in human biology and disease. *Nature* 2009; **461**:1071-1078.
80. Georgakilas A. Formation of Clustered DNA Damage after High-LET Irradiation: A Review. *Journal of Radiation Research*. 2008; **49**(3): 203-210.
81. Wang H, Iliakis G. *et al.* Biochemical evidence for Ku-independent backup pathways of NHEJ *Nucleic Acid Research* 2003; **31**(18):5377-88.
82. Wang H, Wang Y, *et al.* The Ku-dependent non-homologous end-joining but not other repair pathway is inhibited by high linear energy transfer ionizing radiation *DNA repair* 2008; **8**:725-733.

83. Wang H, Wang Y, *et al.* Characteristics of DNA-binding proteins determine the biological sensitivity to high-linear energy transfer radiation. *Nucleic Acids Research* 2010; **38**(10):3245–3251.
84. Lord CJ, Ashworth AA. The DNA damage response and cancer therapy. *Nature 2012;* **481**, 287-289.
85. Bhoumik A, Ronai Z. ATM-dependent phosphorylation of ATF2 is required for the DNA damage response. *Mol. Cell* 2005; **18**:577-587.
86. Gautier J. Double-strand break end resection and repair pathway choice. *Annual review of genetics.* 2011; **45**:247-271.
87. Stucki M, and Jackson SP. gammaH2AX and MDC1: anchoring the DNA-damage response machinery to broken chromosomes. *DNA Repair (Amst) 2006;* **5**:534-543.
88. Lavin MF, Kozlov S. ATM activation and DNA damage response. *Cell Cycle* 2007; **6**:931-942.
89. Savic V,B, Bassing CH, *et al.* Formation of dynamic gamma-H2AX domains along broken DNA strands is distinctly regulated by ATM and MDC1 and dependent upon H2AX densities in chromatin. *Mol Cell 2009;* **34**:298-310.
90. Wilson GD. Radiation and the cell cycle, revisited. *Cancer Metastasis Rev* 2004; **23**:209-225.
91. Matsuoka S, Solimini N, *et al.* ATM and ATR substrate analysis reveals extensive protein networks responsive to DNA damage. *Science 2007;* **316**:1160-1166.
92. Lees-Miller SP, *et al*. DNA damage-induced activation of ATM and ATM-dependent signaling pathways. *DNA repair*. 2004; **3**(8):889-900.
93. Kastan MB, Bartek J. Cell-cycle checkpoints and cancer. *Nature* 2004; **432**:316-323.
94. Vogelstein B, Levine AJ. Surfing the p53 network. *Nature* 2000; **408**:307- 310.
95. Bartek J, Lukas J. Checking on DNA damage in S phase. *Nat. Rev. Mol. Cell. Biol.* 2004; **5**:792-804.
96. Xu N, Gillespie DA, *et al.* Akt/PKB suppresses DNA damage processing and checkpoint activation in late G2. *J Cell Biol 2010;* **190**:297-305.
97. Chistiakov DA, Chistiakov PA, *et al.* Genetic variations in DNA repair genes, radiosensitivity to cancer and susceptibility to acute tissue reactions in radiotherapy-treated cancer patients. *Acta Oncologica* 2008; **47**:809-824.
98. West, SC. Molecular views of recombination proteins and their control. *Nat. Rev. Mol. Cell. Biol.* 2003; **4**:435-445.
99. Buisson R, Masson JY, *et al.* Cooperation of breast cancer proteins PALB2 and piccolo BRCA2 in stimulating homologous recombination. *Nature structural and molecular biology*. 2010; **17**:1247-1254.
100. Pardo B, Gomez-Gonzalez B, Aguilera A, DNA repair in mammalian cells: DNA double-strand break repair: how to fix a broken relationship. *Cell Mol Life Sci* 2009; **66**:1039-1056.
101. Hiom K. Coping with DNA double strand breaks. *DNA Repair (Amst)* 2010; **9**:1256-1263.
102. Huertas P. DNA resection in eukaryotes: deciding how to fix the break. *Nat Struct Mol Biol 2010;* **17**:11-16.
103. Zou L. RPA-coated single-stranded DNA as a platform for post-translational modifications in the DNA damage response. Cell Res. 2014; **147**.

104. Powell SN, Kachnic LA. Roles of BRCA1 and BRCA2 in homologous recombination. DNA replication fidelity and the cellular response to ionizing radiation. *Oncogene* 2003; **22**:5784-5791.
105. Amitani, I, Baskin J, Kowalczykowski SC. Visualization of Rad54, a chromatin remodeling protein, translocating on single DNA molecules. *Mol Cell 2006;* **23**, 143-148.
106. Sebesta M, Krejci L, *et al.* Reconstitution of DNA repairsynthesis in vitro and the role of polymerase and helicase activities. *DNA Repair (Amst)* 2011.
107. Helleday T, Engelward BP, *et al.* DNA double-strand breakrepair: from mechanistic understanding to cancer treatment. *DNA Repair (Amst)* 2007; **6**:923-935.
108. Bennardo N, Stark JM, *et al.* Alternative-NHEJ is a mechanistically distinct pathway of mammalian chromosome break repair. *PLoS Genet* 2008; **4**.
109. Weaver D, et al. Isolation and Characterization of the Human *MRE11* Homologue. *Genomics* 1995; **29**(1):80-86.
110. Williams RS, Tainer JA, *et al.* Mre11-Rad50-Nbs1 is a keystone complex connecting DNA repair machinery, double-strand break signaling, and the chromatin template. *Biochem. Cell Biol.* 2007; **85**:509-520.
111. Chen PL*, et al.* The Nijmegen breakage syndrome protein is essential for Mre11 phosphorylation upon DNA damage. *J. Biol. Chem.* 1999; **274**:19513-19516.
112. Sung LP, *et al.* Nuclease activities in a complex of human recombination and DNA repair factors Rad50, Mre11 and p95. *J. Biol. Chem.* 1998; **273**:21447-21450.
113. Williams CJ, Tainer JA, *et al.* Mre11-Rad50-Nbs1 conformations and the control of sensing, signaling and the effector responses at DNA double strand breaks. DNA repair 2010; **9**:1299-1306.
114. Guenther G, *et al.* Mre11 Dimers Coordinate DNA End Bridging and Nuclease Processing in Double-Strand-Break Repair. *Cell* 2008; **135**:97-109.
115. Vispe S, Defais M, *et al.* Overexpression of Rad51 protein stimulates homologous recombination and increases resistance of mammalian cells to ionizing radiation. *Nucleic Acids Research* 1998; **26**:2859-2864.
116. Thompson LH, Schild D. Homologous recombinational repair of DNA ensures mammalian chromosome stability. *Mutat Res-Fund Mol M* 2001; **477**:131-153.
117. Wiese C. Overexpression of RAD51 suppresses recombination defects: a possible mechanism to reverse genomic instability. *Nucleic Acids Res*. 2010; **38**(4):1061-70.
118. Hine CM, Gorbunova V. Use of the Rad51 promoter for targeted anti-cancer therapy. *Proc Natl Acad Sci USA*. 2008; **105**(52): 20810–20815.
119. Flygare Benson JF, Hellgren D. Expression of the human RAD51 gene during the cell cycle in primary human peripheral blood lymphocytes. *Bba-Mol Cell Res* 1996; **1312**:231-236.
120. Arias-Lopez C, Silva A, *et al.* P53 modulates homologous recombination by transcriptional regulation of the RAD51 gene. *Embo Rep* 2006; **7**:219-224.
121. Slupianek A, Skorski T, *et al.* BCR/ABL regulates mammalian RecA homologs, resulting in drug resistance. *Molecular Cell* 2001; **8**:795-806.

122. Wiegmans AP, Silva LD, *et al.* Rad51 supports triple negative breast cancer metastasis. Oncotarget 2014.
123. Zhang J, Powell SN. The role of the BRCA1 tumor suppressor in DNA double strand break repair. *Mol. Cancer Res.* 2005; 3:531-539.
124. Yuan SFL, Chen G. BRCA2 Is Required for Ionizing Radiation-induced Assembly of Rad51 Complex in Vivo. *Cancer Res* 1999; **59**:3547-3551.
125. Baer R. Effect of DNA damage on a BRCA1 complex. *Nature* 2001; **414**(6859):36.
126. Yun M, Hiom K. CtIP-BRCA1 modulates the choice of DNA double-strand-break repair pathway throughout the cell cycle. *Nature* 2009; **459**(7245):460-463.
127. Lieber MR. The mechanism of human non-homologous DNA end joining. *J. Biol. Chem.* 2008; **283**:1-5.
128. Povirk, LF. Biochemical mechanisms of chromosomal translocations resulting from double-strand breaks. *DNA repair* 2006; **5**:1199-1212.
129. Verkaik NS, Van Gent DC *et al.* Different types of V(D)J recombination and end joining defects in DNA double-strand break repair mutant mammalian cells. *Eur. J. Immunol.* 2002; **32**:701–709.
130. Downs A, Jackson SP. A means to a DNA end: The many roles of Ku. *Nat Rev Mol Cell Bio* 2004; **5**:367-378.
131. Mimori T, Hardin JA. Mechanism of Interaction between Ku Protein and DNA. *Journal of Biological Chemistry* 1986; **261**:375-379.
132. Yaneva M, Kowalewski T, Lieber MR, *et al.* Interaction of DNA-dependent proteinkinase with DNA and with Ku: biochemical and atomic-force microscopy studies. *EMBO Journal* 1997; **16**:5098–5112.
133. Neal JA, Meek K. Choosing the right path: Does DNA-PKcs help make the decision? *Mutation Research* 2011; **711**:73-86.
134. Jeggo PA, Lobrich M. Artemis links ATM to double-strand break rejoining. *Cell Cycle* 2005; **4**:316-323.
135. Moon AF, Pedersen LC, et al. The X family portrait: Structural insights into biological functions of X family polymerases. *DNA Repair* 2007; **6**:1709-1725.
136. Iliakis G. *The Pathways of Double-Strand Break Repair. DNA Repair - On the Pathways to Fixing DNA Damage and Errors* (2011).
137. J. R. Walker, R. A. Corpina, J. Goldberg. *Structure of the Ku heterodimer bound to DNA and its implications for double-strand break repair*. *Nature* 412 (6847), s. 607–614, 2001
138. Drouet J, Calsou P*, et al.* DNA-dependent protein kinase and XRCC4-DNA Ligase IV mobilization in the cell in response to DNA double-strand breaks. *J. Biol. Chem.* 2005; **280**:7060-7069.
139. Roberts SA, Ramsden DA, *et al.* Ku is a 5'-dRP/AP lyase that excises nucleotide damage near broken ends. *Nature* 2010; **464**:1214-1214.

140. Suwa A, Hardin JA, et al. DNA-dependent protein kinase (Ku protein-p350 complex) assembles on double-stranded DNA. *Proc. Natl. Acad. Sci.* USA 1994; **91**:6904-6908.
141. DeFazio LG, Chu G, *et al.* Synapsis of DNA ends by DNA-dependent protein kinase. EMBO J. 1999; **18**:1114-1123.
142. Pawelczak KS, Turchi JJ, *et al.* Differential activation of DNA-PK based on DNA strand orientation and sequence bias. Nucleic Acid Res. 2005; **33**:152-161.
143. Wang H, Wang Y. Heavier Ions with a Different Linear Energy Transfer Spectrum Kill More Cells Due to Similar Interference with the Ku-Dependent DNA Repair Pathway. *Radiation Research*, 2014; 182(4):458-461.
144. Boskovic J, Llorca O, *et al.* Visualization of DNA-induced conformational changes in the DNA repair kinase DNA-PKcs. *Embo J* 2003; **22**, 5875-5882.
145. Dobbs T, Lees-Miller SP, *et al*. A structural model for regulation of NHEJ by DNA-PKcs autophosphorylation. DNA repair 2010; **9**(12):1307-1314.
146. Kurimasa A, Chen DJ, *et al*. Requirement for the kinase activity of human DNA-dependent protein kinase catalytic subunit in DNA strand break rejoining, *Mol. Cell Biol.* 1999; **19**:3877–3884.
147. Zhao Z, Curtin NJ, *et al.* Preclinical evaluation of a potent novel DNA-dependent protein kinase inhibitor NU7441, *Cancer Res.* 2006; 66:5354–5362.
148. Van Gent DC, *et al*. A *DNA-PKcs* mutation in a radiosensitive $T^{-}B^{-}$ SCID patient inhibits Artemis activation and nonhomologous end-joining. *J Clin Invest.* 2009; 119(1):91–98.
149. De Villartay JP, *et al*. Artemis, a Novel DNA Double-Strand Break Repair/V(D)J Recombination Protein, Is Mutated in Human Severe Combined Immune Deficiency. *Cell* 2001; **105**(2):177
150. Guirouilh-Barbat J, Lopez BS, *et al.* Defects in XRCC4 and Ku80 differentially affect the joining of distal nonhomologous ends. Proc Natl Acad Sci 2007; **104**:20902–20907.
151. Wang H, Iliakis G. *et al.* Biochemical evidence for Ku-independent backup pathways of NHEJ *Nucleic Acid Research* 2003; 31(18):5377-5388.
152. McVey M, Lee SE. MMEJ repair of double-strand breaks (director's cut): deleted sequences and alternative endings, *Trends Genet.* 2008; **24**:529– 538.
153. Simsek D, Jasin M. DNA ligase III promotes alternative nonhomologous end-joining during chromosomal translocation formation, *PLoS Genet.* 2011; **7**:e1002080.
154. Wang M, Iliakis G, *et al.* PARP-1 and Ku compete for repair of DNA double strand breaks by distinct NHEJ pathways, Nucleic Acids Res. 2006; 34:6170–6182.
155. Shrivastav M, Nickoloff JA, *et al.* Regulation of DNA double-strandbreak repair pathway choice. *Cell Res* 2008; **18**:134-147.
156. Brugmans L, Essers J, *et al.* Analysis of DNA double-strand break repair pathways in mice. *Mutation Research* 2007; **614**:95-108.
157. Shibata A, Jeggo PA, *et al.* Factors determining DNA double-strand break repair pathway choice in G2 phase, *EMBO J.* 2011; **30**:1079–1092.
158. Beucher A, Lobrich M, *et al.* ATM and Artemis promote homologous recombination of radiation-induced DNA double-strand breaks in G2, EMBO J. 2009; **28**:3413–3427.

159. Bau DT, Shen SY, *et al.* Breast cancer risk and the DNA double-strand break end-joining capacity of nonhomologous end-joining genes are affected by BRCA1, Cancer Res. 2004; 64:5013–5019.
160. Bothmer A, Nussenzweig MC, *et al.* 53BP1 regulatesDNAresection and the choice between classical and alternative end joining during class switch recombination. *J. Exp. Med*. 2010; **207**:855–865.
161. Chapman JR, Jackson SP. BRCA1-associated exclusion of 53BP1 from DNA damage sites underlies temporal control of DNA repair. *J. Cell Sci.* 2012; **125**:3529–3534.
162. Zhong Q, Lee WH, *et al.* BRCA1 facilitates micro-homology mediated end-joining of DNA double-strand breaks, *J. Biol. Chem.* 2002; 207:28641–28647.
163. Kozin SV. Relative biological effectiveness of proton beams in clinical therapy. *Radiother. Oncology* 1999; **50**(2):135-142.
164. Whitmore G. The RBE issues in ion-beam therapy: conclusions of a joint IAEA/ICRU working group regarding quantities and units. *Radiat Prot Dosimetry.* 2006; **122**(1-4):463-70.
165. Dale RG, Carabe-Fernandez A. Why more needs to be known about RBE effects in modern radiotherapy. *Appl Radiat Isot*. 2009; **67**(3):387-92.
166. Raju MR, Robertson JB, *et al.* A heavy particle comparative study. Part III: OER and RBE. *Br J Radiol* 1978; **51**:712-719.
167. Green LM, Tran DT, et al. Response of thyroid follicular cells to gamma irradiation compared to proton irradiation. I. Initial characterization of DNA damage, micronucleus formation, apoptosis, cell survival, and cell cycle phase redistribution. *Radiat. Res.* 2001; **155**:32-42.
168. Genet SC, Kato TA. *et al.* Comparison of cellular lethality in DNA repair-proficient or -deficient cell lines resulting from exposure to 70 MeV/n protons or 290 MeV/n carbon ions. *Oncol. Rep.* 2012; **28**(5):1591-6.
169. Takashi S. Repair of DNA damage induced by accelerated heavy ions in mammalian cells proficient and deficient in the non-homologous end-joining pathway. *Radiat Res*. 2006; **165**(1):59-67.
170. Grosse N, Pruschy MN, et al. Deficiency in homologous recombination renders Mammalian cells more sensitive to proton versus photon irradiation. *Int J Radiat Oncol Biol Phys.* 2014; **88**(1):175-81.

3 Results

3.1 Deficiency in Homologous Recombination renders Mammalian Cells more Sensitive to Proton versus Photon Irradiation

Nicole Grosse[1], Andrea O. Fontana[1], Eugene B Hug[2], Anthony J. Lomax[3], Adolf Coray[1], Marc A. Augsburger[1], Harald Paganetti[4], Alessandro A. Sartori[5], Martin N. Pruschy[1]

[1] Department of Radiation Oncology, University Hospital Zurich, Zurich, Switzerland
[2] Procure, Oklahoma City OK, USA
[3] Paul Scherrer Institute, Villigen, Switzerland
[4] Department of Radiation Oncology, Massachusetts General Hospital and Harvard Medical School, Boston MA, USA
[5] Institute for molecular cancer research, University of Zurich, Zurich, Switzerland

Status of the manuscript: Published in International Journal of Radiation Oncology, Biology, Physics. 2014 Jan; 88(1):175-81.

Author contribution A.O. Fontana:
Set-up and planning of the chromosomal aberration experiment and MTT assay, participation in manuscript drafting, revision and editing.

International Journal of Radiation Oncology biology • physics

www.redjournal.org

Biology Contribution

Deficiency in Homologous Recombination Renders Mammalian Cells More Sensitive to Proton Versus Photon Irradiation

Nicole Grosse, PhD,[*] Andrea O. Fontana, MSc,[*] Eugen B. Hug, MD,[†] Antony Lomax, PhD,[†] Adolf Coray, PhD,[†] Marc Augsburger, MSc,[*] Harald Paganetti, PhD,[‡] Alessandro A. Sartori, PhD,[§] and Martin Pruschy, PhD[*]

Laboratory for Molecular Radiobiology, University Hospital Zurich, Zurich, Switzerland; [†]Center for Proton Therapy, Paul Scherrer Institute, Villigen, Switzerland; [‡]Department of Radiation Oncology, Massachusetts General Hospital and Harvard Medical School, Boston, Massachusetts; and [§]Institute of Molecular Cancer Research, University of Zurich, Zurich, Switzerland

Received Apr 10, 2013, and in revised form Sep 12, 2013. Accepted for publication Sep 16, 2013.

Summary

A differential requirement of the 2 major DSB repair pathways in response to proton versus photon irradiation was demonstrated in an accepted model of genetically defined cells with defects in different DNA repair systems. Cells lacking HR proteins were specifically more sensitive to proton than to photon irradiation, which translated into an increased RBE_{37} and RBE_{10} for the

Purpose: To investigate the impact of the 2 major DNA repair machineries on cellular survival in response to irradiation with the 2 types of ionizing radiation.

Methods and Materials: The DNA repair and cell survival endpoints in wild-type, homologous recombination (HR)-deficient, and nonhomologous end-joining-deficient cells were analyzed after irradiation with clinically relevant, low-linear energy transfer (LET) protons and 200-keV photons.

Results: All cell lines were more sensitive to proton irradiation compared with photon irradiation, despite no differences in the induction of DNA breaks. Interestingly, HR-deficient cells and wild-type cells with small interfering RNA-down-regulated Rad51 were markedly hypersensitive to proton irradiation, resulting in an increased relative biological effectiveness in comparison with the relative biological effectiveness determined in wild-type cells. In contrast, lack of nonhomologous end-joining did not result in hypersensitivity toward proton irradiation. Repair kinetics of DNA damage in wild-type cells were equal after both types of irradiation, although proton irradiation resulted in more lethal chromosomal aberrations. Finally, repair kinetics in HR-deficient cells were significantly delayed after proton irradiation, with elevated amounts of residual γH2AX foci after irradiation.

Conclusion: Our data indicate a differential quality of DNA damage by proton versus photon irradiation, with a specific requirement for homologous recombination for DNA repair and enhanced

Reprint requests to: Martin Pruschy, PhD, Laboratory for Molecular Radiobiology, University Hospital Zurich, Raemistrasse 100, 8091 Zurich, Switzerland. Tel: (41) 44-255-8549; E-mail: martin.pruschy@usz.ch

Portions of these data, including published abstracts, were presented at several conferences: the 55th Annual Meeting of the American Society for Radiation Oncology, Atlanta, GA, September 22-25, 2013, the International Conference on Translational Research in Radiation Oncology - Physics for Health in Europe (ICTR-PHE) 2012 Conference, February 2-3, 2012, Geneva, Switzerland; and the 12 International Wolfsberg Meeting on Molecular Radiation Oncology, June 25-27, 2011, Ermatingen, Switzerland.

This study was supported by grants from the Swiss Cancer League (to M.P.), the University of Zurich (to E.B.H.), the Swiss National Science Foundation, and the Vontobel Foundation (to A.A.S.)

Conflict of interest: none.

Supplementary material for this article can be found at www.redjournal.org.

Acknowledgments—The authors thank Terence Böhringer, Lin Shixiong, Benno Rohrer, and Stefan König for excellent technical support at the Paul Scherrer Institute (Villigen, Switzerland), Malgorzata Z. Zdzienicka (Bydgoszcz, Poland) for all Chinese hamster ovary cell lines, and Adrian Begg (Amsterdam, The Netherlands) for critical input to the manuscript.

0360-3016/$ - see front matter
http://dx.doi.org/10.1016/j.ijrobp.2013.09.041

HR-deficient cells. These results might become relevant for clinical stratification of patients carrying mutations in specific DNA damage response pathways.

cell survival. This has potential relevance for clinical stratification of patients carrying mutations in the DNA damage response pathways. © 2013 Elsevier Inc.

Introduction

A generic relative biological effectiveness (RBE) value of 1.1 is currently used in the clinic for proton radiation therapy. However, this RBE can vary significantly depending on the tissue, cell line, or endpoint investigated (1-4). Only a minimal number of studies have been performed to understand the differential response on the molecular and cellular levels. For example, free 3′ DNA ends are more abundant 1 hour after proton irradiation (222 MeV) than after photon irradiation, as demonstrated in thyroid follicular cells. Micronuclei formation and the immediate apoptotic cell response are also augmented in these cells in response to proton versus photon irradiation (5). Furthermore, in vitro experiments performed with genomic T7 DNA revealed the highest ratio of clustered DNA double-strand breaks (DSBs) after proton irradiation. Finally, a significant fraction of complex types of chromosomal aberrations and an increased frequency of sister chromatid exchanges were demonstrated in different cell lines after proton irradiation (6, 7). These studies indicate that either more initial DNA breaks or a qualitatively different type of damage are induced by these different, low-linear energy transfer (LET) types of ionizing radiation.

Cells have evolved 2 major DSB repair pathways (8, 9): homologous recombination (HR) is initiated through the recognition of DSBs by the Mre11, Rad50 and Nbs1 (MRN)-complex followed by MRN- and CtBP-interacting protein (CtIP)-dependent 3′−5′ DNA resection (10). The resulting single-stranded DNA tails are first stabilized by replication protein A (RPA) that is later replaced by Rad51 (9) to form Holliday junctions. Ultimately, these structures are resolved by several Holliday junction processing factors (10, 11). Double-strand break repair by nonhomologous end-joining (NHEJ) relies on the initial binding of the Ku70/80 heterodimer, which results in the recruitment of DNA-PKcs (9). The XRCC4-DNA Ligase IV complex will eventually re-ligate the 2 broken strands (12).

In the study reported here we have investigated the treatment response to photon and proton irradiation in an accepted model of genetically defined cells with defects in one of the major DNA repair systems (13-15).

Methods and Materials

Cell lines

The Chinese hamster ovary (CHO) cells AA8, CHO9, UV5, Irs1sf, and XR-C1 were cultured in Ham F10 cell culture media containing 10% fetal bovine serum and penicillin−streptomycin (100 U/mL-100 μg/mL) and kept at 37°C, at 5% CO_2 atmosphere.

Irradiation procedures

To irradiate exponentially growing cultures, 3×10^5 cells were plated into 25-cm^2 flasks 24 hours before irradiation. To irradiate plateau phase cultures, 1×10^6 cells were plated into 25-cm^2 flasks 72 hours before irradiation. Photon irradiation was performed using a Gulmay (Suwanee, GA) 200-kV x-ray unit at 1 Gy/min (kVp = 200 kV; half-value layer (HVL) = 1.03 mm Cu; Filter: 1 mm Al and 0.45 mm Cu). Proton irradiations were delivered using spot scanning (16). The maximal instantaneous dose rate at the Bragg peak is 4 Gy/s; however, cells were placed in the center of the spread-out Bragg peak (SOBP), with a length of 5 cm and maximum proton energy of 138 MeV. The LET is generally low in the middle of the SOBP, because most of the dose is deposited by plateau doses, and very little is deposited from Bragg peaks. The field size orthogonal to the beam was 15 × 11 cm. Dosimetry of the fields was performed using both small-diameter cylindrical ionization chambers (active volume 0.3 cm^3) and a farmer-type NE2571 ionization chamber using the International Atomic Energy Agency TRS-398 protocol.

Clonogenic survival

Twenty hours after irradiation, cells were trypsinized, and single-cell suspensions were seeded into petri dishes. The number of plated cells per dish was adjusted to obtain approximately 50-200 colonies under all experimental conditions. After colony formation for 7-10 days, colonies were fixed (methanol/acetic acid; 3:1) and stained with crystal violet (2%). Colonies (containing >50 cells) were counted manually. To calculate RBE values, α and β values for each survival curve were determined. Survival data were fitted by weighted, stratified, linear regression to obtain the linear and quadratic parameters. Linear regression was performed in SPSS (Chicago, IL) as described in reference 17. The RBE values at 37% and 10% survival level were calculated according to reference 18.

Transfection of CHO cells

Transfection of AA8 wild-type cells was performed 1 day before plating for irradiation. Cells were irradiated 48 hours after transfection. Small interfering RNAs (siRNAs) were used at a concentration of 40 nM with 1.7 μL/mL Lipofectamine RNAiMAX (Invitrogen, Carlsbad, CA). The following siRNA sequences were used: siLuc: 5′-CGTACGCGGAATACTTCGAdTdT-3′; siRad51: 5′-GAGCUUGACAAACUACUUCdTdT-3′.

Immunofluorescence microscopy

Twenty-four hours before irradiation, cells were plated onto Ibidi-μ-slides $VI^{0.4}$ (Ibidi, 80606, Munich, Germany) at the same cell density as used for clonogenic survival assays. After irradiation, cells were washed twice with phosphate-buffered saline (PBS), fixed with 4% formaldehyde/PBS for 20 minutes, washed with PBS (4 × 5 minutes), and finally with 0.1 M glycine, for storage at 4°C until staining. Cells were permeabilized for 5 minutes with 0.2% ice-cold Triton-X-100, blocked for 30 minutes with 3%

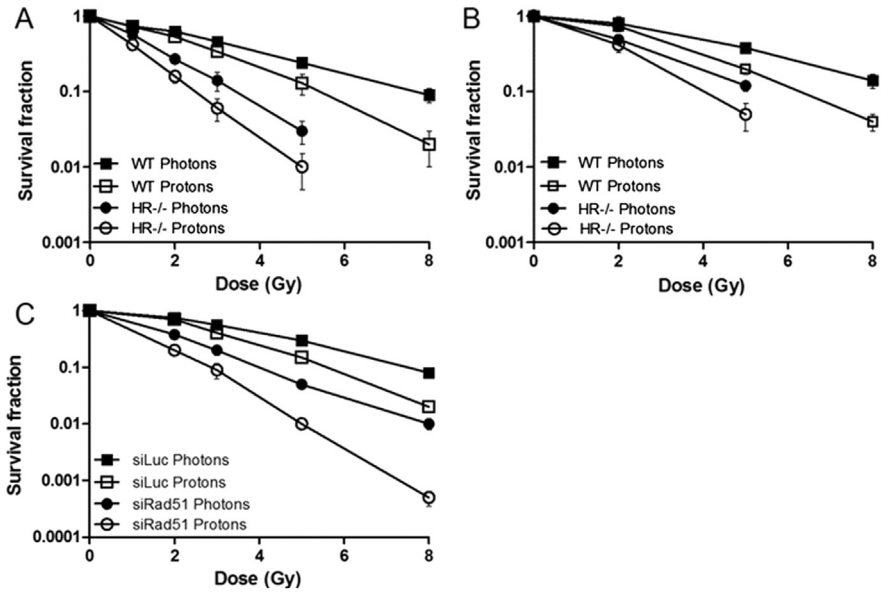

Fig. 1. Clonogenic cell survival of proton- and photon-irradiated cell lines. Chinese hamster ovary wild-type (WT) cells (AA8) and corresponding homologous recombination (HR)-deficient cells (XRCC3-/-; Irs1sf) were irradiated in exponential growth phase (A) and in plateau phase (B). Data were pooled from at least 3 independent experiments. (C) Clonogenic survival of Chinese hamster ovary wild-type cells (AA8) transfected with either control small interfering RNA (siLuc) or with 2 different Rad51-directed small interfering RNAs. Clonogenic survival data from both siRad51-treated cells were pooled. Points represent mean ± SD.

bovine serum albumin (BSA)/0.1% Tween-20/PBS, followed by 1-hour incubation with primary antibodies, diluted 1:100 in 1% BSA/PBS (mouse monoclonal anti-H2AX-pSer139 (Millipore, Billerica, MA), rabbit polyclonal anti-Rad51, and rabbit polyclonal anti-DNA-PKcs-pS2056 (Abcam, Cambridge, United Kingdom). After washing with 1% BSA/PBS (4 × 10 minutes), cells were incubated with the appropriate secondary antibody 1:1000 (Alexa-488 and/or Alexa-546; Invitrogen, Gibco, Basel, Switzerland) and incubated with PBS/4′,6-diamidino-2-phenylindole (1 μg/mL). Slides were examined with a Leica SP5 confocal microscope and a Leica DFC 350 FX camera (Leica Microsystems, Wetzlar, Germany). Merged z-stacks were analyzed with LAS AF Lite software (Leica, free version). At least 50 cells per condition were analyzed.

Chromosomal aberrations

Twenty-one hours after irradiation, cells were blocked in metaphase by the addition of 0.2 μg/mL Colcemid (Gibco) for 3 hours. Thereafter, cells were treated in hypotonic KCl solution (0.075 M) and fixed 2× in Carnoy's fixative (3:1; methanol:acetic acid). Cell concentration was adjusted (approximately 1×10^6 cells/mL), and fixed cells were dropped onto wet slides, stained with 2% Giemsa (Sigma, St. Louis, MO), and embedded with Entellan (Merck, Whitehouse Station, NJ). Light microscopy pictures of at least 100 metaphases per condition were acquired with a Leica SP5 microscope. Metaphase spreads were screened for fragments, rings, dicentrics, sister unions, and complex exchanges.

Statistical analysis

Data were presented as the mean ± standard error of the mean (SEM) or standard deviation (SD) of at least 3 independent experiments. The results were tested for significance using the 2-sided unpaired Student *t* test or the Wilcoxon-Mann-Withney *U* test. Results were considered statistically significant at $P<.05$ (*) or highly significant at $P<.001$ (**).

Results

Experiments conducted during the last decades revealed an approximately 10% higher RBE of proton versus photon irradiation (3). However, the cause for this increased RBE on the physical−chemical and molecular−cellular level is far from clear. To determine the relevance of intact DNA DSB repair machineries to the RBE, clonogenic survival assays were performed in a panel of isogenic CHO cells with known deficiencies in specific DSB repair pathways in response to clinically relevant proton (low-LET, 138 MeV) and photon radiation (19). Exponentially growing cells were exposed to either type of radiation and reseeded 20 hours after irradiation to determine clonogenic survival. Before reseeding, cells were recounted and analyzed for cell cycle distribution. No type of radiation-related differences in cell cycle distribution and amount of cells were observed (Supplementary Figs. e1-e3, available online). At 37% and 10% clonogenic cell survivals, all cells were more sensitive to proton versus photon irradiation, with an RBE_{37} and RBE_{10} of 1.25 ± 0.05 and 1.29 ± 0.04, respectively. As expected, the HR-deficient cell line Irs1sf, which lacks XRCC3, displayed increased hypersensitivity in response to both types of irradiation. Interestingly though, the RBE significantly increased in the HR-deficient cells to an RBE_{37} and RBE_{10} of 1.54 ± 0.1 and 1.44 ± 0.06, respectively (Fig. 1, Table 1).

To confirm enhanced sensitivity of HR-mutated cells to proton versus photon irradiation, clonogenic survival assays were performed in cells lacking the HR-related key factor Rad51. Chinese

Table 1 Relative biological effectiveness (RBE) values at 37% and 10% clonogenic survival after proton and photon irradiation

% Survival	Parameter 1	Parameter 2	*P*
	HR-WT log	HR-/- log	
37	1.25 ± 0.05	1.54 ± 0.10	.02
10	1.29 ± 0.04	1.44 ± 0.06	.03
	HR-WT plateau	HR-/- plateau	
37	1.27 ± 0.08	1.26 ± 0.08	.98
10	1.29 ± 0.03	1.27 ± 0.03	.99
	HR-WT siLuc	HR-WT siRad51	
37	1.32 ± 0.06	1.67 ± 0.07	.03
10	1.32 ± 0.02	1.52 ± 0.04	.03
	NHEJ-WT log	NHEJ-/- log	
37	1.32 ± 0.12	1.08 ± 0.07	.11
10	1.20 ± 0.05	1.09 ± 0.08	.38
	NHEJ-WT plateau	NHEJ-/- plateau	
37	1.27 ± 0.06	1.33 ± 0.05	.31
10	1.25 ± 0.03	1.32 ± 0.05	.21
	NER-WT log	NER-/- log	
37	1.25 ± 0.05	1.41 ± 0.12	.14
10	1.29 ± 0.04	1.28 ± 0.06	.62

Abbreviations: HR = homologous recombination; NER = nucleotide excision repair; NHEJ = nonhomologous end-joining; WT = wild-type.
The RBE values were calculated with the α and β values derived from the survival curves, as explained in the Methods and Materials section.

hamster ovary wild-type cells (AA8) were transfected with either a control siRNA (siLuc) or siRNA targeting the Rad51 recombinase (Supplementary Fig. e4) and irradiated with increasing doses of ionizing radiation. Both siLuc- and siRad51-transfected cells were more sensitive to proton than to photon irradiation, but the RAD51 knockdown cells were significantly more sensitive to proton irradiation (RBE_{37} and RBE_{10} of 1.32 ± 0.06 and 1.32 ± 0.06 for the siLuc-transfected cells versus RBE_{37} and RBE_{10} of 1.67 ± 0.07 and 1.52 ± 0.04 for the siRad51-transfected cells) (Fig. 1C).

Homologous recombination requires an intact sister chromatid and is therefore only active during S and G2 phases of the cell cycle (9, 20). Thus, confluent (plateau phase) cells, which are arrested in the G0/G1 phase of the cell cycle, primarily depend on NHEJ for efficient DSB repair. Wild-type and HR-deficient cells were grown to confluence, and clonogenic survival was determined in response to proton and photon irradiation. Overall, confluent cells were less radiosensitive than their proliferating counterpart cells. A slightly enhanced radiosensitivity remaining in the HR-deficient cell population under these conditions might be due to the small percentage of cells slipping into S/G2 phase (Fig. 1B; see Supplementary Fig. e5 for cell cycle distribution). Interestingly, under these conditions, the differentially enhanced sensitivity of HR-deficient cells to proton irradiation was absent, supporting a critical role of HR-mediated repair of proton irradiation-induced lesions in dividing cells (see Table 1 and Supplementary Tables e1 and e2 for RBE values).

Nonhomologous end-joining is the predominant repair pathway for irradiation-induced DSBs in mammalian cells. As expected, DNA-PKcs-deficient CHO cells (XR-C1) were hypersensitive to both types of radiation (Fig. 2A, Table 1). However, compared with the corresponding wild-type cells (CHO9), we could not detect a statistically significant change of the RBE in the NHEJ-deficient cells. The NHEJ-deficient cells were also irradiated in plateau phase. Under these conditions radiosensitivity was further increased toward both types of irradiation but without a significant change of the RBE (Fig. 2B, Table 1).

Lack of nucleotide excision repair has been found not to affect clonogenicity in response to irradiation. As an additional control experiment, clonogenic survival assays were therefore performed with nucleotide excision repair-deficient hamster cells lacking ERCC2 (alias XPD, UV-5) (21, 22). No statistically significant change of the RBE was observed in the nucleotide excision repair-deficient but otherwise isogenic CHO cells in comparison with the wild-type cells (Fig. 2C).

These results suggest a specific DNA repair machinery–dependent treatment response and point to a differential DNA damage complexity or amount of DNA damage after proton versus photon irradiation. To test for the amount of initial DSBs, γH2AX foci were quantified in an RBE-independent approach 12 minutes after irradiation (1 Gy) with the 2 types of ionizing radiation. At this early time point, we could not detect any significant differences in the amount of γH2AX foci per cell induced by the 2 types of irradiation and in the different cell lines (Fig. 3A). Thus, according to the numbers of irradiation-induced γH2AX foci, enhanced proton sensitivity is unlikely to be due to an increased number of DSBs induced by proton versus photon irradiation.

Ultimately it is the amount of residual DNA damage misrepaired or left unrepaired that affects treatment outcome in response to irradiation. Therefore, we analyzed levels of γH2AX foci per cell over a 24-hour time course in the different cell lines in response to 1 Gy of ionizing radiation (Fig. 3B) (20, 23-25). Repair kinetics in the wild-type cell lines were identical in response to both proton and photon irradiation. As expected, γH2AX focus removal was delayed in both HR- and NHEJ-deficient cell lines, with only 20-30% of γH2AX foci disappearing during the initial time period. Remarkably, however, delayed disappearance of γH2AX foci was most prominent in the HR-deficient cells in response to proton irradiation, at all time points measured (Fig. 3B for 1 Gy), with 45% of γH2AX foci still being detectable 24 hours after proton irradiation (compared with 27% after photon irradiation). Cell cycle analysis at 6, 12, and 24 hours after irradiation displayed no difference in cell cycle distribution for the HR-mutated cells in response to the 2 types of radiation (Supplementary Fig. e3). In contrast, the kinetic profile of γH2AX focus disappearance in NHEJ-mutated cells was indistinguishable between photon and proton irradiation (Fig. 3B) (20, 23). It is important to note that the very low levels of γH2AX foci after 24 hours are due to the fact that only intact and not already cell death-related, fragmented nuclei were considered.

To further investigate a differential requirement for competing DSB repair systems in response to proton versus photon irradiation, foci kinetics of the major constituents of HR (Rad51) and NHEJ (pDNA-PKcs) were determined (Supplementary Fig. e6). We observed a significant increase in Rad51 foci in DNA-PKcs-deficient cells in response to both irradiation treatments compared with wild-type cells. This was most likely due to the absence of NHEJ, which would normally compete with HR for the recognition and repair of DSBs (8). In HR-deficient cells, pDNA-PKc foci persisted much longer in response to both types of irradiation, which may indicate problems for DNA-PKcs to deal with a certain class of DNA damage. Furthermore, only minimal differences in DNA damage signalling in response to the 2 sources of irradiation could be detected in both wild-type and HR-deficient cells

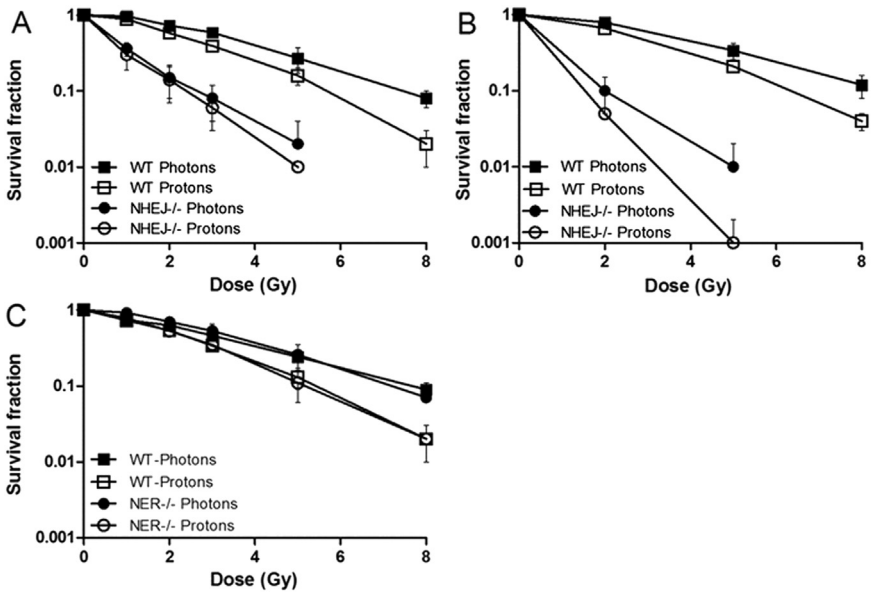

Fig. 2. Clonogenic cell survival of proton- and photon-irradiated cell lines. Chinese hamster ovary wild-type (WT) cells (CHO9) and corresponding nonhomologous end-joining (NHEJ)-deficient cells (DNA-PKcs-/-) were irradiated in exponential growth phase (A) and in plateau phase (B). Chinese hamster ovary wild-type (AA8) cells and corresponding nucleotide excision repair (NER)-deficient (UV-5; ERCC5-/-) cells were irradiated in exponential growth phase (C). Data were pooled from at least 3 independent experiments. Points represent mean ± SD.

(Supplementary Fig. e6C; see also Supplementary Figs. e7-e9 for representative images of irradiation-induced γH2AX, Rad51, and pDNA-PKc foci).

Quantification of residual chromosomal aberrations in wild-type and HR-deficient cells (at 2 Gy) revealed a slightly enhanced total amount of chromosomal aberrations in the HR-deficient cells in response to both types of irradiation. Proton irradiation resulted primarily in more fragments, especially in the HR-deficient cells (Fig. 4; see also Supplementary Fig. e11 for NHEJ-deficient cells). As previously described by Natarajan et al (26) for these cell lines in response to photon irradiation, we also observed a shift from chromosome- to more chromatid-type aberrations in HR-deficient

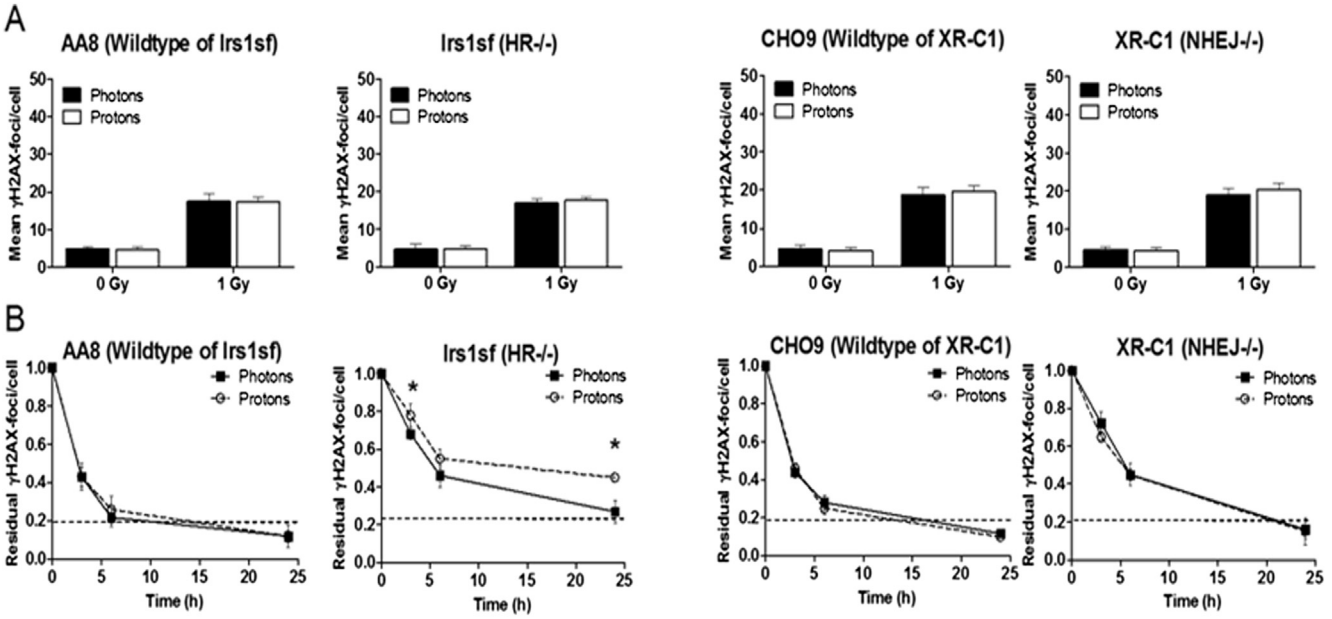

Fig. 3. Quantification of initial and residual γH2AX foci after proton and photon irradiation with 1 Gy. (A) Initial amount of γH2AX foci in Chinese hamster ovary wild-type cells (AA8, CH9) and corresponding homologous recombination (HR)-deficient (Irs1sf) and nonhomologous end-joining (NHEJ)-deficient (XR-C1) cells, detected 12 minutes after irradiation (n = 5, mean ± SD). (B) Residual amount of γH2AX foci 3, 6, and 24 hours after irradiation. The initial amount of foci is set as 1; the dotted line indicates the background level of γH2AX foci in unirradiated cells; n = 3, mean ± SD. *$P < .05$.

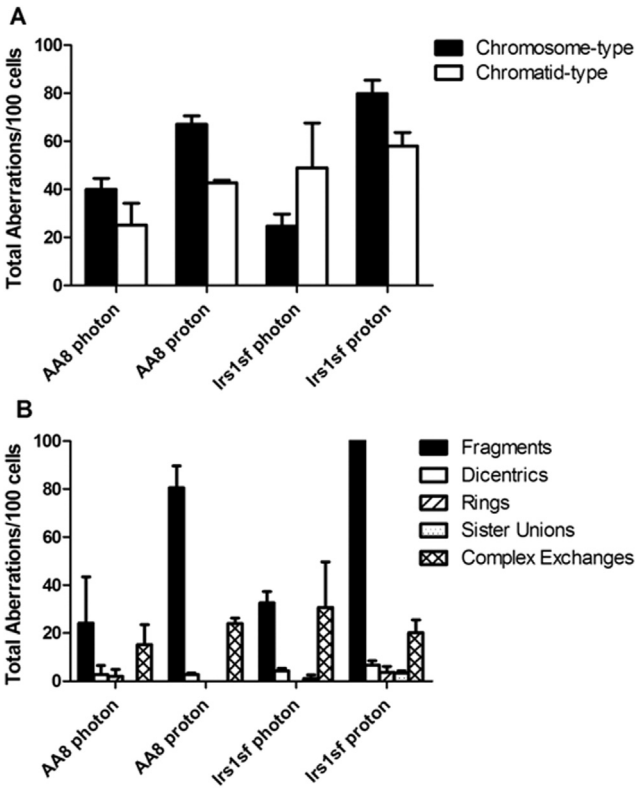

Fig. 4. Chromosomal aberrations after proton and photon irradiation with 2 Gy in wild-type and homologous recombination-deficient cells. (A) Chromosomal aberrations grouped into chromosomal-type and chromatide-type aberrations, and (B) amounts of fragments, dicentrics, rings, sister unions, and complex exchanges abundant in 100 cells 24 hours after irradiation.

cells. After proton irradiation the amount of chromatid-type aberrations increased even further in the HR-deficient cells but was still lower than the amount of chromosome-type aberrations, which include the high level of proton irradiation-induced fragments.

Discussion

To the best of our knowledge, our study is the first to investigate a differential requirement of the 2 major DSB repair pathways in response to proton versus photon irradiation using accepted models of genetically defined, isogenic wild-type cells and mutants thereof with defined defects in the different DNA repair systems (13-15). Overall, clonogenic survival in the wild-type cell lines was lower in all proton-irradiated in comparison with photon-irradiated cells, which is consistent with the well-known RBE of high-energy, sparsely ionizing protons (1, 3, 5, 27-29). Of note, the RBEs determined in these in vitro studies are in general higher than the generically used RBE value of 1.1 used for clinical studies (3). This is mainly caused by the cell lines and endpoints chosen in these studies and does not necessarily point to a difference between in vivo and in vitro response. Clinically, this generic RBE value is used because it represents a reasonable average over various endpoints.

Proliferating cells lacking HR proteins were even more sensitive to proton than to photon irradiation than their corresponding wild-type cells, which also translated into a further increase in RBE_{37} and RBE_{10} for the HR-deficient cells. On the other hand, DNA-PKcs-deficient cells with compromised NHEJ did not display enhanced proton sensitivity. These results suggest an enhanced dependence of a part of proton-induced DNA DSBs on HR, which might become relevant for clinical stratification of patients carrying mutations in specific DNA damage response pathways. Future studies will determine this HR-dependent shift of the RBE in other cell line systems and in animal tumor models.

Proton irradiation resulted in more lethal DNA aberrations than photon irradiation, even though the initial amount of DNA DSB marks were in the same range. These results suggest that the spatial distribution or the quality of the DNA damage is different after proton versus photon irradiation, which eventually could result in primarily increased levels of fragments and lethal chromosomal rearrangements. Increased amounts of small DNA fragments could enhance chromosome deletions and cell death.

Within a clinically relevant SOBP the LET varies only modestly. However, experiments with radioresistant melanoma cells revealed an increased RBE across the SOBP (30), which might be due to a slight increase of LET across the SOBP, and corresponds to enhanced cell killing per gray of irradiation as LET increases (30). We cannot exclude that this minimal enhanced LET contribution within the multiple near-monoenergetic proton beams might shift the DNA damage profile also relevant for this study.

Interestingly, enhanced HR dependence was only observed in proliferating cells. Thus, despite the lack of an intact HR machinery, confluent, plateau phase cells can sufficiently cope with proton-induced DNA damage, most probably owing to enhanced potentially lethal damage repair (31).

Nonhomologous end-joining and HR might compete with each other, particularly during S/G2 phase, but there are also data suggesting that initial, fast repair of DNA DSBs is carried out by NHEJ, whereas the more time-demanding HR occurs at a later stage (32, 33). This model also suggests that in mammalian cells, NHEJ first attempts to repair DSBs but grants access for the HR machinery in case rejoining does not rapidly proceed (15, 34). Interestingly, the slow repair kinetic in HR-defective cells indicates continuing checkpoint signaling and DNA repair at these sites. These different phenotypes might indeed result from an initial but unsuccessful attempt of NHEJ to repair all proton irradiation-induced DSBs.

Overall, our studies demonstrate that the major DNA DSB machineries are challenged in a differential way after proton and photon irradiations. Our data suggest that the overall DNA damage is different at least to a certain extent, requiring preferentially homologous recombination after proton irradiation. Future studies will specifically investigate whether these differential requirements can be exploited and will translate into biology-based rationales to choose between proton- and photon-based radiation therapy.

References

1. Raju MR, Amols HI, Bain E, et al. A heavy particle comparative study. Part III: OER and RBE. *Br J Radiol* 1978;51:712-719.
2. De Ruysscher D, Mark Lodge M, Jones B, et al. Charged particles in radiotherapy: A 5-year update of a systematic review. *Radiother Oncol* 2012;103:5-7.
3. Paganetti H, Niemierko A, Ancukiewicz M, et al. Relative biological effectiveness (RBE) values for proton beam therapy. *Int J Radiat Oncol Biol Phys* 2002;53:407-421.

4. Raju MR. Proton radiobiology, radiosurgery and radiotherapy. *Int J Radiat Biol* 1995;67:237-259.
5. Green LM, Murray DK, Bant AM, et al. Response of thyroid follicular cells to gamma irradiation compared to proton irradiation. I. Initial characterization of DNA damage, micronucleus formation, apoptosis, cell survival, and cell cycle phase redistribution. *Radiat Res* 2001;155: 32-42.
6. Hada M, Sutherland BM. Spectrum of complex DNA damages depends on the incident radiation. *Radiat Res* 2006;165:223-230.
7. Manti L, Durante M, Grossi G, et al. Measurements of metaphase and interphase chromosome aberrations transmitted through early cell replication rounds in human lymphocytes exposed to low-LET protons and high-LET 12C ions. *Mutat Res* 2006;596:151-165.
8. Shrivastav M, Miller CA, De Haro LP, et al. DNA-PKcs and ATM co-regulate DNA double-strand break repair. *DNA Repair (Amst)* 2009;8: 920-929.
9. Hiom K. Coping with DNA double strand breaks. *DNA Repair (Amst)* 2010;9:1256-1263.
10. Pardo B, Gomez-Gonzalez B, Aguilera A. DNA repair in mammalian cells: DNA double-strand break repair: How to fix a broken relationship. *Cell Mol Life Sci* 2009;66:1039-1056.
11. Goetz JD, Motycka TA, Han M, et al. Reduced repair of DNA double-strand breaks by homologous recombination in a DNA ligase I-deficient human cell line. *DNA Repair (Amst)* 2005;4:649-654.
12. Lieber MR. The mechanism of double-strand DNA break repair by the nonhomologous DNA end-joining pathway. *Annu Rev Biochem* 2010; 79:181-211.
13. Hinz JM, Yamada NA, Salazar EP, et al. Influence of double-strand-break repair pathways on radiosensitivity throughout the cell cycle in CHO cells. *DNA Repair* 2005;4:782-792.
14. Kuhfittig-Kulle S, Feldmann E, Odersky A, et al. The mutagenic potential of non-homologous end joining in the absence of the NHEJ core factors Ku70/80, DNA-PKcs and XRCC4-LigIV. *Mutagenesis* 2007;22:217-233.
15. Rothkamm K, Kruger I, Thompson LH, et al. Pathways of DNA double-strand break repair during the mammalian cell cycle. *Mol Cell Biol* 2003;23:5706-5715.
16. Pedroni E, Bacher R, Blattmann H, et al. The 200-Mev proton therapy project at the Paul-Scherrer-Institute: Conceptual design and practical realization. *Med Phys* 1995;22:37-53.
17. Franken NA, Rodermond HM, Stap J, et al. Clonogenic assay of cells in vitro. *Nat Protoc* 2006;1:2315-2319.
18. Staab A, Zukowski D, Walenta S, et al. Response of Chinese hamster v79 multicellular spheroids exposed to high-energy carbon ions. *Radiat Res* 2004;161:219-227.
19. Thacker J, Zdzienicka MZ. The mammalian XRCC genes: Their roles in DNA repair and genetic stability. *DNA Repair* 2003;2:655-672.
20. Jeggo PA, Geuting V, Lobrich M. The role of homologous recombination in radiation-induced double-strand break repair. *Radiother Oncol* 2011;101:7-12.
21. Friedberg EC. How nucleotide excision repair protects against cancer. *Nat Rev Cancer* 2001;1:22-33.
22. Thompson LH, Rubin JS, Cleaver JE, et al. A screening method for isolating DNA repair-deficient mutants of CHO cells. *Somatic Cell Genet* 1980;6:391-405.
23. Shibata A, Conrad S, Birraux J, et al. Factors determining DNA double-strand break repair pathway choice in G2 phase. *EMBO J* 2011;30:1079-1092.
24. Klokov D, MacPhail SM, Banath JP, et al. Phosphorylated histone H2AX in relation to cell survival in tumor cells and xenografts exposed to single and fractionated doses of X-rays. *Radiother Oncol* 2006;80:223-229.
25. Olive PL. Retention of gammaH2AX foci as an indication of lethal DNA damage. *Radiother Oncol* 2011;101:18-23.
26. Natarajan AT, Berni A, Marimuthu KM, et al. The type and yield of ionising radiation induced chromosomal aberrations depend on the efficiency of different DSB repair pathways in mammalian cells. *Mutat Res* 2008;642:80-85.
27. Allen C, Borak TB, Tsujii H, et al. Heavy charged particle radiobiology: Using enhanced biological effectiveness and improved beam focusing to advance cancer therapy. *Mutat Res* 2011;711:150-157.
28. Gueulette J, Gregoire V, Octave-Prignot M, et al. Measurements of radiobiological effectiveness in the 85 MeV proton beam produced at the cyclotron CYCLONE of Louvain-la-Neuve, Belgium. *Radiat Res* 1996;145:70-74.
29. Gueulette J, Blattmann H, Pedroni E, et al. Relative biologic effectiveness determination in mouse intestine for scanning proton beam at Paul Scherrer Institute, Switzerland. Influence of motion. *Int J Radiat Oncol Biol Phys* 2005;62:838-845.
30. Petrovic I, Ristic-Fira A, Todorovic D, et al. Response of a radioresistant human melanoma cell line along the proton spread-out Bragg peak. *Int J Radiat Biol* 2010;86:742-751.
31. Rasey JS, Nelson NJ. Repair of potentially lethal damage following irradiation with X rays or cyclotron neutrons: Response of the EMT-6/uw tumor system treated under various growth conditions in vitro and in vivo. *Radiat Res* 1981;85:69-84.
32. Mao Z, Bozzella M, Seluanov A, et al. DNA repair by nonhomologous end joining and homologous recombination during cell cycle in human cells. *Cell Cycle* 2008;7:2902-2906.
33. Mladenov E, Kalev P, Anachkova B. The complexity of double-strand break ends is a factor in the repair pathway choice. *Radiat Res* 2009; 171:397-404.
34. Jeggo P, Lobrich M. Radiation-induced DNA damage responses. *Radiat Prot Dosimetry* 2006;122:124-127.

3.2 Differential Requirement for Homologous Recombination Repair and Non-Homologous End Joining after High-Energy Proton and Photon Irradiation

Andrea O. Fontana[1], Marc A. Augsburger[1], Alessandro A. Sartori[2], Anthony J. Lomax[3], Nicole Grosse[2] and Martin N. Pruschy[1]

[1] Department of Radiation Oncology, University Hospital Zurich, Zurich, Switzerland
[2] Institute for Molecular Cancer Research, University of Zurich, Zurich, Switzerland
[3] Paul Scherrer Institute, Villigen, Switzerland

Status of the manuscript: Submitted to International Journal of Radiation Oncology, Biology, Physics.

Author contribution A.O. Fontana:
Planning, data acquisition at USZ and PSI, analysis and interpretation of the experiments, manuscript drafting, revision and editing.

Abstract:

Purpose:
A 10% higher efficacy of proton- versus photon irradiation (IR) is already implemented in the clinics. However little is known about the radiobiology of the relative biological effectiveness (RBE). Non-homologous end-joining (NHEJ) and homologous recombination repair (HRR) both contribute to promote the repair of radiation-induced DNA double strand breaks (DSBs). We previously investigated this higher efficacy of proton-irradiation in genetically-defined Chinese hamster ovary cells and observed that HRR-deficient, but not NHEJ-deficient cells were significantly more sensitive to proton-IR than to photon-IR when compared to their wild-type cells. We have now investigated the impact of the two major DNA repair machineries for cellular survival of human tumor cells in response to irradiation with the two types of ionizing radiation.

Methods and Materials:
In this study, DNA-repair and cell survival endpoints were analyzed in wildtype, homologous recombination (HR)-deficient and non-homologous end joining (NHEJ)-deficient cells after irradiation with clinically relevant, high-energy protons (136 MeV) and 200 keV photons.
We further analyzed DNA damage repair and cell survival endpoints in the non-small cells lung cancer (NSCLC) cell line A549 with compromised HRR- and NHEJ-repair and the effect of the DNA-PKcs inhibitor NU7026 in response to both types of ionizing radiation.

Results:
A549 cells depleted of DNA-PKcs were equally sensitive to both types of ionizing radiation (RBE_{10}=0.94), whereas transient inhibition by the DNA-PKcs-inhibitor NU7026 strongly radiosensitized the DNA-PKcs-proficient A549 and M059K cell lines to photon, but to a much lower extent to proton irradiation (DMF_{10}=1.91 vs 1.49 for A549 cells). Interestingly, we observed a reduced phosphorylation of DNA-PKcs at ser-2056 and thr-2609 clusters after proton irradiation, compared to photon radiation. In contrast, A549 cells depleted of the RAD51 recombinase (HRR) were markedly hypersensitive to proton radiation in comparison to control cells (RBE_{10}=1.27 vs 1.0). Likewise, human BRCA2-deficient cells (PEO1), but not the DNA-PKcs-deficient cells (M059J) were markedly hypersensitive towards proton irradiation.

Conclusion:
Our data demonstrate an enhanced susceptibility of HRR-deficient cancer cells to proton radiation, due to a compromised capability of the DNA-PK-dependent NHEJ pathway in repairing proton-induced damages, resulting in an enhanced RBE. This might become relevant for clinical stratification of patients carrying mutations in the DNA damage response pathways and for combined treatment modalities with specific inhibitors of the two major DNA repair machineries to be selectively used with either photon- or proton-based radiotherapy.

Introduction:

Currently, a generic RBE value of 1.1 is used in the clinic for proton radiotherapy. This value however does not always reflect the sensitization observed at the tissue or cellular level [1-5]. Reasons for this variable RBE may be several, including a different type of damage or involvement of DNA repair machineries, but only a limited number of studies have been performed to understand these differences in detail at the cellular and molecular level. Ionizing radiation is usually regarded as a prototypic double-strand break (DSB)-producing agent. Unrepaired DBS can be lethal for the cell, by causing chromosomal rearrangements ultimately leading to cell death [6-7]. Cells have evolved two major pathways to cope with DNA damage and genome integrity, namely homologous recombination repair (HRR) and non-homologous end joining (NHEJ) [8-9]. HRR is a slow process, primarily active through the S/G_2-phase of the cell cycle and results in preserved sequence integrity. First, damage recognition by the Mre_{11}-RAD_{50}-NBS_1 (MRN) complex initiate the CtIP-dependent DNA end resection [10]. The single-strand DNA (ssDNA) is first bound by RPA, thus preventing the ssDNA from forming secondary structures [11]. Thereafter, the nucleoprotein binds to RAD51 and its accessory factors to initiate search for homologous sequence in sister chromatids to form Holliday Junctions. Finally, resolution of the heteroduplex by several helicases takes place [12]. Non-homologous end joining can be divided in *canonical* and *alternative* NHEJ. Canonical-NHEJ (cNHEJ, also called Ku-dependent EJ) is active throughout the cell cycle, and is responsible for the repair of most IR-induced DSBs in eukaryotic cells, other than being involved in V(D)J recombination [13-15]. Although very efficient in a quantitative way, the quality of repair can steadily decrease by increasing amount of DNA damage [16]. It consists primarily on three steps: first, DNA break recognition by the Ku70/Ku80 heterodimer, which in turn recruits DNA-PKcs to form the DNA-PK complex (called, together with DNA, the synaptic complex) [17]. This binding step is followed by DNA processing to remove non-ligatable ends by several enzymes, including Artemis, MRN and several DNA polymerases.

End processing promotes the kinase activity of DNA-PKcs, leading to its autophosphorylation and release of the autophosphorylated catalytic subunit from the synaptic complex [18]. Finally, the XRCC4-DNA Ligase IV complex will relegate the two broken ends [19].

Alternative EJ (aEJ) has recently been identified as a Ku80- or DNA-PKcs-independent pathway [20-22] and requires $PARP_1$, MRN and LIG3 for break recognition, processing and ligation [23]. It is usually associated with deletions at repair junctions, and thus with high mutagenic potential. Several studies using pulsed field gel electrophoresis or γH2AX as DNA damage markers indicate that either the initial amount or the quality of the initial DNA damage caused by irradiation of different linear energy transfer (LET), including protons, may be different [24-26]. These high-LET radiations generate complex DNA damages, called *cluster damages*, are opposite to single isolated damages, which are typical for very low-LET photon radiation and can be generally readily repaired by the cell. As the LET increases the number of induced DSB/track traversal and the complexity of the break also increases, potentially leading to damages which are usually resistant to repair or can be repaired but with a strong mutagenic potential [27-28]. Recently, a differential involvement of these two major pathways after particle irradiation has been described. Particularly, it has been showed that high-LET particle radiation interferes with the Ku-dependent EJ, but not with HRR pathway [29-32]. This is probably due to the combined effect of high-LET radiation producing coordinated ionizing events along the path resulting in very small DNA fragments, and the inability of the Ku70/Ku80 heterodimer to efficiently bind these fragments, therefore preventing NHEJ to properly function.

In this report we now investigate the treatment response to high energy, low-LET proton (136 MeV) and photon (200 KeV) irradiation in an accepted model of genetically-defined cells with defects in one of the major DNA repair systems. We have now shown that cells with compromised HRR are more sensitive to treatment with low-LET hadron therapy compared to photon therapy, whereas cells with compromised NHEJ are equally sensitive to both low-LET proton and photon radiation.

Materials and Methods:

Cell lines. The human non-small cell lung cancer cell line A549 and the triple-negative breast cancer cell line MDA-MB-231 were obtained from ATCC and cultured in RPMI cell culture media supplemented with 10% FBS, glutamine (2mM) and penicillin-streptomycin (100U/ml-100μg/ml). The glioblastoma cell lines M059K and M059J were kindly provided by Prof P. O'Neil (Oxford University, UK) and maintained in 1:1 MEM/F12 Ham's mixture supplemented with 10% FBS, glutamine (2mM) and penicillin-streptomycin (100U/ml-100μg/ml). The Ovarian cancer cell lines PEO4 and PEO1 were purchased from the Health Protection Agency Culture Collections **(**Salisbury, UK) and maintained in RPMI cell culture media supplemented with 10% FBS, glutamine (2mM), sodium pyruvate (2mM) and penicillin-streptomycin (100U/ml-100μg/ml). All cells were kept at 37°C and 5% CO_2 atmosphere.

Drug Treatment. NU7026 [10μM] and KU60019 [1μM] were added to the cells 1 h prior to irradiation. Vorinostat [2μM] was added 24 h prior to irradiation. All chemicals were purchased from Selleckchem (Huston TX, USA) and dissolved in DMSO.

Antibodies. The following antibodies were used at the specified dilutions: rabbit monoclonal anti- H2AX-pSer139 (1:200 immunofluorescence, IF - Abcam, Cambridge, UK); rabbit monoclonal anti- H2AX-pSer139 (1:1000 western blot, WB - Cell Signaling, Boston MA, USA); rabbit monoclonal anti-RPA32 (1:1000 IF or 1:2000 WB - Bethyl Science, Bethesda, USA); rabbit polyclonal anti-DNA-PKcs-pS2056 (1:100 (IF) or 1:1000 (WB) - Abcam, Cambridge, UK); mouse monoclonal anti-DNA-PKcs-pT2609 (1:200 (IF) - Abcam, Cambridge, UK); mouse monoclonal anti-DNA-PKcs (1:500 (WB) - Abcam, Cambridge, UK); rabbit polyclonal anti-53BP1 (1:200 (IF) - Cell Signaling, Boston MA, USA); mouse anti-ATM-p1981(1:100 (IF) or 1:2000 (WB) - Abcam, Cambridge, UK); mouse anti-ATM (1:2000 (WB) - Abcam, Cambridge, UK); mouse monoclonal anti-RAD51 (1:100 (IF) or 1:500 (WB) -

Novus Biological, A-8 Littleton CO, USA); mouse monoclonal anti-Ku80 (1:1000 (WB) - Abcam, Cambridge, UK); mouse monoclonal anti-BRCA1 (1:1000 (WB) - Abcam, Cambridge, UK); mouse monoclonal anti-β-actin (1:1000 (WB) - Sigma-Aldrich, St. Louis MO, USA).

Irradiation procedures. To irradiate exponentially growing cell cultures, $1.5x10^5$ cells were plated into 25 cm^2 TPP flasks 24 hours prior to irradiation (IR). Photon irradiation was performed using a Gulmay 200 kV X-ray unit at 1 Gy/min (kVp = 200kV; Amperage=15mA, HVL = 1.03mm Cu, Filter: 1mm Al and 0.45mm Cu). Proton irradiation was delivered using spot scanning technique at the Paul Scherrer Institute [33]. The maximal instantaneous dose rate at the Bragg peak is 4Gy/s; however cells were placed in the center of the Spread-Out-Bragg-Peak (SOBP), with a length of 5 cm and maximum proton energy of 138 MeV. The LET was estimated at 2 KeV/μM in the center of the SOBP. The field size was orthogonal to the beam with an area of 15x11cm. Dosimetry of the field was performed using both small diameter cylindrical ionization chambers (active volume 0.3cm3) and a Farmer NE2571 ionization chamber using the IAEA TRS-398 protocol.

Clonogenic survival. Twenty hours following irradiation, cells were trypsinized and single cell suspensions were seeded into 10cm-petri dishes. The number of plated cells per dish was adjusted to obtain approx. 50-100 colonies under all experimental conditions. After colony formation (depending on cell lines, between 7-21 days), colonies were fixed (methanol/acetic acid; 3:1) and stained with 2% crystal violet. Colonies were then counted manually.
In order to calculate RBE and DMF values, α- and ß-values for each survival curve were determined. Survival data were fitted by weighted, stratified, linear regression to obtain the linear and quadratic parameters. Linear regression was performed in SPSS (Version 23) as described in [34]. RBE and DMF values at the 10 % survival level (termed RBE_{10} and DMF_{10}) were calculated according to [35].

siRNA Transfection. Transfection of A549 cells was performed one or two days before plating for irradiation, according to the specific siRNA. Cells were irradiated 48 or 72 h after transfection. siRNAs were used at a concentration of 20 nM (siDNA-PK_{cs}) or 40 nM (siRAD51) with 1.7 µL/ml Lipofectamin RNAiMAX (Invitrogen). The following siRNA sequences were used: siLuc: 5'-CGTACGCGGAATACTTCGAdTdT-3'**.**
siRad51: 5'-GAGCUUGACAAACUACUUCdTdT-3'.
siDNA-PK_{cs}, Dharmacon SMARTpool against human PRKDC (GE Healthcare).

Immunofluorescence microscopy. 24 hours prior to irradiation cells were plated onto Ibidi µ-slides $VI^{0.4}$ (Ibidi, Munich) at the same cell density as used for clonogenic survival assay. At the desired time points, cells were washed twice with PBS, fixed with 4% formaldehyde/PBS for 10 min, washed with PBS (4 x 5min) and stored at 4°C until further staining. Cells were permeabilized for 5 min with 0.5% ice cold Triton-X-100/PBS, blocked for at least 20 min with 1% BSA, followed by 1h incubation with the selected primary antibody (diluted in 1%BSA/PBS). After washing with 1%BSA/PBS (3 x 10min), cells were incubated with the appropriate secondary antibody diluted 1:1000 in 1%BSA/PBS (Alexa-488 or/and Alexa-546; Invitrogen), washed with 1%BSA/PBS (2 x 10min) followed by PBS (1 x 10min) and incubated with DAPI/Methanol (1µg/ml) for 3 min. Cells were then mounted in Ibidi mounting Medium (Ibidi, Munich) and stored at 4°C. Slides were examined with a Leica SP5 confocal microscope and a Leica DFC 350 FX camera. Merged z-stacks (z=0.49µm) were analyzed with LAS AF Lite software (Leica, free-version). At least 50 cells per condition were analyzed.

Western blotting. At the indicated time points cells were collected by scratching them on ice for 5 min, counted, and lysates were prepared with about 10 µL Laemmli-buffer/45'000 cells (2% SDS, 10% glycerol, 0.004% bromphenol blue, 62.5 mM Tris-HCl, pH 6.8). After scratching and collection of the lysates, they were frozen on dry ice and stored at -20°C until

analysis. An equal amount of protein was subjected to SDS-PAGE to separate the proteins. Due to the different sizes of the proteins different grades of acrylamide polymerization were used (ATM, DNA-PKcs and BRCA1: 7.5% SDS-gel/ γH2AX, RAD51, RPA32, Ku80: 12% SDS-gel). Proteins were blotted from the SDS-gel onto Amersham Hybond-P polyvinylidene difluoride membranes. Depending on the molecular mass of the protein of interest, the time for transfer was different (> 150 kDa = over-night, 30 V at 4°C/ < 15 0 kDa = 1 h, 60V at 4°C). Membranes were blocked for 1 h with 5% milk /TBS. Antibodies were diluted in 5% milk/TBS. Primary antibody detection was achieved by enhanced chemiluminescence using a corresponding horseradish peroxidase conjugated second antibody, according to the manufacturer's protocol (Amersham, Freiburg, Germany).

Statistical Analysis. Data were presented as the mean ± standard deviation (SD) of at least three independent experiments. The results were tested for significance using the two-sided unpaired Student's t-test or the Wilcoxon-Mann-Withney-UTest.
Results were considered statistically significant when $p < 0.05$ (*) or highly significant $p < 0.001$ (**).

Results:

In the last years, several reports indicate a differential role for NHEJ and HRR in recognizing and repairing DNA damages induced by low- and high-LET radiation [29, 36]. In NHEJ, after binding of the high-affine Ku70/Ku80 heterodimer to the free DNA ends [37-38], DNA-dependent protein kinase catalytic subunit (DNA-PKcs) is recruited within a few seconds to the DSB site through its interaction with the Ku heterodimer and DNA, forming the synaptic complex. This is followed by its own autophosphorylation at several sites, the two more important being Serine-2056 (called the PQR cluster) and Threonine-2609 (called the ABCDE cluster) [39].

To examine whether high-energy, low-LET proton irradiation (136 MeV) and photon irradiation have a different effect on DNA repair and particularly on DNA-PKcs phosphorylation, we compared the sensitivities of NSCLC A549 cells to proton and photon radiation. We first determined formation of phospho-DNA-PKcs foci using specific antibodies directed against Ser-2056 and Thr-2609 loci. Interestingly, proton irradiation of A549 cells resulted in a reduced activation of DNA-PKcs at both Ser-2056 and Thr-2609 sites, in comparison to DNA-PKcs activation in response to photon irradiation (Fig 1A and B). These results indicated a differential activation and requirement of the Ku-dependent NHEJ DNA repair machinery in response to proton irradiation.

Therefore, we decided to investigate the radiosensitizing effect of the selective DNA-PKcs inhibitor NU7026 in combination with either type of ionizing radiation [40]. This compound reportedly inhibits the PI3-kinase DNA-PKcs with improved selectivity over the ATM and ATR kinases by interfering with the Ser-2056 autophosphorylation site, but not with phosphorylation at Thr-2609, which is ATM-mediated. As expected, NU7026 sensitized A549 cells for both types of irradiation, but interestingly to a much higher extent for photon irradiation. The DMF_{10} was significantly increased after photon irradiation, as compared to proton, with a DMF_{10} of 1.91±0.05 and 1.49±0.06, respectively (Fig 1C).

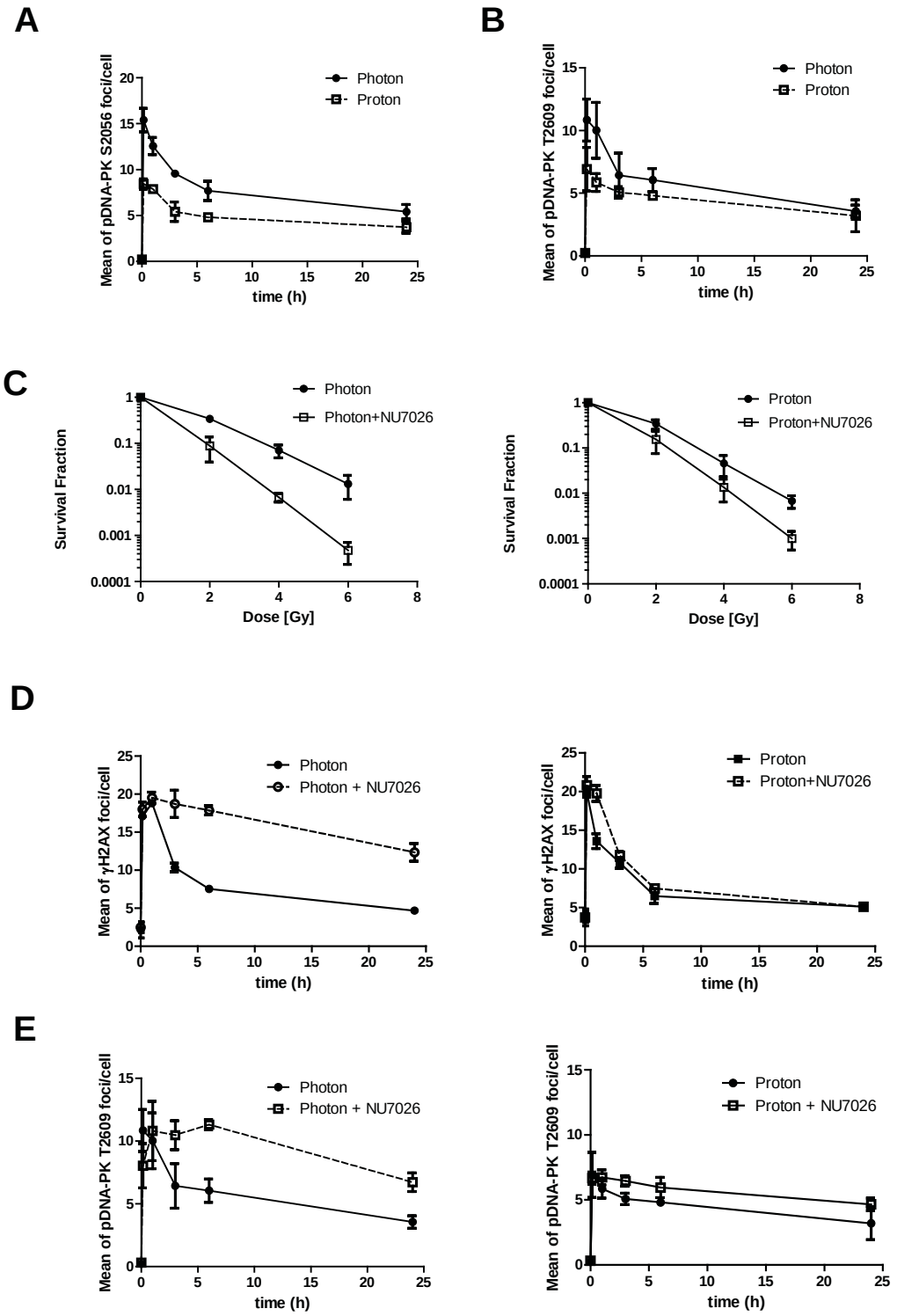

Figure 1. Radiosensitizing effect of NU7026 on A549 cells. Phosphorylation of DNA-PKcs at the Ser-2056 (A) and Thr-2609 (B) cluster sites in response to 1Gy of low-LET proton and photon irradiation. (C) Effect of cellular pretreatment with the selective DNA-PKcs inhibitor NU7026 on A549 cells. Cells were incubated for 1 hour with 10μM NU7026 in DMSO followed by photon and proton irradiation. Kinetics of γH2AX (D) and pDNA-PK (Thr-2609) (E) foci removal after 1Gy of proton and photon irradiation. Cells were treated 1hour prior to irradiation and fixed at the indicated time points.

NU7026 did not further sensitized A549 cells pretransfected with siRNA against DNA-PKcs (siDNA-PKcs-A549) supporting the kinase selectivity of the inhibitor (S2B and S2C).

The amount of DNA damage left unrepaired or misrepaired is a strong determinant of the outcome of ionizing radiation [41-42]. Therefore, we analyzed the levels of several DNA damage markers over a 24 hour time course in response to 1Gy of proton and photon radiation. Treatment of A549 cells with 1Gy of both photon and proton radiation resulted in the same amount of initial γH2AX and 53BP1-foci (S3). Likewise, removal of these foci over time was similar in response to both types of irradiation. As expected, cellular pretreatment with NU7026 strongly delayed γH2AX -foci removal after photon radiation, but surprisingly the time course of γH2AX -foci after proton irradiation was only minimally affected (Fig 1D). The same foci removal pattern was observed with 53BP1-foci (S4). To exclude a possible involvement of a differential cell cycle arrest in response to photon and proton irradiation, cell cycle analysis was performed 18 hours after irradiation with 5 Gy. Cell cycle arrest profiles after both proton and photon irradiation were identical, with most of irradiated cells in G2 (S5). Pretreatment of the cells with NU7026 further increased the amount of cells in G2-arrest, but again no difference was observed between photon and proton irradiation (S2D).

To complement the experiments performed with the small molecular inhibitor of DNA-PKcs, we investigated the effect of downregulating the NHEJ-factor DNA-PKcs in A549 cells. Cells were transfected with either control-siRNA (siLuc) or siRNA targeting the DNA-PK catalytic subunit (Fig 2A). As expected, downregulation of DNA-PKcs also rendered A549 cells more sensitive to ionizing radiation, but interestingly and in comparison to pretreatment with NU7026, we observed a reduction of clonogenic survival in DNA-PKcs-depleted cells to the same extent for both types of ionizing radiation (RBE_{10}=0.94±0.07). The kinetics of γH2AX-focus removal was also equal after photon and proton irradiation in DNA-PKcs-knockdown cells (Fig 2B), even though strongly delayed in comparison to siLuc-treated cells. This can be due to the fact that in cells with compromised NHEJ, HRR is the only active pathway and

usually DSB repair mediated by HRR is a slow process. RPA32-foci resolution analysis showed that siDNA-PKcs-transfected cells had a much slower activation of HRR, compared to control cells (S6).

NU7026 treatment inhibits autophosphorylation at the Ser-2056 site, but it does not alter the phosphorylation at the Thr-2609 site (ABCDE cluster). Therefore, we further analyzed Thr-2609 phosphorylation in response to the DNA-PKcs inhibitor. Similar to γH2AX and 53BP1, we observed a strong delay in pDNA-PKcs (Thr-2609)-foci removal after photon radiation, but the time course of pDNA-PKcs (Thr-2609)-foci after proton irradiation was only minimally affected (Fig. 1E). It is known that inhibition of the DNA-PK catalytic by NU7026 subunit not only leads to a complete blockade of NHEJ, but also of the HRR pathway [43].

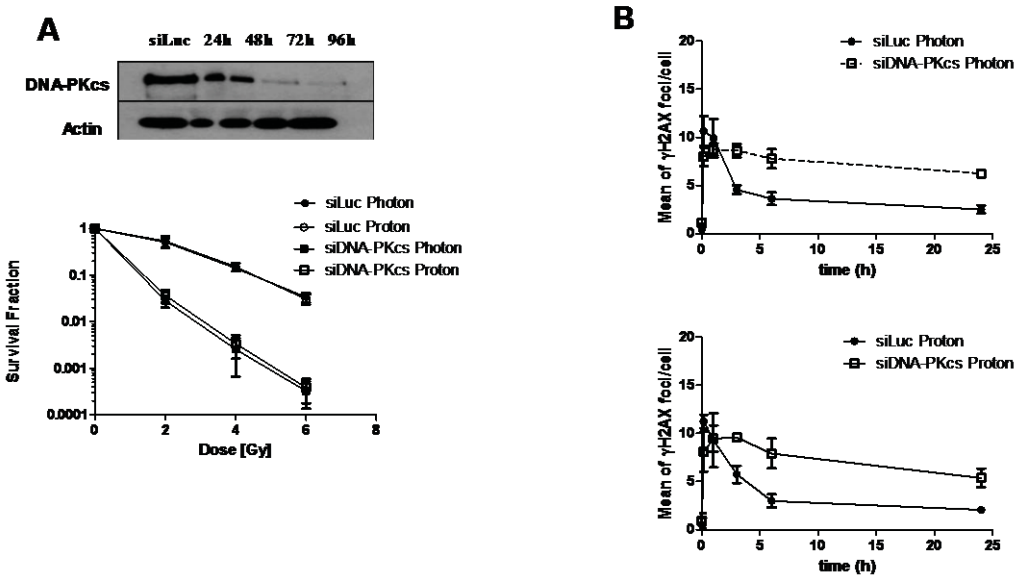

Figure 2. Comparison of low-LET proton and photon radiation-induced cell killing in DNA-PKcs-knockdown A549 cells. (A) DNA-PKcs protein levels of siDNA-PKcs-treated A549 cells, determined at the indicated time points and clonogenic cell survival of proton- and photon-irradiated cell lines either treated with control siRNA (siLuc) or siRNA against DNA-PKcs (siDNA-PKcs). Points represent mean ±SD. (B) Kinetics of γH2AX-foci removal after 1Gy of proton and photon irradiation in siLuc- and siDNA-PKcs-treated cells.

The autophosphorylation step at Ser-2056 is necessary to promote dissociation of the catalytic subunit from the DNA damage site. Inhibition by NU7026 does not allow enzyme dissociation to effectively take place by preventing this step, therefore inhibiting not only further repair by

NHEJ, but also MRN complex, and thus HRR, to promote repair. We assumed that the delay observed in γH2AX-foci repair in NU7026-pretreated cells after photon irradiation would be caused by the DNA-PKcs stuck to DNA damage site, preventing efficient repair by NHEJ and HRR. In contrast, we reasoned that the reduced activation of DNA-PKcs after proton-induced DNA damage, as measured by Ser-2056-foci, would result in a reduced blockade of the DNA damage site by NU7026. This would allow HRR or alternative-EJ to properly repair DNA damage. To eventually detect a differential HRR activation, we analyzed RPA32-foci formation, a known marker for HRR, in absence and presence of NU726 (Fig. 3A and 3B). We observed a time-dependent increase of RPA32-foci formation in these cells 1 hour and 4 hour after photon ionizing radiation. DNA-PKcs inhibition by NU7026 strongly reduced RPA32-foci formation in response to photon irradiation, with only about 35% of foci detectable 4 hour after photon radiation. Proton irradiation induced similar amount of RPA32 foci compared to photon radiation, however foci formation in response to proton irradiation was not affected by cellular pretreatment with the DNA-PKcs inhibitor.

Overall, these results indicate a differential sensitivity to DNA-PKcs inhibition with NU7026 and DNA-PKcs-knockdown in response to photon and proton radiation, respectively. To confirm our results in an additional cell system, we investigated cell survival and the kinetics of γH2AX-focus removal in the DNA-PKcs-deficient cells M059J and their proficient, isogenic counterpart cells, M059K (Fig. 4A and Table 1 and 2) [44]. Similarly to DNA-PKcs-downregulated A549 cells, the DNA-PKcs-deficient cells M059J were equally sensitive to proton and photon radiation (RBE_{10}=0.88±0.05) and the kinetics of γH2AX-focus removal was also equal after photon and proton irradiation in DNA-PKcs-deficient cells. Treatment of the DNA-PKcs proficient cells M059K with NU7026 resulted in a stronger radiosensitizing effect after photon radiation, compared to proton radiation, with a DMF_{10} of 1.49±0.02 and 1.2±0.11, respectively (Fig. 4B and Table 2).

In CHO cells, we have previously demonstrated a differential quality of DNA damage by proton- versus photon-irradiation with a specific requirement for homologous recombination for DNA repair and enhanced cell survival in response to proton irradiation [45]. We reasoned that, in a HRR-deficient system, the reduced dependence on NHEJ repair after proton radiation would result in a complete abrogation of DSB repair, enhancing proton over photon radiosensitisation.

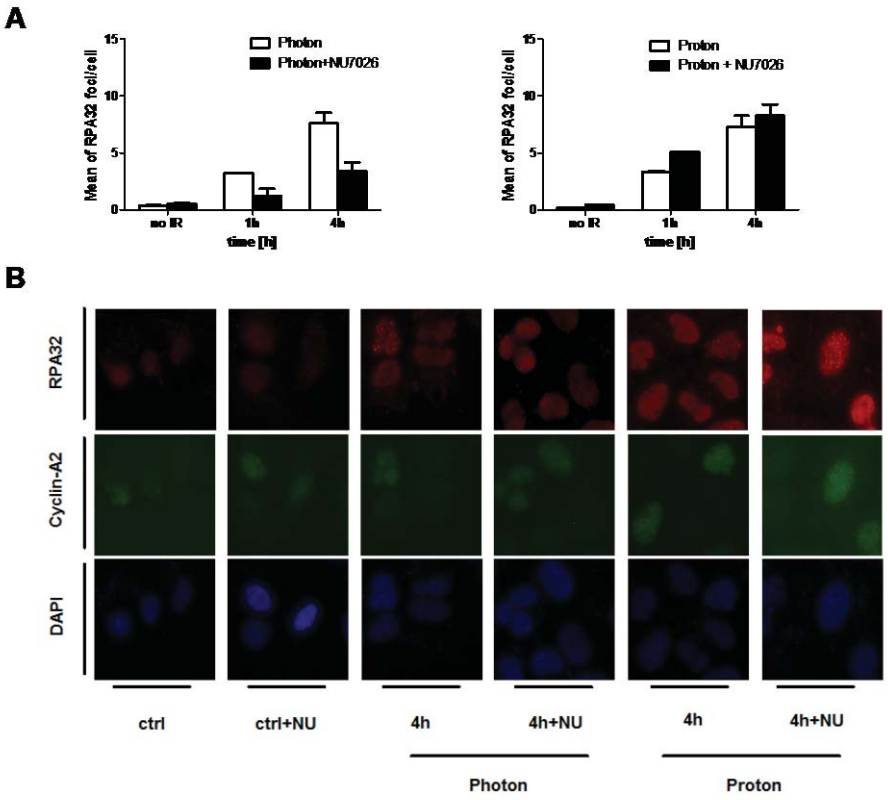

Figure 3. Analysis of RPA32 recruitment in A549 cells pretreated with NU7026. (A) RPA32 foci were determined at 1 hour and 4 hour after radiation with 10Gy. Cells were co-stained for Cyclin-A2 to identify S/G2-phase cells. (B) Representative pictures of RPA32 foci.

We first analyzed RAD51- and RPA32-foci formation in response to proton and photon irradiation, two major components of the HRR pathway, and did not observe any quantitative difference in response to the two types of ionizing radiation (S1A and S1B). To probe the enhanced sensitivity of HRR-mutated cells, we downregulated the key HRR-recombinase RAD51 in A549 cells by siRNA targeting RAD51 (Fig. 5A). A549 cells with siRNA-downregulated

RAD51 (siRAD51-A549) were markedly hypersensitive to proton radiation (RBE_{10} of 1.27±0.08 for the RAD51-depleted cells vs RBE_{10} of 1.±0.04 for the siLuc-transfected cells). To confirm enhanced sensitivity of HRR-mutated cells to proton radiation, we investigated cell survival in the BRCA2-deficient cells PEO1 and their wild-type, isogenic counterpart cells PEO4 in response to both types of ionizing radiation (S7A) [46]. Both PEO4 and PEO1 cells were more sensitive to proton than to photon-irradiation, but the BRCA2-deficient cells PEO1 were markedly more sensitive to proton-irradiation (RBE_{10} of 1.08±0.06 for PEO4 vs RBE_{10} of 1.2±0.02 for PEO1 cells). To further exclude any cell cycle-related effects, we analyzed the time course of cell cycle distribution after both types of irradiation. Both PEO4 and PEO1 cells experienced a G2-arrest already after 12 hours and up to 48 hours after radiation, with no significant difference between proton and photon irradiation (S7B).

Direct pharmacological targeting of the DNA repair pathways, and particularly of the HRR pathway, has proven to be unsuccessful in the past years, mostly due to the lack of druggable target proteins. Interestingly though, several chemotherapeutic agents exists, which originally were designed to target unrelated biological processes, that eventually downregulate the protein level of RAD51. Although through different molecular mechanisms, cellular pretreatment with the broad-range histone deacetylase inhibitor SAHA (Vorinostat) and the selective Bcr-Abl Tyrosine kinase inhibitor Imatinib Mesylate (Gleevec) lead to downregulation of RAD51, and both clinically relevant agents sensitize for ionizing radiation *in vitro* and also *in vivo* [47-53]. Due to the essential role of the RAD51 recombinase and the fact that it is often overexpressed in several cancer types, RAD51 is an attractive target for tumor-selective inhibitors. Based on our previous results, which showed a strong dependence on HRR to repair proton-induced damages, we tested if the histone deacetylase inhibitor SAHA would lead to an increased efficacy in combination with proton radiation in comparison to photon radiation. Continuous exposure with 2µM SAHA for 24 hours was sufficient to reduce RAD51 levels down to approximately 10 % of its basal level, but without any effect on Ku80 or DNA-PKcs protein levels (Fig. 6A).

Pretreatment of A549 cells radiosensitized only mildly to photon irradiation, whereas radiosensitization to proton irradiation was much stronger (DMF_{10} of 1.11±0.07 vs. 1.45±0.15, Fig. 6 and Table 2).

Histone acetylation has an important role in the recruitment of DNA repair factors at the DSB site. Therefore, we investigate the effect of cellular pretreatment with SAHA on γH2AX and DNA-PKcs (Thr-2609) foci formation after both proton and photon irradiation (Fig. 6C). Similar to the results obtained in RAD51-knockdown cells, γH2AX foci removal was strongly delayed after proton irradiation, but only minimally after photon irradiation. In contrast, pDNA-PKcs (Thr-2609) foci removal was almost identical after both types of irradiation.

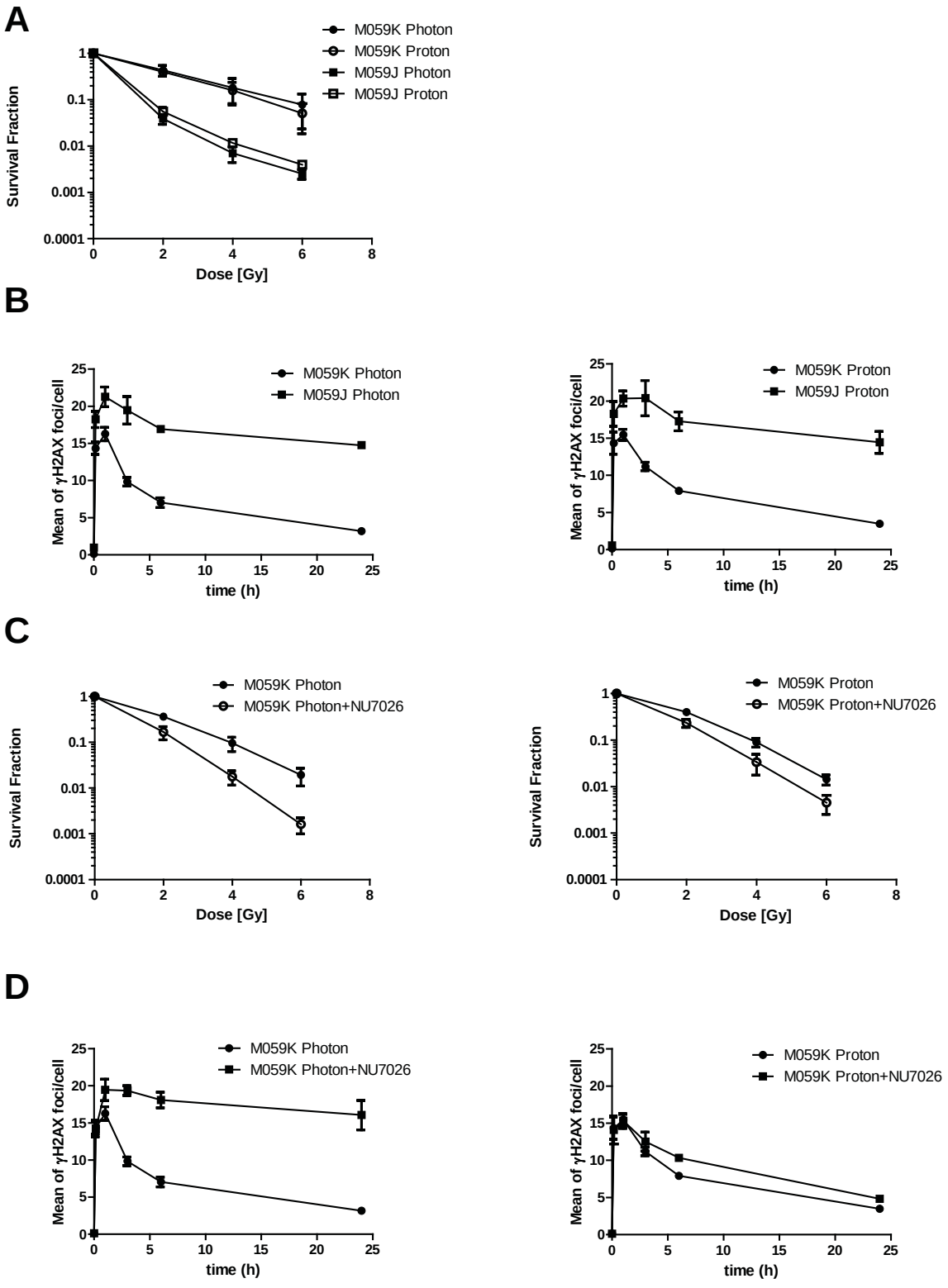

Figure 4. Clonogenic survival and DSB repair in cells pretreated with NU7026 or DNA-PKcs deficiency. Clonogenic survival of DNA-PKcs-proficient (M059K) and DNA-PKcs-deficient (M059J) cells in response to low-LET proton and photon radiation (A) and DSB repair by γH2AX -foci removal (B). Clonogenic survival of M059K cells pretreated with NU7026 (C) and γH2AX-foci removal (D). M059K cells were incubated with 10μM NU7026 in DMSO for 1 hour prior to radiation.

Discussion:

In the present study we have investigated the role and differential requirement of the two major repair pathways, HRR and NHEJ, in response to DSB induced by photon and proton irradiation in a human cancer cells. We previously demonstrated that proliferating cells lacking HRR were more sensitive to proton irradiation than photon irradiation. In contrast, lack of NHEJ did not result in hypersensitivity towards proton-irradiation [45].

In our human cell system studied, depletion of DNA-PKcs by siRNA treatment in A549 cells or genetic deficiency in M059J cells rendered cells more sensitive than their DNA-PKcs proficient counterpart, but they did not display increased sensitivity toward proton radiation. A549 cells depleted of DNA-PKcs showed increased HRR levels after irradiation, as detected by RPA32 recruitment. RPA32-foci occurred mainly in Cyclin-A positive cells, compatible with an S/G_2-arrest in DNA-PKcs-compromised cells [54].

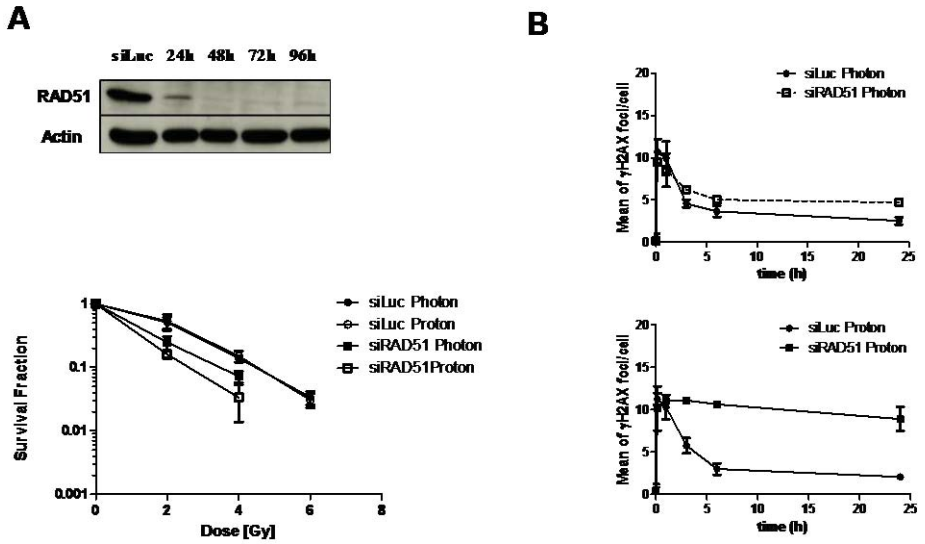

Figure 5. Low-LET proton and photon radiation-induced cell killing in RAD51-knockout A549 cells. (A) RAD51 protein levels of siRAD51-treated A549 cells, determined at the indicated time points and clonogenic cell survival of proton- and photon-irradiated cell lines either treated with control siRNA (siLuc) or siRNA against RAD51. Points represent mean ±SD. (B) Kinetics of γH2AX-foci removal after 1Gy of proton and photon irradiation in siLuc- and siRAD51-treated cells.

We have now demonstrated that DNA-PKcs activation is strongly hampered in response to proton irradiation compared to photon irradiation. Furthermore, selective inhibition of the catalytic subunit of the kinase by NU7026 strongly radiosensitized cells to photon radiation, but to much a less extent to photon radiation. γH2AX- and 53BP1-foci resolution analysis matched the survival data. Interestingly, in DNA-PKcs-deficient cells we observed a strong delay in γH2AX-foci resolution after both types of radiation. In contrast, when the enzyme was present but its catalytic activity inhibited, the strong delay in γH2AX-foci resolution was observed after photon, but not proton irradiation. The reason may rely in the fact that cells with absent DNA-PKcs primarily depend on HRR to repair DNA damage. ATM is expressed at low levels in DNA-PKcs-null cells, but restored to wild-type level in cells expressing a kinase-death form of DNA-PKcs [59]. Therefore, DNA-PKcs-null cells or where the enzyme has been downregulated by siRNA would show a strongly hampered γH2AX-foci resolution, which is strongly ATM dependent. Furthermore, pathway oversaturation may further slowdown the repair process. On the contrary, enzyme inhibition would result in a delay of γH2AX-foci resolution after photon radiation, because DNA-PKcs would be stuck at the DSB site not allowing HRR other than NHEJ to promote repair. Because DNA-PKcs is much less involved in the repair of proton-induced damages, its inhibition would not particularly affect HRR and its ability to promote DNA-damage repair after proton irradiation. This would translate in the fast γH2AX-foci resolution observed after proton radiation in cells pretreated with NU7026, but not where DNA-PKcs is missing. It has been reported that an alternative form of end joining can repair damages, independently of Ku70/Ku80 or DNA-PKcs [21, 55]. This pathway mainly requires PARP1 and Ligases 1 and 3 to repair DSBs. Wang *et al.* [36] showed that PARP1-dependent EJ is not inhibited by high-LET radiation. Despite this, we cannot completely exclude an involvement of this pathway in repairing complex, proton-induced damages.

In our study, A549 cells depleted of RAD51 or treated with the chemotherapeutic agent SAHA were significantly more sensitive to proton radiation than photon radiation. These results point towards an enhanced cellular dependence on HRR to repair proton-induced DNA damages.

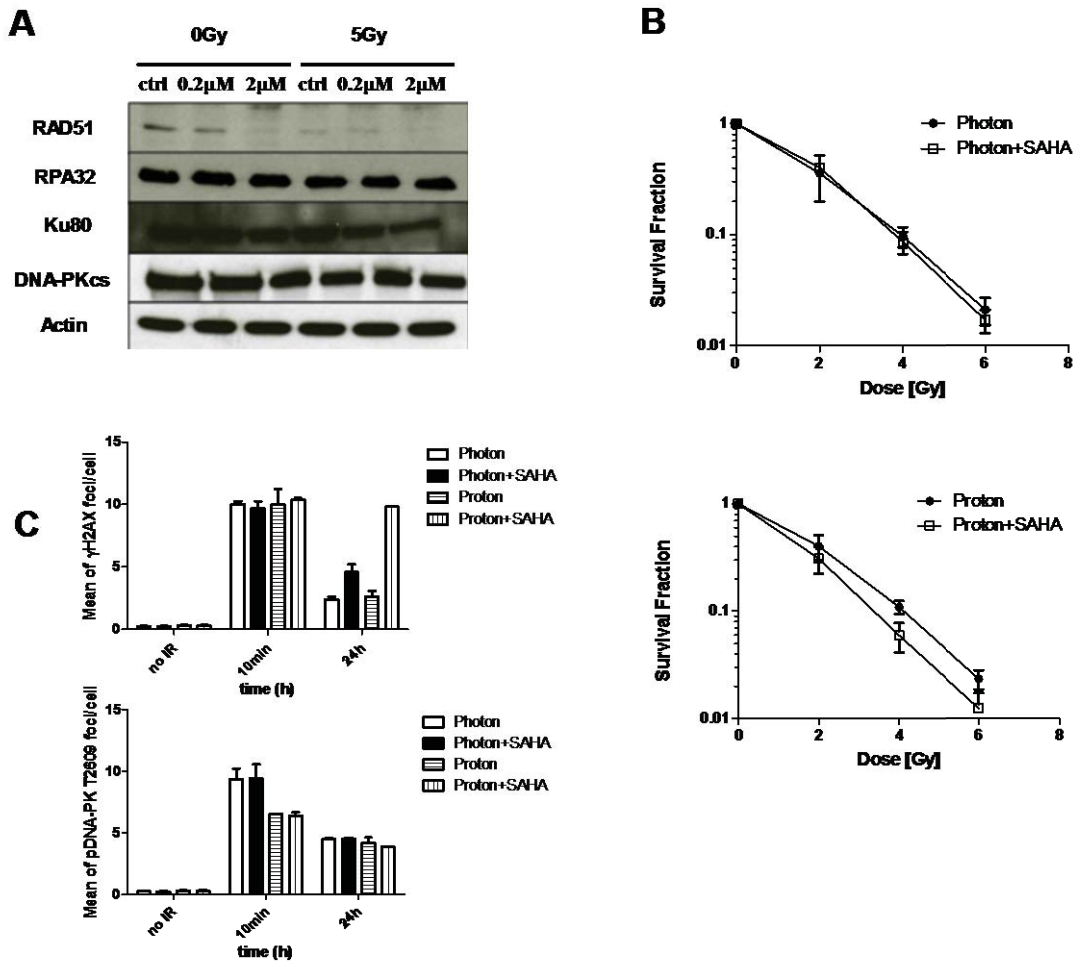

Figure 6. Effect of SAHA (Vorinostat) in A549 cells. (A) Levels of DSB-repair proteins in A549 cells pretreated with SAHA. Cells were incubated with SAHA at the indicated concentrations, irradiated (either mock or 5Gy photon) and cell lysates prepared 24 hours thereafter. (B) Clonogenic survival of A549 cells pretreated with SAHA. Cells were incubated for 24 hour with 2μM SAHA, followed by radiation at the indicated doses. Points represent mean ±SD. (C) Quantification of initial and residual γH2AX and pDNA-PKcs (Thr-2609) foci after 1Gy of proton and photon irradiation.

ATM kinase plays a key role in DSB recognition and signaling [56, 57]. ATM is essential in promoting HRR through DNA-PKcs [58]. Therefore, inhibition of ATM may results in an increased sensitivity to proton radiation. In A549 cells pretreated with KU-60019, a potent and selective ATM inhibitor, a strong radiosensitizing response was observed, with higher DEF_{10}

values after proton irradiation, compared to photon irradiation (*data not shown*). Because of the broad effects of the ATM kinase on the cells, we cannot exclude DSB repair-unrelated effects, as for example p53-dependent effects, to be partially responsible. In conclusion, taken together our results suggest a differential role of NHEJ factors in the recognition and repair of proton-induced DNA damage. In our study, we have shown that NHEJ, but not HRR is inhibited by high energy, low-LET proton radiation, as depicted by the RBE_{10} values of DNA-PKcs-knockdown cells and RAD51-knockdown cells (respectively 0.94±0.07 and 1.27±0.08 vs. 1±0.04 for wild-type). The reason may rely in the inability of DNA-PKcs to fully promote NHEJ repair of complex, proton radiation-induced DNA damage; therefore leading to a situation in which HRR becomes the main repair pathway available. Consequently, cells with reduced or absent HRR are highly susceptible to proton-induced complex damages.

To further develop and exploit novel combined treatment options with proton irradiation, new chemotherapeutic agents have to be developed. We have shown that the histone deacetylase inhibitor SAHA, through its effect on RAD51 protein levels, can lead to an increased radiosensitivity in combination with proton therapy compared to photon therapy. Due to the broad and unspecific effects of these substances on the cell, their specificity and efficacy is strongly cell-type dependent. Recently, selective inhibitors of the RAD51 protein have been developed, like RI-1 and IBR2, widening the spectrum of potential agents which could be used in combination with proton irradiation [51-53]. On the contrary, we have shown that inhibition of DNA-PKcs by NU7026 potently radiosensitize cells in combination with conventional, photon radiation but it is not particularly effective in combination with proton radiation.

Altogether, this may translate in the future in a clinical advantage for proton therapy over the conventionally used, photon-based radiotherapy for selected patients carrying specific mutations or new combined treatment approaches using selective HRR inhibitors, whereas patients treated with conventional, photon-based radiotherapy should strongly profit from DNA-PKcs inhibitors.

Table 1 Relative biological effectiveness (RBE) values at 10% clonogenic survival after proton and photon irradiation

Cell line	Genetic deficiency	RBE_{10}
A549	wild type	1 ± 0.04
A549 siDNA-PKcs	$DNA - PKcs$	0.94 ± 0.07
A549 siRAD51	RAD51	1.27 ± 0.08
M059K	wild type	1.02 ± 0.11
M059J	$DNA - PKcs$	0.88 ± 0.05
PEO4	wild type	1.08 ± 0.06
PEO1	BRCA2	1.20 ± 0.02

Table 2 Dose modifying factors (DMF) values at 10% clonogenic survival after proton and photon irradiation

Cell line	inhibitor	DMF_{10} Photon	DMF_{10} Proton
A549	NU7026 [10µM]	1.91 ± 0.05	1.49 ± 0.06
A549+siDNA-PKcs	NU7026 [10µM]	1 ± 0.07	-
M059K	NU7026 [10µM]	1.49 ± 0.02	1.2 ± 0.11
A549	KU60019 [1µM]	2.32 ± 0.07	3.19 ± 0.34
A549	SAHA [2µM]	1.11 ± 0.07	1.45 ± 0.15

References:

1. Raju MR, Amols HI, Bain E*, et al.* A heavy particle comparative study. Part III: OER and RBE. *Br J Radiol* 1978; 51:712-719.
2. De Ruysscher D, Mark Lodge M, Jones B*, et al.* Charged particles in radiotherapy: a 5-year update of a systematic review. *Radiother Oncol* 2012; 103:5-7.
3. Paganetti H, Niemierko A, Ancukiewicz M*, et al.* Relative biological effectiveness (RBE) values for proton beam therapy. *Int J Radiat Oncol Biol Phys* 2002; 53:407-421.
4. Raju MR. Proton radiobiology, radiosurgery and radiotherapy. *Int J Radiat Biol* 1995; 67:237-259.
5. Cometto A, Russo G, Attili A, et al. Direct evaluation of radiobiological parameters from clinical data in the case of ion beam therapy: an alternative approach to the relative biological effectiveness. *Phys med boil* 2014; 11;59(23):7393-7417.
6. D'Adda di Fagagna F, Living on a break: cellular senescence as a DNA-damage response. *Nat. Rev. Cancer* 2008; 7:512–522.
7. Ward JF, Biochemistry of DNA lesions *Radiat. Res.* 1985; 150 **(suppl.)**:s60-s7.
8. Shrivastav M, De Haro LP*, et al.* DNA-PKcs and ATM co-regulate DNA double-strand break repair. *DNA Repair (Amst)* 2009; 8:920-929.
9. Hiom K. Coping with DNA double strand breaks. DNA Repair (Amst) 2010; 9:1256-1263.
10. Pardo B, Gomez-Gonzalez B, Aguilera A. DNA repair in mammalian cells: DNA double-strand break repair: how to fix a broken relationship. *Cell Mol Life Sci*. 2009; 66:1039-1056.
11. Wold, MS Replication protein A: heterotrimeric, single-stranded DNA-binding protein required for eukaryotic DNA metabolism. *Annual Review of Biochemistry* 1997; 66:61–92.

12. Sung P, Klein H. Mechanism of homologous recombination: mediators and helicases take on regulatory functions. *Nature Reviews Molecular Cell Biology* 2006; **7**(10):739–750.

13. Karagiannis TC, El-Osta A, Double-strand breaks: signaling pathways and repair Mechanisms. *Cell. Mol. Life Sci.* 2004; (61):2137–2147.

14. N.S. Verkaik NS, Van Gent DC *et al.* Different types of V(D)J recombination and end joining defects in DNA double-strand break repair mutant mammalian cells. *Eur. J. Immunol.* 2002; (32):701–709.

15. Branzei D, Foiani M *et al.* Regulation of DNA repair throughout the cell cycle *Nat. Rev. Mol. Cell Biol.* 2008; 9, 297–308

16. Povirk LF *et al.* Biochemical mechanisms of chromosomal translocations resulting from DNA double-strand breaks *DNA Repair* 2006; 5(1):199–1212.

17. Yaneva M, Kowalewski T, Lieber MR, *et al.* Interaction of DNA-dependent protein kinase with DNA and with Ku: biochemical and atomic-force microscopy studies, *EMBO J.* 1997; 16:5098–5112.

18. Dobbs TA, Miller SL et al. A structural model for regulation of NHEJ by DNA-PKcs Autophosphorylation DNA Repair 2010; (9):1307–1314

19. Lieber MR. The Mechanism of Double-Strand DNA Break Repair by the Nonhomologous DNA End-Joining Pathway. *Annual Review of Biochemistry,* 2010; 79:181-211. Guirouilh-Barbat J, Lopez BS, *et al.*

20. Defects in XRCC4 and KU80 differentially affect the joining of distal nonhomologous ends. Proc Natl Acad Sci 2007; 104: 20902–20907.

21. Wang H, Iliakis G. *et al.* Biochemical evidence for Ku-independent backup pathways of NHEJ *Nucleic Acid Research* 2003; 15;31(18):5377-88.

22. Mansour WY, Dahm-Daphi J, *et al.* The absence of Ku but not defects in classical non homologous end-joining is required to trigger PARP1-dependent end-joining. *DNA Repair* 2013; 12:1134– 1142

23. Bennardo N, Cheng A, Stark JM, *et al.* Alternative-NHEJ is a mechanistically distinct pathway of mammalian chromosome break repair, *PLoS Genet.* 2008; 4:100-110.

24. Goodhead DT, Cox R, et al. Effect Radiation of different qualities on cells, molecular mechanism of damage and repair *Int. J. Radiat. Biol.* 1993; 63:543-556.

25. Sutherland BM, Sutherland J, *et al.* Clustered DNA damages induced by High and Low LET radiation, including heavy ions. *Phys. Med.* 2001; 17 (suppl.):202-204.

26. Karlsson KH, Stenerlöw B, Focus formation of DNA repair proteins in normal and repair deficient cells irradiated with high-LET ions. Radiation Research 2004; 161(5):517 –527.

27. Ward JF, the complexity of DNA damage: relevance to biological consequences. *Int. J. Radiat. Biol.* 1994; 63:543-556.

28. Leatherbarrow M, O'Neil P, et al. Induction and quantification of γH2AX foci following low and high LET-irradiation. Int. J. Radiat. Biol. 2006; 82(2):111-118.

29. Wang H, Wang Y, *et al.* The Ku-dependent non-homologous end-joining but not other repair pathway is inhibited by high linear energy transfer ionizing radiation *DNA repair* 2008; 8:725-733.

30. Li Y, Cucinotta FA, *et al.* Modeling Damage Complexity-Dependent Non-Homologous End-Joining Repair Pathway. *PLOS One* 2014; 9(2):1-12.

31. Okayasu R, Takahashi S, *et al.* Repair of DNA damage induced by accelerated heavy ions in mammalian cells proficient and deficient in the non-homologous end-joining pathway. *Radiat. Res*. 2006; 165:59–67.

32. Williams RS, Guenther G, *et al.* Mre11 dimers coordinate DNA end bridging and nuclease processing in double-strand-break repair. *Cell* 2008; 135:97–109.

33. Pedroni E, Bacher R, Blattmann H*, et al.* The 200-Mev Proton Therapy Project at the Paul-Scherrer-Institute - Conceptual Design and Practical Realization. *Medical Physics* 1995; 22:37-53.

34. Franken NA, Rodermond HM, Stap J*, et al.* Clonogenic assay of cells in vitro. *Nat. Protoc.* 2006; 1:2315-2319.

35. Staab A, Zukowski D, Walenta S*, et al.* Response of Chinese hamster v79 multicellular spheroids exposed to high-energy carbon ions. *Radiat. Res.* 2004; 161:219-227.

36. Wang H, Wang Y, *et al.* Characteristics of DNA-binding proteins determine the biological sensitivity to high-linear energy transfer radiation. *Nucleic Acids Research* 2010; 38(10):3245–3251.

37. Blier PR, Hardin JA, *et al.* Binding of Ku protein to DNA. Measurement of affinity for ends and demonstration of binding to nicks. *J. Biol. Chem.* 1993; 268:7594–7601.

38. Walker JR, Goldberg J, *et al.* Structure of the Ku heterodimer bound to DNA and its implications for double-strand break repair. *Nature* 2001; 412:607–614.

39. Neal JA, Meek K. Choosing the right path: Does DNA-PK helps make the decision? *Mutation Research* 2011; 711:73-86

40. Hollick JJ, Griffin RJ, *et al.* 2,6-disubstituted pyran-4-one and thiopyran-4-one inhibitors of DNA-Dependent protein kinase (DNA-PK). *Bioorg. Med. Chem. Lett.* 2003; 13(18):3083-3086.

41. Olive PL. Retention of γH2AX foci as an indication of lethal DNA damage. *Radiother. Oncol.* 2006; 101:18-23.

42. Klokov D, Banath JP, et al. Phosphorylated H2AX in relation to cell survival in tumor cells and xenografts exposed to single and fractionated doses of X-rays. Radiother. Oncol. 2006; 80:223-229.

43. Allen C, Halbrook J, Nickoloff JA. Interactive Competition between Homologous Recombination and Non-Homologous End Joining *Mol Cancer Res* 2003; 1:913-920.

44. Allalunis-Turner MJ, Mirzayans R, *et al.* Isolation of two cell lines from a human malignant glioma specimen differing in sensitivity to radiation and chemotherapeutic drugs. *Radiat. Res.* 1993; 134(3):349-54

45. Grosse N, Pruschy MN, et al. Deficiency in homologous recombination renders Mammalian cells more sensitive to proton versus photon irradiation. Int J Radiat Oncol Biol Phys. 2014; 88(1):175-81.

46. Langdon SP, Smyth SJ, *et al.* Characterization and properties of nine human ovarian adenocarcinoma cell lines. Cancer Res. 1988; 48(21):6166-72.

47. Chen X, Wong JY*, et al.* Suberoylanilide hydroxamic acid as a radiosensitizer through modulation of RAD51 protein and inhibition of homology-directed repair in multiple myeloma *Mol. Cancer Res.* 2012; 10(8):1052-64.

48. Konstantinopoulos PA, Khabele D, *et al.* Suberoylanilide hydroxamic acid (SAHA) enhances olaparib activity by targeting homologous recombination DNA repair in ovarian cancer *Gynecol Oncol.* 2014; 133(3):599-606.

49. Choudhury A, Bristow RG, *et al.* Targeting homologous recombination using Imatinib results in enhanced tumor cell chemosensitivity and radiosensitivity *Mol. Cancer Ther.*2009; 8(1):203-13.

50. Quiao B, Kiltie AE, *et al.* Imatinib radiosensitizes bladder cancer by targeting homologous recombination *Cancer Res*. 2013; Mar 1;73(5):1611-20.

51. Budke B, Connell PP, *et al*. RI-1: a chemical inhibitor of RAD51 that disrupts homologous recombination in human cells. *Nucleic acid research* 2012; 40(15):7347-7357.

52. Budke B, Connell PP, *et al*. An optimized RAD51 inhibitor that disrupts homologous recombination without requiring Michael acceptor reactivity. *J Med Chem* 2013; 10;56(1):254-63.

53. Zhu J, Lee WH, *et al.* A novel small molecule RAD51 inactivator overcomes Imatinib resistance in chronic myeloid leukaemia. *EMBO Medical Journal* 2013; 5(3):353-65.

54. Anderson JA, O'Neill P. *et al.* Participation of DNA-PKcs in DSB Repair after Exposure to High- and Low-LET Radiation. *Radiation Research* 2010; 174(2):195-205.

55. Soni A, Iliakis G, *et al.* Requirement for Parp-1 and DNA ligases 1 or 3 but not of Xrcc in chromosomal translocation formation by backup end joining. *Nucleic Acid Research.*2014; 42(10):6380-92.

56. Burma S, Chen DJ, *et al.* ATM phosphorylates histone H2AX in response to DNA double-strand breaks. *The Journal of biological chemistry.* 2001; **276**(45): 42462-42467.

57. Tomita, M. Involvement of DNA-PK and ATM in radiation- and heat-induced DNA damage recognition and apoptotic cell death. *J Radiat Res.* 2010; **51**(5):493-501.

58. Chen BPJ, Chen DJ, *et al.* Ataxia telangiectasia mutated (ATM) is essential for DNA-PKcs phosphorylations at the Thr-2609 cluster upon DNA double strand break. *The Journal of biological chemistry*. 2007; **282**(9):6582-6587.

59. Shrivastav M , Nickoloff JA, *et al.* DNA-PKcs and ATM co-regulate DNA double-strand break repair. *DNA Repair (Amst).* 2009; **8**(8):920-9.

Supplementary procedures:

Proliferation Assay. Growth inhibition was measured using the Thiazoyl blue tetrazolium bromide assay. 24 h prior to drug treatment, cells were plated at a density of 500 cells/well in a 96-wells plate. Cells were then treated with different concentration of NU7026 and incubated for 72 h. Thiazoyl blue tetrazolium bromide solution (Sigma–Aldrich) was then added for 4 hours followed by optical density measurement in a 96-well plate reader at 750 nm.

Cell cycle. Cells were pretreated with 10μM NU7026 for 1 hour before being either treated with mock or 5Gy radiation. 30 min before the desired time point after irradiation, Bromodeoxy-uridine (10μM) was added to the growing cell. Cells were then washed, harvested, and fixed with ice-cold ethanol. Cells were then co-stained with PI (Sigma–Aldrich, Germany) and anti- Bromodeoxy-uridine Fluorescine antibody (Roche Diagnostic GmbH, Germany) and analyzed by flow cytometry (FACS Canto II, BD Biosciences). Cell cycle distribution was analyzed using the FlowJo 7 software package (FlowJo LLC, Oregon, USA).

Supplementary figures:

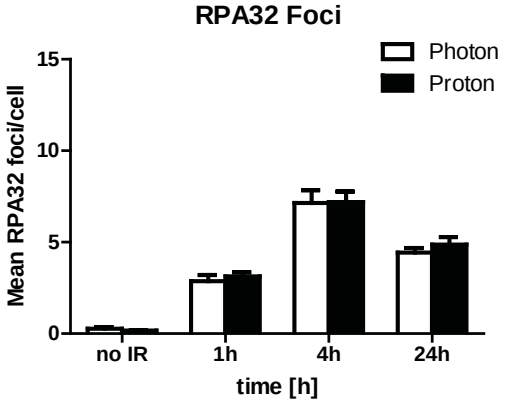

Supplementary figure 1. Analysis of RPA32 and RAD51 recruitment in A549 cells. (A) RAD51 and RPA32 foci were determined at 1 hour, 4 hours and 24 hours after radiation with 10Gy. Cells were co-stained for Cyclin-A2 to identify S/G2-phase cells.

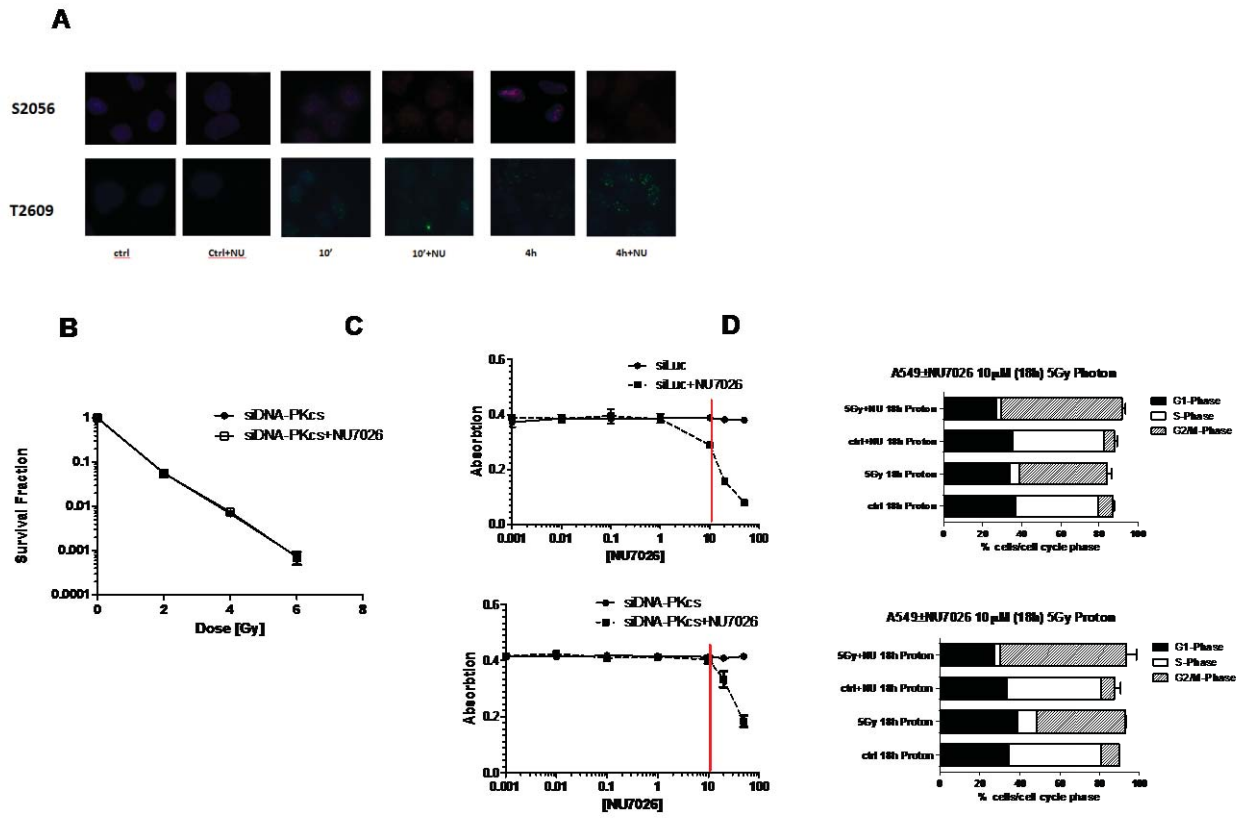

Supplementary figure 2. NU7026 pretreatment strongly affects DNA-PKcs-proficient, but not DNA-PKcs-deficient cells. (A) NU7026 pretreatment potently inhibits autophosphorylation of DNA-PKcs at Ser-2056 site, but not at Thr-2609 site. (B) Clonogenic cell survival of photon-irradiated cell lines pretreated with NU7026 and with siRNA against DNA-PKcs (siDNA-PKcs). Points represent mean ±SD. Cells were incubated for 1 hour with 10µM NU7026 in DMSO followed by photon and proton irradiation. (C) SiLuc-treated and siDNA-PKcs-treated A549 cells were incubated for 72 hours with increasing concentrations of NU7026, and after 72 hours absorption was measured by MTT-assay (D) cell cycle distribution analysis of A549 cells in presence and absence of NU7026. Cells were fixed 18 hours after irradiation with 5Gy of either photons or protons, double-stained for Propidium Iodide and anti-BrdU and cell cycle distribution measured by FACS.

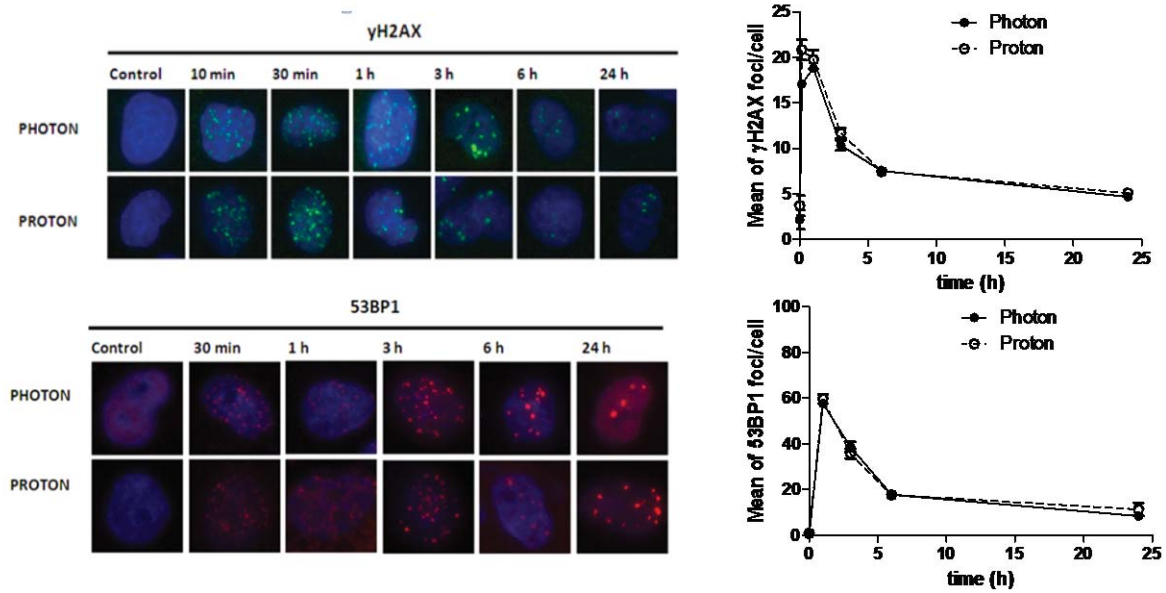

Supplementary figure 3. γH2AX- and 53BP1-foci resolution profile in A549 cells. A549 cells were irradiated with either 1Gy (γH2AX) or 5Gy (53BP1) of both types of ionizing radiation and fixed at the indicated time points.

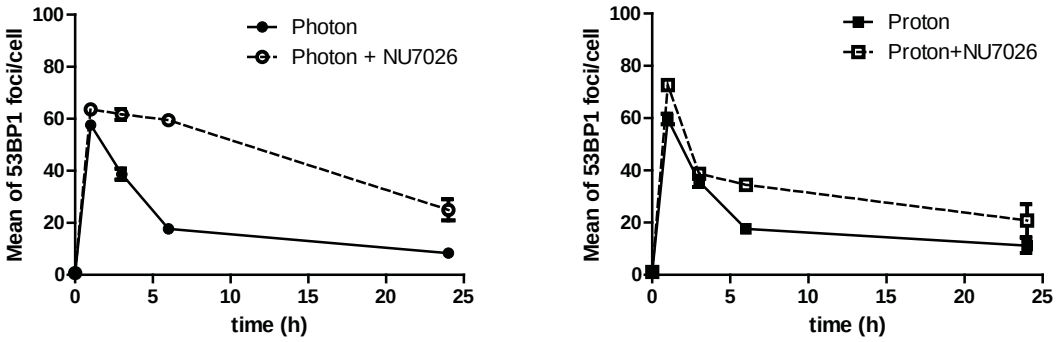

Supplementary figure 4. 53BP1-foci resolution profile in A549 cells pretreated with NU7026. A549 cells were incubated for 1 hour with 10μM NU7026 in DMSO followed by irradiation with 5Gy of proton and photon irradiation and fixed at the indicated time points.

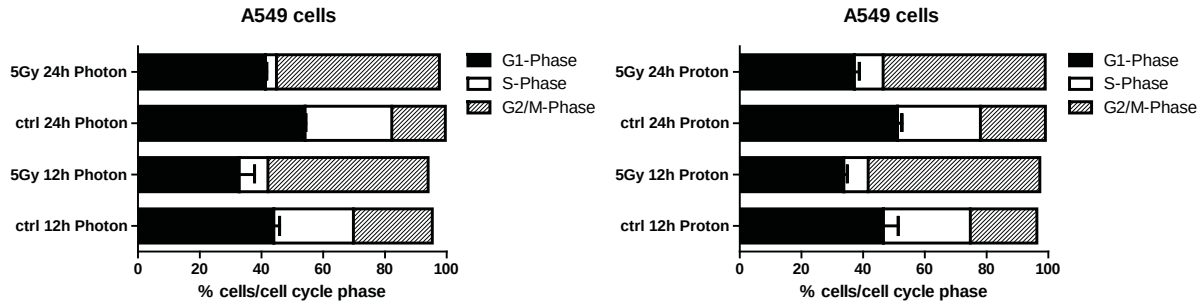

Supplementary figure 5. Cell cycle distribution analysis in A549 cells. A549 cells were fixed at the indicated time points after irradiation with 5Gy of either photons or protons, double-stained for Propidium Iodide and anti-BrdU and cell cycle distribution measured by FACS.

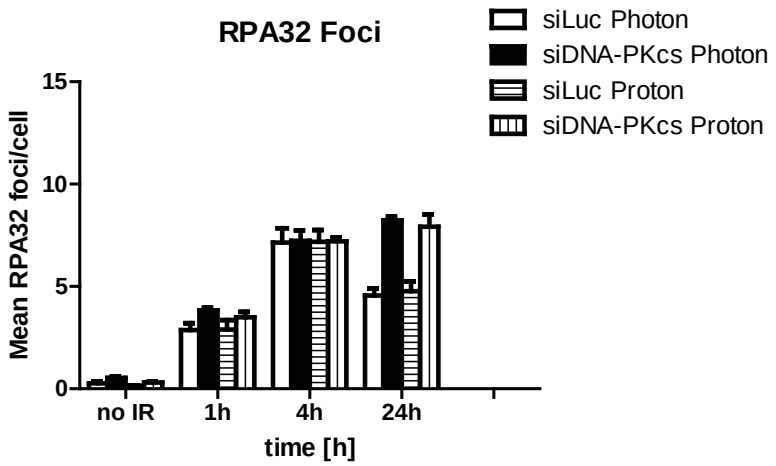

Supplementary figure 6. Analysis of RPA32 recruitment in A549 cells treated with siRNA against Luciferase or DNA-PKcs. (A) RPA32 foci were determined at 1 hour, 4 hours and 24 hours after radiation with 10Gy. Cells were co-stained for Cyclin-A2 to identify S/G2-phase cells.

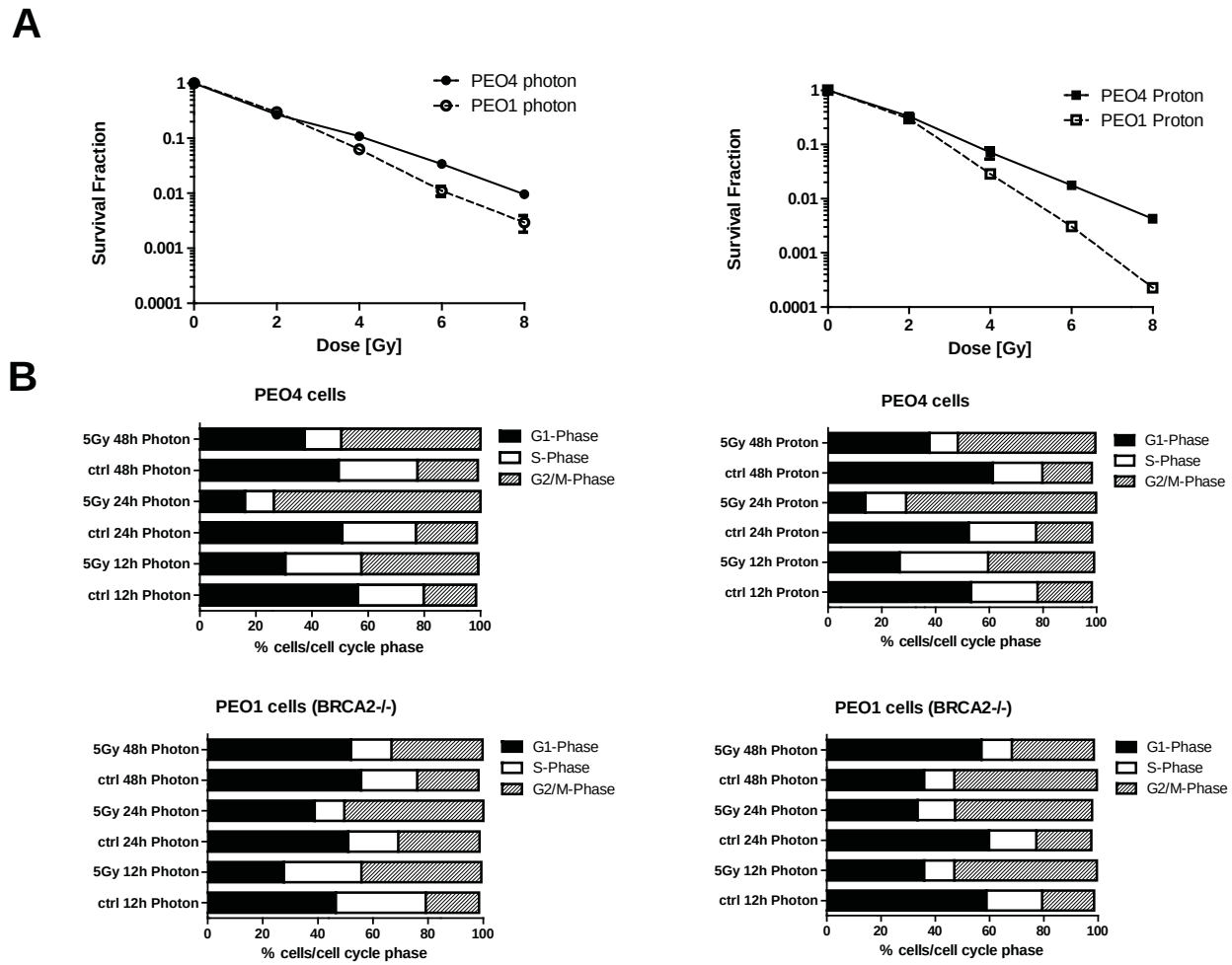

Supplementary figure 7. Comparison of low-LET proton and photon radiation-induced cell killing in BRCA2-deficient PEO1 cells and BRCA2-proficient PEO4 cells.
(A) Clonogenic cell survival of proton- and photon-irradiated PEO4 and PEO1 cell lines. Points represent mean ±SD. (B) cell cycle distribution analysis of PEO4 and PEO1 cells. Cells were fixed at the indicated time points after irradiation with 5Gy of either photons or protons, double-stained for Propidium Iodide and anti-BrdU and cell cycle distribution measured by FACS.

3.3 Complement is a central mediator of radiotherapy-induced tumor-specific immunity and clinical response

Laura Surace[1], Veronika Lysenko[1], Andrea Orlando Fontana[2], Virginia Cecconi[1], Hans Janssen[3], Antonela Bicvic[1], Michal Okoniewski[4], Martin Pruschy[2], Reinhard Dummer[4], Jacques Neefjes[3], Alexander Knuth[6*], Anurag Gupta[1], Maries van den Broek[1].

[1] Institute of Experimental Immunology, University of Zurich, Switzerland

[2] Department of Radiation Oncology, University Hospital Zurich, Switzerland

[3] The Netherlands Cancer Institute, Department of Cell Biology, Amsterdam, the Netherlands

[4] Functional Genomic Centre Zurich, University of Zurich, Switzerland

[5] Department of Dermatology, University Hospital Zurich, Switzerland

[6] Clinic of Oncology, University Hospital Zurich, Switzerland

*present address: National Center for Cancer Care & Research, Hamad Medical Corporation, Doha, Qatar.

Status of the manuscript: Published in Immunity. 2015 April; 42:1-11.

Author contribution A.O. Fontana:

Set-up and conduction of the irradiation procedure at the Gulmay machine, University Hospital Zurich.

Article

Immunity

Complement Is a Central Mediator of Radiotherapy-Induced Tumor-Specific Immunity and Clinical Response

Graphical Abstract

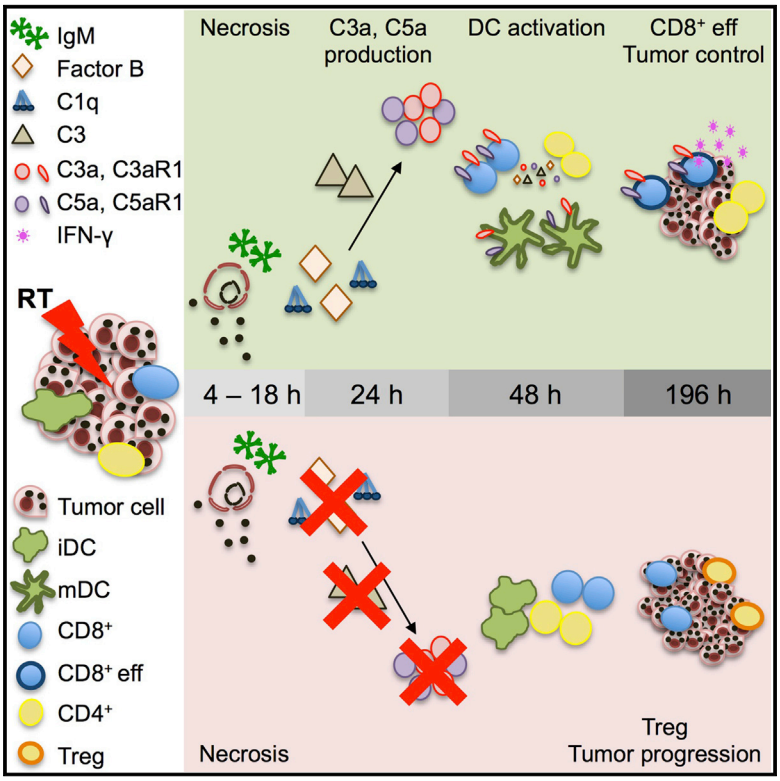

Authors

Laura Surace, Veronika Lysenko, ..., Anurag Gupta, Maries van den Broek

Correspondence

vandenbroek@immunology.uzh.ch

In Brief

Anaphylatoxins are produced upon complement activation and are well-known pro-inflammatory molecules. van den Broek and colleagues demonstrate that anaphylatoxins are produced within a tumor after radiotherapy by immune cells, support tumor-specific immunity, and are essential to therapeutic efficacy.

Highlights

- RT induces local complement activation in mice and humans
- RT-mediated cell death and necrosis activates complement
- C3a and C5a accumulate in the tumor and promote tumor-specific immunity
- Dexamethasone inhibits complement activation and reduces efficacy of RT

Surace et al., 2015, Immunity *42*, 767–777
April 21, 2015
http://dx.doi.org/10.1016/j.immuni.2015.03.009

CellPress

Immunity
Article

Complement Is a Central Mediator of Radiotherapy-Induced Tumor-Specific Immunity and Clinical Response

Laura Surace,[1] Veronika Lysenko,[1] Andrea Orlando Fontana,[2] Virginia Cecconi,[1] Hans Janssen,[3] Antonela Bicvic,[1] Michal Okoniewski,[4] Martin Pruschy,[2] Reinhard Dummer,[5] Jacques Neefjes,[3] Alexander Knuth,[6,7] Anurag Gupta,[1] and Maries van den Broek[1,*]

[1]Institute of Experimental Immunology, University of Zurich, Winterthurerstrasse 190, 8057 Zurich, Switzerland
[2]Department of Radio-Oncology, University Hospital Zurich, Rämistrasse 100, 8091 Zurich, Switzerland
[3]Division Cell Biology II, Netherlands Cancer Institute, Plesmanlaan 121, 1066 CX Amsterdam, the Netherlands
[4]ID Scientific IT Services, Swiss Federal Institute for Technology (ETH), Weinbergstrasse 11, 8092 Zurich, Switzerland
[5]Department of Dermatology, University Hospital Zurich, Rämistrasse 100, 8091 Zurich, Switzerland
[6]Clinic of Oncology, University Hospital Zurich, Rämistrasse 100, 8091 Zurich, Switzerland
[7]Present address: National Center for Cancer Care & Research NCCCR, Hamad Medical Corporation, P.O. Box 3050 Doha, Qatar
*Correspondence: vandenbroek@immunology.uzh.ch
http://dx.doi.org/10.1016/j.immuni.2015.03.009

SUMMARY

Radiotherapy induces DNA damage and cell death, but recent data suggest that concomitant immune stimulation is an integral part of the therapeutic action of ionizing radiation. It is poorly understood how radiotherapy supports tumor-specific immunity. Here we report that radiotherapy induced tumor cell death and transiently activated complement both in murine and human tumors. The local production of pro-inflammatory anaphylatoxins C3a and C5a was crucial to the tumor response to radiotherapy and concomitant stimulation of tumor-specific immunity. Dexamethasone, a drug frequently given during radiotherapy, limited complement activation and the anti-tumor effects of the immune system. Overall, our findings indicate that anaphylatoxins are key players in radiotherapy-induced tumor-specific immunity and the ensuing clinical responses.

INTRODUCTION

It is now well accepted that the immune system can control tumors (Schreiber et al., 2011). For example, there is a positive correlation between tumor infiltration by effector T cells and survival (Fridman et al., 2011), and the risk to develop cancer is increased in immunosuppressed patients (Dunn et al., 2006), and dormant tumors are kept in check by the adaptive immune system (Koebel et al., 2007). Despite the presence of tumor-specific immunity in many cancer patients, complete rejection of clinically apparent tumors by the immune system is rare, presumably due to mechanisms that locally inhibit tumor-specific protective immunity (Schreiber et al., 2011). The clinical efficacy of so-called checkpoint blockade, antibodies that target co-inhibitory molecules such as CTLA-4 or PD-1, underscores the potential of tumor-specific immunity (McDermott and Atkins, 2013; Mellman et al., 2011).

Radiotherapy is a standard treatment for cancer that induces irreversible damage to DNA, thus targeting mainly rapidly dividing cells (Prise and O'Sullivan, 2009). Although radiotherapy was considered an immunosuppressive treatment (Merrick et al., 2005), there is accumulating evidence that it supports local tumor-specific immunity (Apetoh et al., 2007; Matsumura et al., 2008) and, in fact, that immune activation might be an integral part of radiotherapy (Formenti and Demaria, 2012; Gupta et al., 2012; Ma et al., 2010; Sharma et al., 2013). This is clinically relevant because tumor-specific immunity can target dormant lesions (Postow et al., 2012) that are presumably insensitive to radiotherapy. Several studies have addressed the question of how radiotherapy supports tumor-specific immunity, and various factors were suggested, including increased presence or function of tumor-infiltrating $CD8^+$ T cells (Gupta et al., 2012; Lugade et al., 2005; Takeshima et al., 2010), type I interferon (IFN) resulting in enhanced antigen cross-presentation (Burnette et al., 2011; Fuertes et al., 2011), increased expression of major histocompatibility complex (MHC) class I glycoproteins and tumor-associated antigens (Reits et al., 2006), and maturation of tumor-associated dendritic cells (DCs) (Gupta et al., 2012), however, an initial event has not been identified.

We therefore performed an unbiased analysis of immune response-related transcripts after radiotherapy in a preclinical model and noted a strong and transient upregulation of genes associated with the complement pathway. This was unexpected as complement was described as tumor-promoting (Markiewski et al., 2008; Pio et al., 2014), although other studies have shown that complement supports adaptive immunity (Farrar and Sacks, 2014; Kopf et al., 2002; Lalli et al., 2007; Liszewski et al., 2013; Strainic et al., 2013). Because we observed similar changes in human tumor samples, we investigated the impact of complement on the anti-tumor immune response following radiotherapy.

RESULTS

Radiotherapy Induces Complement Activation

To identify the initial event in radiotherapy-induced tumor-specific immunity, we performed an unbiased analysis of immune

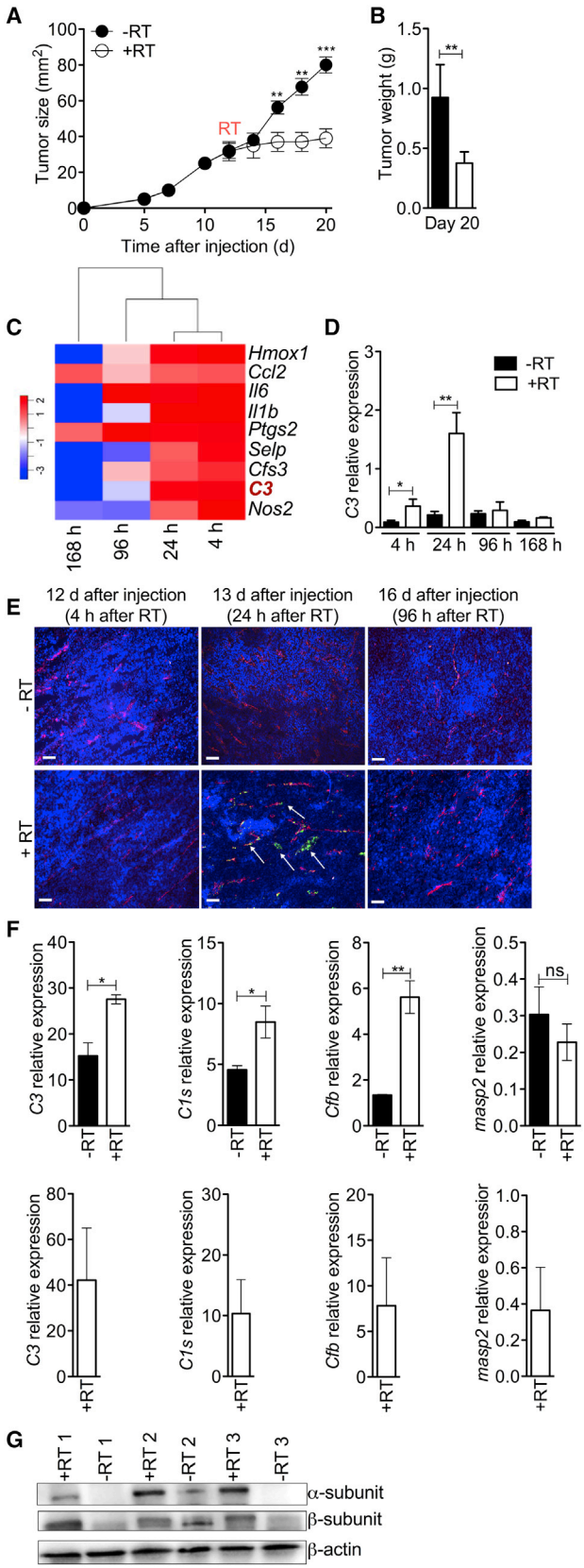

Figure 1. Radiotherapy Results in Transient Upregulation and Activation of Complement in Murine and Human Tumors

(A–E) Mice were injected with B16F10-OVA cells and received radiotherapy 12 days later. (A) Tumor growth curves, (n = 5 mice per group). Representative data from three independent experiments are shown. (B) Tumor weight (day 20). (C) Heatmaps of transcripts were created using the $\log_2$ value of the fold increase of irradiated compared to untreated tumors at different time points after radiotherapy, (n = 6 mice per time point). Representative data from two independent experiments are shown. (D) Relative expression of *C3* mRNA in tumors at different time points after radiotherapy. The data show the mean ± SD of triplicates from three independent analyses. Radiotherapy, RT. (E) Immunofluorescence of irradiated and untreated tumors. Sections were stained with an antibody recognizing C3b, iC3b, and C3c (green), CD31 for blood vessels (red), and DAPI (blue). Scale bars represent 100 μm (n = 6 mice per group). Representative images from two independent experiments are shown.

(F and G) Patient biopsies were collected before and 24–36 hr after radiotherapy (1.5–2 Gy; upper panel) or only after radiotherapy (lower panel). Quantification of complement transcripts by qPCR. Data show the mean ± SD of triplicates from two independent analyses (upper panel). (G) Quantification of C3-α and -β subunits by immuno-blot.

Data are shown as mean ± SD. *p < 0.05, **p < 0.005, ***p < 0.0005 by Student's t test (A, B, and F) or two-way ANOVA with the Bonferroni correction (D). See also Figure S1.

response-related transcripts after radiotherapy. Local irradiation with a single dose of 20 Gy significantly reduced progression of B16F10-OVA tumors in C57BL/6 mice (Figures 1A and 1B). Because transplantable mouse tumors only allow for a short therapeutic window, radiotherapy must be applied as a single high dose (Lugade et al., 2005). To dissect which pathways are crucial to radiotherapy-induced stimulation of the immune response, we quantified immune response-related transcripts in tumors at different time points 4, 24, 96, and 168 hr after local irradiation (Figures 1C and S1A). We observed an upregulation of the complement system (represented in this panel only by *C3*) and the inflammation cascade at 4 and 24 hr, whereas both pathways were downregulated at 96 and 168 hr after irradiation (Figure 1C). Because 20 Gy might be of limited clinical relevance, we performed the same analysis 24 hr after irradiation with a single dose of 5 Gy and observed a similar transcriptional upregulation (Figure S1B).

C3 is the central protein of the complement cascade at which all three known pathways (classical, alternative, and lectin) converge and which gives rise to various bioactive components (Markiewski and Lambris, 2009). Because complement might be tumor-promoting (Markiewski et al., 2008; Markiewski and Lambris, 2009; Pio et al., 2014), we investigated whether radiotherapy-induced upregulation of complement supported or antagonized the efficacy of this treatment. We first quantified four different complement-related transcripts in response to radiotherapy: *C3*, *C1s*, *Masp2* and *Cfb*. The classical and alternative pathways are the main pathways induced by radiotherapy on the transcriptional level (Figures 1D and S1C). Because NF-κB, JAK, and STAT transcriptional pathways (Chen et al., 2011; Fukuoka et al., 2013; Hasegawa et al., 2014; Huang et al., 2002), as well as S100 calcium-binding proteins A8 and A9 (S100A8, S100A9) (Schonthaler et al., 2013) are involved in the transcription of complement factors, we analyzed such pathways by immuno-blot and found an increased production of STAT 1, STAT 2, STAT 3, NF-κB, and JAK and increased phosphorylation of STAT 2, STAT3, and JAK (Figure S1D) 4 hr, but not

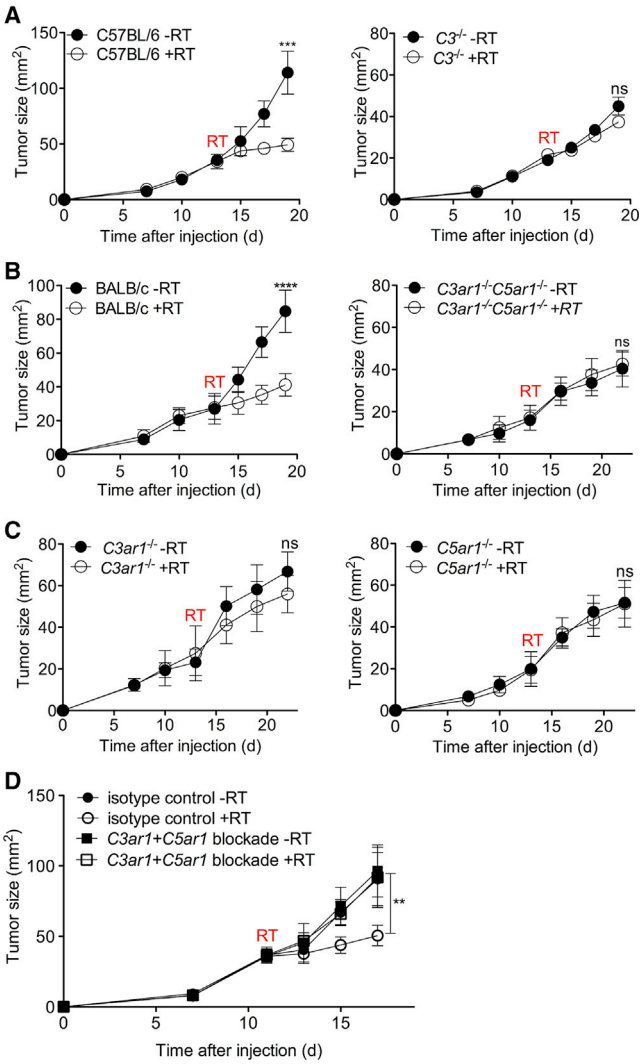

Figure 2. C3a and C5a Are Crucial to the Therapeutic Efficacy of Radiotherapy

(A) Control and $C3^{-/-}$ mice were injected with B16F10-OVA cells and received radiotherapy 13 days later. Growth curves, (n = 5 mice per group). Representative data from two independent experiments are shown. Radiotherapy, RT.

(B) BALB/c, $C3ar1^{-/-}$, $C5ar1^{-/-}$, and $C3ar1^{-/-}C5ar1^{-/-}$ were injected with CT26 cells and received radiotherapy 13 days later. Tumor growth curves (BALB/c n = 5 mice per group; $C3ar1^{-/-}$, $C5ar1^{-/-}$, and $C3ar1^{-/-}C5ar1^{-/-}$ n = 8 mice per group). Representative data from two independent experiments are shown.

(C) Mice were injected with B16F10-OVA cells and received radiotherapy 12 days later. SB290157 was administered at 2 mg/kg to block C3aR1 and anti-C5aR1 mAb 20/70 or an isotype control at 0.6 mg/kg to block C5aR1 (administered every second day starting on day 12 until day 19). (n = 5 mice per group).

Data are shown as the mean ± SD. **p < 0.005, ***p < 0.0005, ****p < 0.00005 by two-way ANOVA with the Bonferroni correction. See also Figure S2.

24 hr, after radiotherapy. Transcripts of *S100a8* and *S100a9* were unaffected (data not shown).

To show that these translated in different complement factor amounts, we analyzed the tumors prior to and after radiotherapy by immunofluorescence (Figure S1E) and by immuno-blot (Figure S1F). Because C1q and Factor B are more abundant compared to mannose-binding lectin C (MBL-C), these results confirmed our qPCR data (Figure S1C). We analyzed the activation status of complement and found deposition of fragments derived from C3 cleavage (C3b, iC3b, and C3c) 24 hr after radiotherapy in the proximity of (green fluorescence) or associated with (yellow fluorescence) blood vessels (Figure 1E). Similarly to C3 cleavage products, we observed C1q and Factor B mainly associated to blood vessels, whereas MBL-C showed a markedly different pattern of deposition. We obtained similar results using B16F10 cells, both at the transcriptional (data not shown) and protein level (Figure S1G). We confirmed radiotherapy-induced complement activation by immuno-blotting using an antibody recognizing C3 plus its fragments C3b, C3c, and C3dg (Figure S1H). Because deposition of C3b, iC3b, and C3c was not detected at other time points besides 24 hr after radiotherapy, this suggests that radiotherapy-induced complement activation is a rapid and transient response.

We analyzed the expression of complement-related transcripts and proteins in paired human tumors that were collected before and 24–36 hr after a single, low dose of radiotherapy (1.5 or 2 Gy) and detected upregulated expression (Figure 1F) and activation of complement (Figure 1G). To exclude that taking the first biopsy prior to radiotherapy rather than radiotherapy was responsible for complement activation, we analyzed additional four biopsies that were taken 24–36 hr after irradiation with 1.5–2 Gy but without previous intervention. The amounts of complement transcripts were comparable to those after radiotherapy in the paired samples, excluding this option (Figure 1F).

Together, we found that radiotherapy induces transient, local production, and activation of the classical and alternative complement pathway in both human and murine tumors.

Therapeutic Efficacy of Radiotherapy Depends on C3a and C5a

To investigate the impact of complement activation on therapeutic efficacy, we applied radiotherapy to tumor-bearing $C3^{-/-}$ mice. Because tumors grew more slowly in $C3^{-/-}$ mice (Figures 2A and S2A) (Markiewski et al., 2008; Qing et al., 2012), $C3^{-/-}$ and C57BL/6 mice were irradiated at two different time points, i.e., 13 (Figure 2A) or 17 days (Figure S2B) after tumor injection. Comparison of C57BL/6 mice irradiated at day 13 (Figure 2A, left panel) with $C3^{-/-}$ mice irradiated at day 17 (Figure S2B, right panel) shows the response of tumors with a similar size (36–40 mm^2) at the time point of irradiation. Radiotherapy was not efficient in $C3^{-/-}$ mice irrespective of the day of therapy (Figures 2A, S2A, and S2B), suggesting that complement activation is crucial to efficacy.

Anaphylatoxins (C3a and C5a) modulate adaptive immunity (Schmudde et al., 2013; Strainic et al., 2013). As we observed higher local amounts of C3a and C5a (Figure S2C) and their receptors (Figures S2D) upon radiotherapy, we investigated their role in the response to radiotherapy using $C3ar1^{-/-}$, $C5ar1^{-/-}$, and $C3ar1^{-/-}C5ar1^{-/-}$ mice. As these mice were only available on a BALB/c background, we confirmed that radiotherapy resulted in local complement activation (Figure S2E), showing that radiotherapy-induced complement activation is a general phenomenon independent of the strain or tumor cell line used. Similar to $C3^{-/-}$ mice, $C5ar1^{-/-}$,

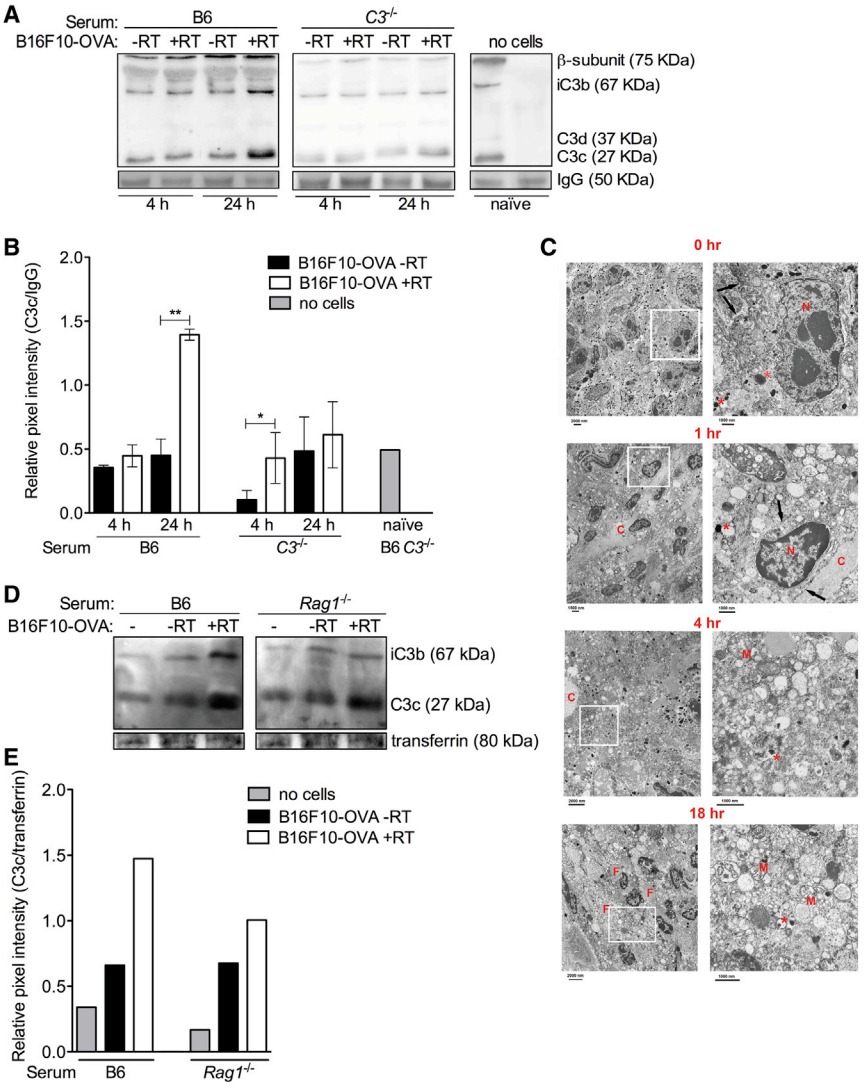

Figure 3. Radiotherapy-Induced Tumor Cells Death Activates Complement

(A and B) B16F10-OVA cells were irradiated in vitro with 20 Gy or left untreated. Serum from C57BL/6 or $C3^{-/-}$ mice was added to the cultures immediately after irradiation and C3 cleavage products were analyzed 4 and 24 hr later in the supernatants by immuno-blot using a polyclonal anti-C3 antibody (n = 3 mice per group). Representative data of two independent experiments are shown. (B) Relative intensities were calculated using Bio1D software. Radiotherapy, RT.

(C) Ultrastructural analysis of tumor response to radiotherapy. B16F10-OVA tumors were isolated from mice prior to and different times after radiotherapy. Fixed tumor tissue was epon embedded and analyzed by EM. Shown are images of tumor tissues before (0 h), 1, 4, and 18 hr after radiotherapy. Left column, overview; Right column, zoom-in of region indicated in left image. Bar indicates magnification. N, nucleus; M, mitochondrion; black arrow, cell boundaries; F, fat bodies; C, collagen; *, melanosomes.

(D and E) B16F10-OVA cells were irradiated in vitro with 20 Gy or left untreated. Serum from $Rag1^{-/-}$ mice was added to the cultures immediately after irradiation and C3 cleavage products were analyzed as described in (A), (n = mice 3 per group). (E) Relative intensities were calculated using Bio1D software.

Data in (B) are shown as the mean ± SD. *$p < 0.05$, **$p < 0.005$, by two-way ANOVA with the Bonferroni correction.

$C3ar1^{-/-}$, and $C3ar1^{-/-}C5ar1^{-/-}$ mice showed no significant impact of radiotherapy on tumor progression, whereas BALB/c mice did (Figures 2B, 2C, and S2F). To avoid the issue of inherent different tumor growth rates in various genetically ablated strains, we blocked C3aR with an antagonist (C3aRA, SB290157) or C5aR with a monoclonal antibody (20/70) (Baelder et al., 2005) just before applying radiotherapy to tumor-bearing C57BL/6 mice. This treatment blocked the improved antitumor effect of radiotherapy (Figures 2D and S2G), which is in line with the results observed in $C3^{-/-}$, $C3ar1^{-/-}$, $C5ar1^{-/-}$, and $C3ar1^{-/-}C5ar1^{-/-}$ mice. These data suggest that radiotherapy induces the intratumoral generation of anaphylatoxins, which are crucial to the therapeutic efficacy.

Radiotherapy-Induced Cell Death Locally Activates Complement

Despite the fact that complement deposition was observed in the vicinity of blood vessels, we failed to detect activated complement in serum irrespective of whether mice received radiotherapy or bore a tumor (Figure 4A). This excludes that radiotherapy or a local tumor results in systemic activation of complement. Local radiotherapy results in apoptosis (Wang, 2008), mitotic catastrophe, and necrosis (Eriksson and Stigbrand, 2010), all of which can be potent activators of complement (Basu et al., 2000; Kemper et al., 2008; Markiewski and Lambris, 2007). We first evaluated the possibility of direct complement activation by radiation and exposed serum from C57BL/6 or $C3^{-/-}$ mice in vitro to a single dose of 20 Gy or left them untreated and analyzed sera 4 and 24 hr after irradiation by immuno-blot. We did not detect any significant changes upon irradiation (data not shown). To investigate whether irradiated tumor cells can activate complement, we either or not exposed B16F10-OVA cells in vitro to a single dose of 20 Gy. Immediately after irradiation, 10-fold diluted serum from C57BL/6 mice or $C3^{-/-}$ mice was added to irradiated or untreated B16F10-OVA cells. Complement activation was detected in the supernatants 24 hr after radiation. Because the culture serum was from $C3^{-/-}$ mice, the complement should have been derived from the tumor cells (Figures 3A and 3B).

To identify the mode of tumor cell death upon a single dose of 20 Gy, we performed electron microscopy (EM) on B16F10-OVA tumors isolated at different time points after radiotherapy as indicated (Figure 3C). The tissue isolated before radiation showed normal nuclei, cell boundaries, intracellular organelles, and melanosomes (the dark vesicular structures) illustrating healthy

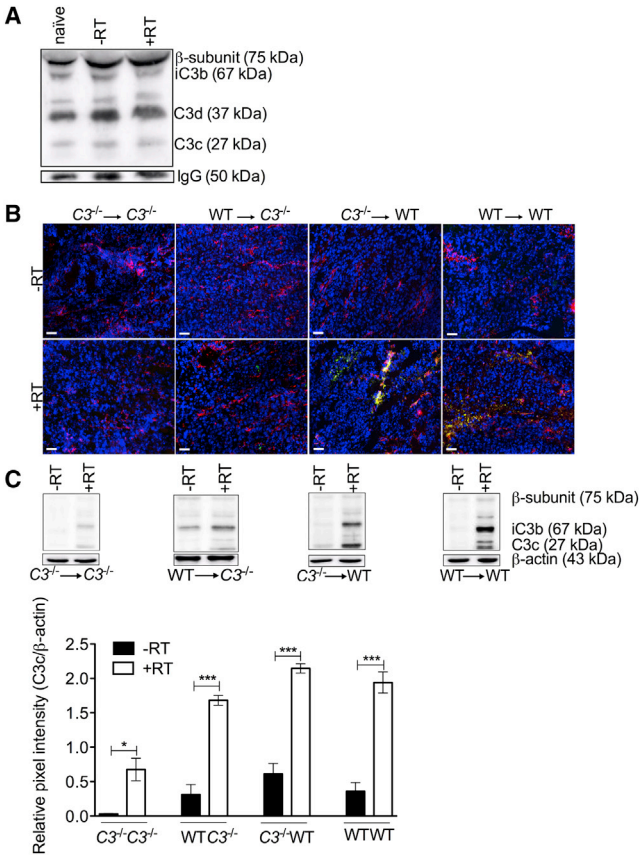

Figure 4. Radiotherapy-Induced, Tumor-Associated Complement Is Mainly Liver-Derived but Partially Produced Locally

(A) Measurement of complement activation by immuno-blot in pooled blood samples from naive, tumor-bearing, and irradiated tumor-bearing mice (24 hr after radiotherapy), (n = 3 mice per group). C3 cleavage products were detected using a polyclonal anti-C3 antibody. Radiotherapy, RT.

(B and C) Bone-marrow chimeras were injected with B16F10-OVA cells and received radiotherapy 13 days later. Tumors were collected 24 hr after radiotherapy (B) Immunofluorescence of irradiated and untreated tumors. Sections were stained with an antibody recognizing C3b, iC3b, and C3c (green), CD31 for blood vessels (red) and DAPI (blue). Scale bars represent 100 μm. Representative images from two independent experiments are shown (n = 4 mice per group). (C) C3 cleavage products in the tumors were analyzed by immuno-blot using a polyclonal anti-C3 antibody, (n = 3 mice per group). Relative expression measured by Bio-1D software. Representative data from two independent experiments are shown.

Data in (C) are shown as the mean ± SD. *$p < 0.05$, ***$p < 0.0005$ by two-way ANOVA with the Bonferroni correction.

tumor tissue. Already 1 hr after radiation, the first signs of radiation damage were detected in the form of extensive vacuolization of tumor cells with normal nuclei and cell boundaries. Already 4 hr after radiation, cell boundaries were dissolved and cellular content fragmented. Mitochondrial structures (M) were swollen and did not show normal cristae. This did not change any further between 4 and 18 hr after radiotherapy. We did not observe any nuclear fragmentation and apoptotic bodies; rather, the irradiated tissue showed marked fields of necrosis with many intracellular materials now entering the extracellular space.

Because immunoglobulin M (IgM) binds to necrotic cells, which results in complement activation (Ciurana et al., 2004; Quartier et al., 2005), we performed the experiment described above using serum from *Rag1*$^{-/-}$ mice. We observed reduced complement activation in supernatants containing *Rag1*$^{-/-}$ serum (Figures 3D and 3E), suggesting that IgM binding to necrotic cells contributes to radiotherapy-induced complement activation. This suggests that necrotic tumor cells express or secrete factors that activate complement.

Microenvironmental Complement Is Produced by Immune Cells

Hepatocytes are the main source of complement proteins, but also extra-hepatic tissues and immune cells can produce them (Farrar and Sacks, 2014; Kolev et al., 2014; Pio et al., 2014; Strainic et al., 2008). To define the source of radiotherapy-induced, tumor-associated complement, we generated *C3*$^{-/-}$→WT, WT→*C3*$^{-/-}$, WT→WT, and *C3*$^{-/-}$→*C3*$^{-/-}$ bone marrow chimeras. B16F10-OVA bearing chimeras received radiotherapy or not and tumors were processed 24 hr later. We detected high amounts of activated complement in *C3*$^{-/-}$→WT and WT→WT mice and less in WT→*C3*$^{-/-}$ mice. The low amount of complement detected in irradiated tumors in *C3*$^{-/-}$→*C3*$^{-/-}$ mice is presumably tumor-derived (Figures 4B and 4C). This is in agreement with the detection of basal expression of complement-related transcripts in cultured B16F10-OVA tumor cells and an increased release of complement proteins by B16F10-OVA cells upon in vitro irradiation (Figures 3A, 3B, and 4C). These experiments suggest that a large fraction of radiotherapy-induced, tumor-associated complement is produced systemically, with a contribution of local production by immune and tumor cells.

Radiotherapy-Induced DC Activation Depends on Anaphylatoxins

Because several immune cells can produce complement components (Li et al., 2007; Strainic et al., 2008), which are essential for full functional development of antigen-presenting cells (APCs) and T cell responses (Peng et al., 2009; Strainic et al., 2008), we investigated which immune cells produce complement or anaphylatoxin receptors in irradiated tumors. We sorted DCs, CD8$^+$ T cells, CD4$^+$ T cells, and other CD45.2$^+$ cells from irradiated and untreated tumors (Figure S3A) and quantified the complement factor related transcripts *C3*, *C1s*, *Masp2*, *Cfb*, *C3ar1*, and *C5ar1* by qPCR. Because the impact of radiotherapy on tumor-associated DCs and T cells is apparent after 24 hr and 5–7 days, respectively (Gupta et al., 2012), we harvested tumors at these time points after radiotherapy exposure. DCs showed increased expression of *C3, Cfb*, *C3ar1*, and *C5ar1* 24 hr and 168 hr after radiotherapy (Figure 5A). We failed to detect expression of *C1s* and *Masp2* transcripts by DCs. The other CD45.2$^+$ cells (mainly containing macrophages) showed upregulated *C5ar1* but no other complement-related transcripts at 168 hr after radiotherapy (Figure S3B).

Recent studies demonstrate that complement factors, in particular anaphylatoxins, directly bind to their receptors on DCs thereby supporting their maturation, which then induces T cell effector activation (Li et al., 2007; Peng et al., 2009; Strainic et al., 2008). Furthermore, we showed previously that radiotherapy-induced activation of tumor-associated dendritic cells locally supports the function of tumor-specific CD8$^+$ T cells

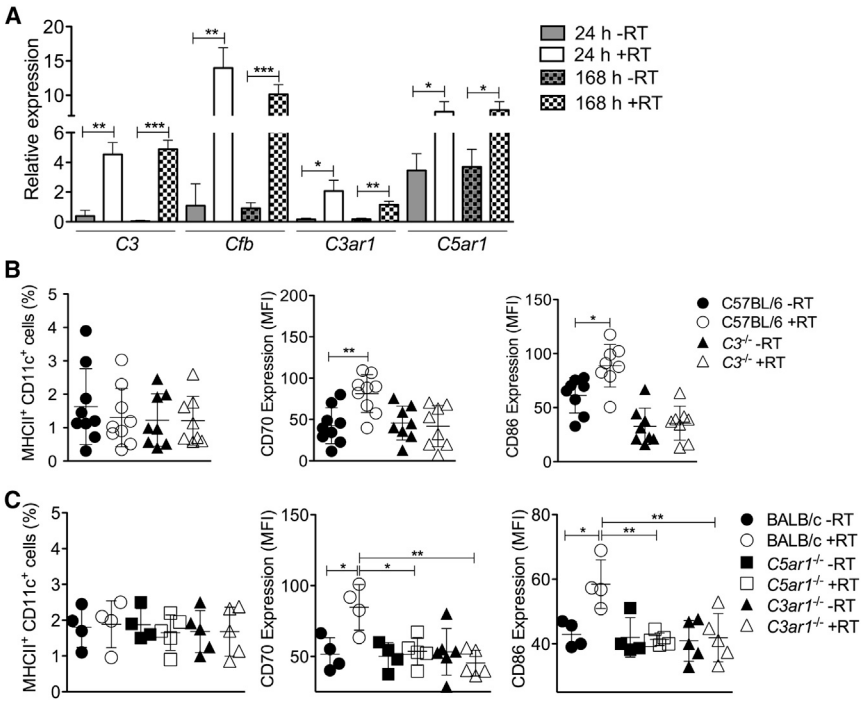

Figure 5. Radiotherapy Induces Upregulation of Transcripts for Complement and Anaphylatoxins Receptors by DCs and Is Essential to Their Maturation

(A) Mice were injected with B16F10-OVA cells and received radiotherapy 12 days later. DCs ($CD45.2^+$ $TCR\beta^-$ $CD11c^+$ MHC-II^{high} gated on live singlets) were sorted from untreated and irradiated tumors 24 and 168 hr after radiotherapy. Complement-related transcripts were quantified by qPCR (n = 5 mice per group). Radiotherapy, RT.

(B) Control and $C3^{-/-}$ mice were injected with B16F10-OVA cells and received radiotherapy 12 days later. CD70 and CD86 expression on tumor-associated DCs in irradiated (48 hr after radiotherapy) and untreated tumors plotted as geometric mean fluorescence intensity (gMFI).

(C) BALB/c, $C3ar1^{-/-}$, and $C5ar1^{-/-}$ mice were injected with CT26 cells and received radiotherapy 12 days later. DCs were analyzed as described in (B).

(B and C) Each symbol represents an individual mouse. Pooled data from two independent experiments are shown. Data are shown as the mean ± SD. *p < 0.05, **p < 0.005, ***p < 0.0005 by two-way ANOVA with the Bonferroni correction. See also Figure S3.

and that this is crucial to therapeutic efficacy (Gupta et al., 2012). Therefore, we analyzed the activation status of DCs upon irradiation in $C3^{-/-}$ and in C57BL/6 mice 2 days after radiotherapy. DCs were equally present in untreated and irradiated tumors of complement-proficient and -deficient mice, however, DC activation as measured by surface expression of CD70 and CD86 (Keller et al., 2008) was observed only in irradiated C57BL/6, but not in $C3^{-/-}$ mice (Figure 5B). These results were confirmed using $C3ar1^{-/-}$, $C5ar1^{-/-}$, and BALB/c mice (Figure 5C). Thus, radiotherapy induces upregulation of anaphylatoxins, and their receptors in tumor-associated DCs controls radiotherapy-induced DC activation.

Radiotherapy-Induced $CD8^+$ T Cell Activation Depends on Anaphylatoxins

T cells express complement components and anaphylatoxin receptors that are critical to T cell co-stimulation (Liszewski et al., 2013; Strainic et al., 2008). $CD8^+$, but not $CD4^+$ T, cells upregulated *C3* and the anaphylatoxin receptors slowly at 168 hr, but not at 24 hr, after radiotherapy (Figures 6A and S3C), whereas *C1s* and *Masp2* were undetectable. C5aR1 and C3aR1 signaling during cognate interaction between DCs and $CD4^+$ T cells promotes IFN-γ production (Liu et al., 2008) and counteracts the development of $FoxP3^+$ regulatory T cells (Strainic et al., 2013). We therefore analyzed the impact of radiotherapy on expression of *Ifng* and *Foxp3* and observed a strong upregulation of *Ifng* in $CD8^+$ T cells 168 hr after the treatment (Figure 6A), but no changes of *Foxp3* within the $CD4^+$ T cell compartment (data not shown).

To investigate the in vivo relevance of those observations, we analyzed the infiltrate in tumors from BALB/c and $C3ar1^{-/-}C5ar1^{-/-}$ mice by flow cytometry 168 hr after radiotherapy. Radiotherapy resulted in higher numbers of $CD45.2^+$ and $CD8^+$ T cells in tumors, which was independent of anaphylatoxins (Figure 6B). Radiotherapy had no effect on $CD4^+$ T cell numbers (Figures 6C and 6D). Therefore, it is unlikely that anaphylatoxins act as chemoattractants for T cells. We analyzed the global IFN-γ production by tumor-infiltrating $CD8^+$ T cells in situ. Therefore, we injected mice with Brefeldin A 4 hr before euthanasia and measured intracellular IFN-γ without in vitro restimulation. IFN-γ production by $CD8^+$ T cells was significantly increased in irradiated tumors in BALB/c, but not $C3ar1^{-/-}C5ar1^{-/-}$ mice compared to untreated controls (Figures 6C, S4A, and S4B). This presumably involves anaphylatoxin-mediated DC maturation (Strainic et al., 2013), although a direct activity of anaphylatoxins on $CD8^+$ T cells cannot be excluded. In agreement with earlier data (Strainic et al., 2013), we observed higher numbers of $FoxP3^+$ T cells in $C3ar1^{-/-}C5ar1^{-/-}$ mice independent of radiotherapy (Figures 6D, S4C, and S4D). Flow cytometry results thus confirmed the qPCR data on sorted cells (Figure 6A). We obtained similar results using B16F10-OVA-bearing C57BL/6 mice in which C3aR1 and C5aR1 were blocked (Figure S4E). A recent publication shows that blocking C3 improves the efficacy of fractionated radiotherapy given as multiple daily fractions of 1.5 Gy (Elvington et al., 2014), which is an apparent controversy with our findings. We found that 5× 1.5 Gy equally diminished tumor growth as 1× 20 Gy did. However, in contrast to a single high dose, 5× 1.5 Gy resulted in prolonged activation of complement and did not support accumulation of $CD8^+$ T cells nor their function in the tumor (Figures S4G–S4I).

To generate a complete immune cell profile related to irradiation responses, we analyzed $CD19^+$ B cells and found low numbers (Figure S4F), regardless of radiotherapy or blockade of C5aR1 and C3aR1. Tumors contained substantial numbers of $NK1.1^+$ cells that significantly increased upon

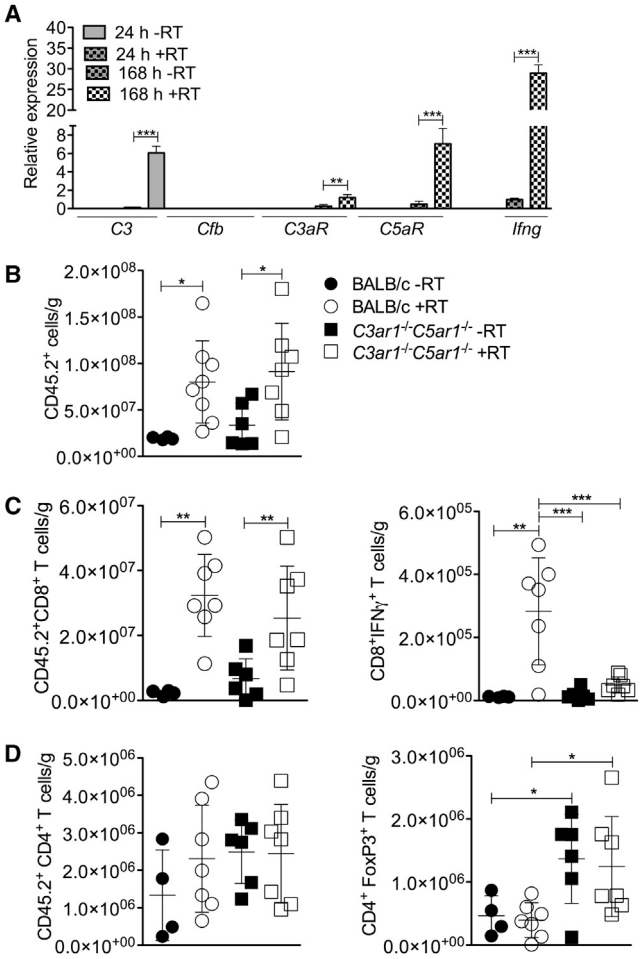

Figure 6. Radiotherapy Induces Upregulation of Transcripts for Complement and Anaphylatoxins Receptors by CD8$^+$ T Cells and Supports Tumor-Specific Immunity

(A) C57BL/6 mice were injected with B16F10-OVA cells and received radiotherapy 12 days later. CD8$^+$ T cells (CD45.2$^+$ TCRβ$^+$ CD8$^+$ gated on live singlets) were sorted from untreated and irradiated tumors 24 and 168 hr after radiotherapy. Complement-related transcripts were quantified by qPCR (n = 5 mice per group). Radiotherapy, RT.

(B–D) BALB/c and *C3ar1*$^{-/-}$*C5ar1*$^{-/-}$ mice were injected with CT26 cells and received radiotherapy 12 days later. Flow cytometric analysis was performed 7 days after radiotherapy. (B) The total number of infiltrating leukocytes (CD45.2$^+$), (C) CD8$^+$ cells (left panel), and CD8$^+$ T cells that produce IFN-γ in vivo (right panel), (D) CD4$^+$ (left panel) and FoxP3$^+$ CD4$^+$ T cells (right panel) were determined per gram tumor tissue. Mice were injected with Brefeldin A 4 hr before euthanasia.

Each symbol represents an individual mouse. Data are shown as the mean ± SD. *p < 0.05, **p < 0.005, ***p < 0.0005 by two-way ANOVA with the Bonferroni correction. See also Figure S4.

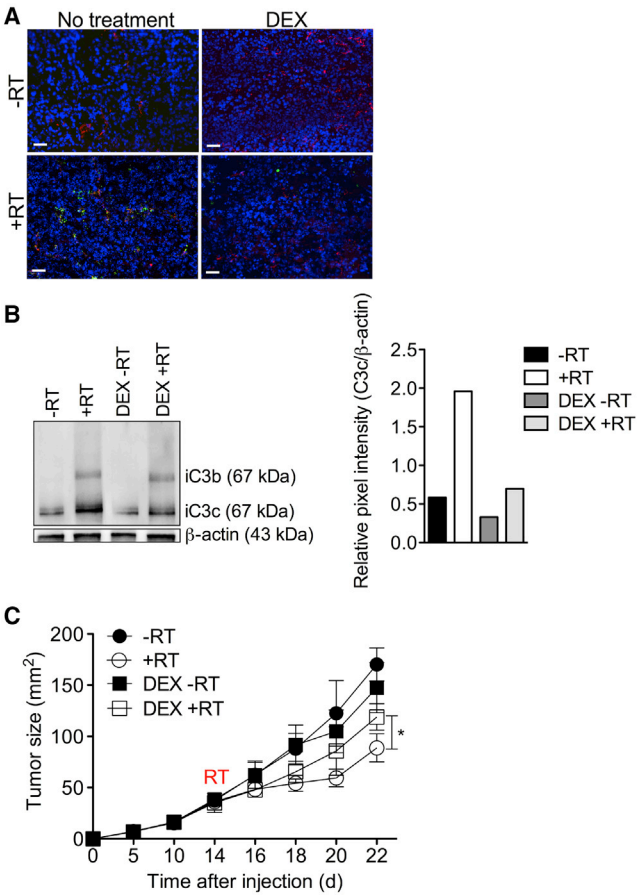

Figure 7. Dexamethasone Inhibits Complement Activation and Reduces the Clinical Efficacy of Radiotherapy

(A–C) Mice were injected with B16F10-OVA cells and received radiotherapy 14 days later. DEX (0.3 mg/kg) was injected daily from day 12 until day 22, (n = 6 mice per group). (A) Immunofluorescence of irradiated (24 hr) and untreated tumors. Sections were stained with an antibody recognizing C3b, iC3b, and C3c (green), CD31 for blood vessels (red), and DAPI (blue). Scale bars represent 100 μm. Representative images are shown. (B) C3 cleavage products in the tumors 24 hr after radiotherapy were analyzed by immuno-blot using a polyclonal anti-C3 antibody. Relative expression measured by Bio-1D software. Representative data are shown. (C) Tumor growth curves.

The data are shown as the mean ± SD. *p < 0.05 by two-way ANOVA with the Bonferroni correction. Radiotherapy, RT.

radiotherapy and seemed independent of anaphylatoxin receptor blockade. We observed very low numbers of NKp46$^+$ cells that remained similar in all four groups (Figure S4F). Thus, following a single dose of 20 Gy, the DC-CD8-arm of the immune system appears to be selectively activated in irradiated tumors, which is essential for tumor control and depends on complement.

Dexamethasone (DEX) is a glucocorticoid with anti-inflammatory and immunosuppressive properties (Auphan et al., 1995). In addition, it inhibits the activation of complement (Engelman et al., 1995; Packard and Weiler, 1983). Given the important role of complement in promoting adaptive immunity and supporting the efficacy of radiotherapy, we treated mice with DEX starting 1 day before radiotherapy. DEX treatment significantly reduced the extent of local complement activation (Figure 7A) and importantly, also the efficacy of radiotherapy (Figures 7B and 7C).

Thus, radiotherapy-induced, local production of anaphylatoxins is essential to activation of DCs and protective effector function of CD8$^+$ T cells in the tumor and as such to therapeutic efficacy.

DISCUSSION

In this study, we have demonstrated that radiotherapy induces an acute and transient local activation of complement, which is pivotal for tumor-specific immunity and therapeutic efficacy. Complement has traditionally been considered only to "complement" the action of the immune system in the antibody-mediated defense against pathogens. The current appreciation is that complement is involved in many different pathological processes such as transplant rejection, autoimmunity, neurodegeneration, and cancer.

The role of complement in cancer is still confusing as the production of complement-inhibiting proteins by tumor cells or stroma has been suggested to promote tumor growth (Kolev et al., 2011), whereas it is also proposed that complement in the context of chronic inflammation promotes tumor growth, migration and angiogenesis (Markiewski et al., 2008; Pio et al., 2014). This is in line with a previous publication (Elvington et al., 2014) showing increased efficacy of fractionated radiotherapy when C3 was blocked. Repeated irradiation might thus induce a chronic inflammatory response that interferes with protective adaptive immunity. In addition, the infiltrating T cells might be killed by the next dose before they could execute their anti-tumor effect. A different radiotherapy protocol that either introduces a radiotherapy holiday of 7–10 days between the fractions of radiotherapy or provides a single high-dose of radiotherapy might be required to optimally support tumor-specific immunity (Favaudon et al., 2014).

Pathogen- and damage-associated molecular patterns can activate C1q, MBL, and the alternative complement pathway. The latter can also be activated by spontaneous hydrolysis of C3 or by non-complement proteins (Markiewski and Lambris, 2007). Furthermore, modified membranes of late apoptotic and necrotic cells are potent activators of complement (Ricklin et al., 2010). In fact, every disturbance of homeostasis or assault might result in activation of complement (Kolev et al., 2014). Our data suggest that factors released from necrotic tumor cells upon radiotherapy are responsible for local complement activation. The leakiness of tumor-associated blood vessels (Carmeliet and Jain, 2011) might further promote accumulation of complement in the tumor.

The liver is the main source of complement, but many complement components can be produced by a variety of tissues and immune cells either constitutively or in response to stress (Kolev et al., 2014; Li et al., 2007). For example, locally produced C1q contributes to removal of apoptotic material and immune complexes (Roumenina et al., 2011) and supports T cell responses (Baudino et al., 2014). We have shown here that tumor-associated T cells, DCs, other CD45$^+$ cells, as well as tumor cells can be a source of anaphylatoxins and their receptors in response to radiotherapy. It is plausible to consider that tumor-associated stroma might also contribute to the production of complement upon radiotherapy.

Sensing immune cell-derived complement during cognate interactions between T cells and DCs is essential for development of protective immunity (Lalli et al., 2007; Liszewski et al., 2013; Peng et al., 2009; Strainic et al., 2008). Moreover, when signaling through C3aR1 and C5aR1 is prevented during cognate interactions, CD4$^+$ T cells develop into FoxP3$^+$ regulatory T (Treg) cells instead of effectors (Strainic et al., 2013), in line with our observation that tumors contained more Treg cells in the absence of anaphylatoxin receptor signaling. We found that tumor-associated DCs produced complement factors and upregulated the expression of C3aR1 and C5aR1 upon radiotherapy, which appeared to be essential for radiotherapy-induced DCs maturation. It has been shown that anaphylatoxins directly can induce DC maturation in vitro and that C3 upregulation precedes the expression of IL-1, IL-12, and IL-23 (Strainic et al., 2008), suggesting a direct effect of anaphylatoxins on DCs. DC maturation is crucial to development and/or maintenance of T cell effector function within the tumor and efficacy of radiotherapy (Gupta et al., 2012), and indeed, tumor-infiltrating CD8$^+$ T cells failed to produce IFN-γ after radiotherapy in the absence of signaling through C3aR1 and C5aR1.

Given the importance of complement activation and immune response following local radiotherapy, the administration of glucocorticoids, anti-inflammatory, and immunosuppressive drugs for managing post-radiation symptoms (Hempen et al., 2002; Hughes et al., 2005) might have a modulating impact on the efficacy of radiotherapy. Indeed, DEX given around the time of radiotherapy significantly diminishes its efficacy, suggesting that treatment with glucocorticoids or other anti-inflammatory or immunosuppressive drugs might decrease the clinical response of cancer patients to radiotherapy.

The stimulation of tumor-specific immunity by standard therapies including radio- and chemotherapy has been documented in several publications (Formenti and Demaria, 2012; Gupta et al., 2012; Matsumura et al., 2008; Reits et al., 2006; Sharma et al., 2013) and this phenomenon might actually be of great clinical importance: dormant metastases are intrinsically resistant to standard treatments that mainly target rapidly dividing cells but might still be susceptible to immune-mediated control (Koebel et al., 2007). The abscopal effect—a situation in which not only the irradiated tumor but also distant lesions show a clinical response—can be explained as such. When radiotherapy is combined with immune stimulation by anti-CTLA-4 antibodies, the abscopal effect becomes readily apparent (Postow et al., 2012; Verbrugge et al., 2014).

Our data expand the role of complement in the defense against tumors. Tumor-specific immunity is unleashed by locally produced anaphylatoxins in response to radiotherapy that activate DCs and then CD8$^+$ T cells for optimal tumor control following radiotherapy.

EXPERIMENTAL PROCEDURES

Mice and Cell Lines

C57BL/6, *C3*$^{-/-}$, BALB/cJ, *C5ar1*$^{-/-}$, *C3ar1*$^{-/-}$, and *Rag1*$^{-/-}$ mice were purchased from the Jackson Laboratory. *C3*$^{-/-}$ mice were on a C57BL/6.129S4 background; *C3ar1*$^{-/-}$ and *C5ar1*$^{-/-}$ mice on a BALB/cJ background, *Rag1*$^{-/-}$ mice were on a C57BL/6 background. We generated *C5ar1*$^{-/-}$ *C3ar1*$^{-/-}$ mice by crossing *C5ar1*$^{-/-}$ and *C3ar1*$^{-/-}$ mice. All mice were bred and maintained in specific pathogen-free facilities at the University of Zurich and University Hospital of Zurich. C57BL/6 → *C3*$^{-/-}$, *C3*$^{-/-}$ → C57BL/6, *C3*$^{-/-}$ → *C3*$^{-/-}$, and C57BL/6 → C57BL/6 bone-marrow chimeras were generated as previously described (Probst et al., 2003). All experiments were performed with age- and sex-matched mice in accordance with the guidelines of the Swiss federal and cantonal laws on animal protection.

B16F10 melanoma cells (ATCC) and B16F10-OVA (B16F10 stably transfected to express chicken ovalbumin as neo-antigen, provided by Melody

Swartz, EPFL) were cultured in Dulbecco's modified Eagle's medium (DMEM, GIBCO Invitrogen), CT26 murine colon carcinoma (ATCC) cells in MEM medium (Invitrogen). Media were supplemented with 10% fetal calf serum, 5×10^{-5} M 2-mercaptoethanol, 10 mM sodium pyruvate 2 mM L-glutamine, and antibiotics.

In Vivo Experiments

2×10^5 B16F10-OVA, B16F10 or CT26 were injected s.c. in 100 μl of a 1:1 mix of PBS and Matrigel Basement Membrane Matrix (BD Biosciences).

Local radiotherapy with a single dose of 20 or 5 Gy was performed at indicated time points using a Xstrahl 200 kV X-ray unit at 1 Gy/min as described (Gupta et al., 2012). Prior to radiotherapy, mice were anaesthetized by i.p. injection of 50 mg/kg ketamine and 10 mg/kg xylazine.

The C3aR1 antagonist (C3aRA) N2-[(2,2-Diphenylethoxy)acetyl]-L-arginine (SB290157, Calbiochem) was administered i.p. at 2 mg/kg body weight in 100 μl PBS. Anti-C5aR1 mAb 20/70 (Hycult Biotech) or an isotype control (rat IgG2b anti-HLA-DR, clone SFRF8B6) was administered i.p. at 0.6 mg/kg in 100 μl PBS (Baelder et al., 2005; Godau et al., 2004; Sun et al., 2011). C3aRA and anti-C5aR1 mAb were administered every second day starting at the day of radiotherapy until the end of the experiment.

To measure the cytokine production in vivo, we injected Brefeldin A (BFA, Sigma-Aldrich). A 20-mg/ml stock was prepared in DMSO. Further dilution to 0.5 mg/ml was made in PBS, and 500 μl was injected i.p. 4 hr before mice were sacrificed (Liu and Whitton, 2005). DEX (Sigma-Aldrich) was administered daily at 0.3 mg/kg in PBS p.o., starting 1 day before radiotherapy. Tumors were measured with a caliper every 2–3 days in two dimensions (length and width). Excised tumors were weighed and processed for flow cytometry, histology, or isolation of RNA and proteins.

In Vitro Experiments

C57BL/6 and *C3*$^{-/-}$ mice were bled from the sublingual vein and sera were collected with Microtainer SST tubes (BD). Sera were diluted 1:10 with PBS, irradiated with 20 Gy (YXLON Y.SMART582, YXLON International GmbH, Hamburg, D) and subsequently incubated at 37°C. B16F10-OVA cells were cultured in 6-well plates (10^6 cells per well) and irradiated as described above. Immediately after irradiation, 60 μl of serum from C57BL/6 or *C3*$^{-/-}$ mice diluted in 500 μl of PBS was added to the cells. Control samples were not irradiated but treated similarly otherwise. Supernatants were taken 4 hr and 24 hr after irradiation and were stored at −80°C until further use.

Human Samples

Two sets of biopsies were provided by the Department of Dermatology, University Hospital Zurich. Patients signed informed consent. The ethical committee of the canton of Zurich approved this study (EK647). (1) Paired biopsies were collected from two patients with basal cell carcinoma and one with lentigo maligna melanoma immediately before and 24–36 hr after radiotherapy (1.5–2 Gy) and were snap frozen. (2) Four biopsies were collected from four patients (two with basal cell carcinoma, one with melanoma, and one with squamous cell carcinoma) 24–36 hr after radiotherapy (1.5–2 Gy) but without previous interventions and were snap frozen.

Statistical Analysis

Results are presented as mean ± SD. Statistical significance was determined by ANOVA using GraphPad Prism 5 software (GraphPad). When multiple groups were compared, we used the Bonferroni post-test correction. When two groups were compared, we used the two-tailed Student's t test. *, $p < 0.05$; **, $p < 0.01$; ***, $p < 0.001$.

SUPPLEMENTAL INFORMATION

Supplemental Information includes four figures and Supplemental Experimental Procedures and can be found with this article online at http://dx.doi.org/10.1016/j.immuni.2015.03.009.

AUTHOR CONTRIBUTIONS

L.S., A.K., A.G., and M.v.d.B. conceptualized the study and designed experiments; L.S. conducted the majority of the experiments; V.L. and A.B. performed immuno-blot experiments; M.O. created heatmaps and performed bioinformatics analyses; A.O.F. and M.P. irradiated mice; V.C. sorted cells and performed some experiments; R.D. provided patient biopsies; H.J. and J.N. performed electron microscopy; and L.S. and M.v.d.B. wrote the manuscript.

ACKNOWLEDGMENTS

We thank Melody Swartz (EPFL Lausanne, Switzerland) for providing the B16F10-OVA cell line; Jovan Pavlovic (Institute of Medical Virology, University of Zurich) for providing antibodies against JAK and STAT; James Di Santo (Department of Immunology, Institute Pasteur, Paris) for providing anti-NK1.1 antibody; Claudia Matter (Clinic for Oncology, University Hospital Zurich, Switzerland) and Karina Silina (Institute of Experimental Immunology, University of Zurich) for technical assistance; personnel from the Biologisches Zentrallabor (University Hospital of Zurich) for expert animal care; Alessandra Curioni-Fontecedro (Clinic for Oncology, University Hospital of Zurich) for helpful discussion; and Burkhard Becher, Christian Münz, Ali Bransi (Institute of Experimental Immunology, University of Zurich), Sabine Werner (Institute of Cell Biology, ETH, Zurich), Stefano Ferrari (Institute of Molecular Cancer Research, University of Zurich), Mark Robert Nicolls (Department of Medicine, Stanford Medicine), and John Lambris (Department of Pathology, University of Pennsylvania) for scientific support and critically reading the manuscript. This work was financially supported by the Swiss National Science Foundation (SNSF), the Vontobel Foundation Zurich, and the University Research Priority Program (URPP) "Translational Cancer Research."

Received: July 1, 2014
Revised: January 16, 2015
Accepted: March 21, 2015
Published: April 14, 2015

REFERENCES

Apetoh, L., Ghiringhelli, F., Tesniere, A., Obeid, M., Ortiz, C., Criollo, A., Mignot, G., Maiuri, M.C., Ullrich, E., Saulnier, P., et al. (2007). Toll-like receptor 4-dependent contribution of the immune system to anticancer chemotherapy and radiotherapy. Nat. Med. *13*, 1050–1059.

Auphan, N., DiDonato, J.A., Rosette, C., Helmberg, A., and Karin, M. (1995). Immunosuppression by glucocorticoids: inhibition of NF-kappa B activity through induction of I kappa B synthesis. Science *270*, 286–290.

Baelder, R., Fuchs, B., Bautsch, W., Zwirner, J., Köhl, J., Hoymann, H.G., Glaab, T., Erpenbeck, V., Krug, N., and Braun, A. (2005). Pharmacological targeting of anaphylatoxin receptors during the effector phase of allergic asthma suppresses airway hyperresponsiveness and airway inflammation. J. Immunol. *174*, 783–789.

Basu, S., Binder, R.J., Suto, R., Anderson, K.M., and Srivastava, P.K. (2000). Necrotic but not apoptotic cell death releases heat shock proteins, which deliver a partial maturation signal to dendritic cells and activate the NF-kappa B pathway. Int. Immunol. *12*, 1539–1546.

Baudino, L., Sardini, A., Ruseva, M.M., Fossati-Jimack, L., Cook, H.T., Scott, D., Simpson, E., and Botto, M. (2014). C3 opsonization regulates endocytic handling of apoptotic cells resulting in enhanced T-cell responses to cargo-derived antigens. Proc. Natl. Acad. Sci. USA *111*, 1503–1508.

Burnette, B.C., Liang, H., Lee, Y., Chlewicki, L., Khodarev, N.N., Weichselbaum, R.R., Fu, Y.X., and Auh, S.L. (2011). The efficacy of radiotherapy relies upon induction of type i interferon-dependent innate and adaptive immunity. Cancer Res. *71*, 2488–2496.

Carmeliet, P., and Jain, R.K. (2011). Molecular mechanisms and clinical applications of angiogenesis. Nature *473*, 298–307.

Chen, G., Tan, C.S., Teh, B.K., and Lu, J. (2011). Molecular mechanisms for synchronized transcription of three complement C1q subunit genes in dendritic cells and macrophages. J. Biol. Chem. *286*, 34941–34950.

Ciurana, C.L., Zwart, B., van Mierlo, G., and Hack, C.E. (2004). Complement activation by necrotic cells in normal plasma environment compares to that

by late apoptotic cells and involves predominantly IgM. Eur. J. Immunol. *34*, 2609–2619.

Dunn, G.P., Koebel, C.M., and Schreiber, R.D. (2006). Interferons, immunity and cancer immunoediting. Nat. Rev. Immunol. *6*, 836–848.

Elvington, M., Scheiber, M., Yang, X., Lyons, K., Jacqmin, D., Wadsworth, C., Marshall, D., Vanek, K., and Tomlinson, S. (2014). Complement-dependent modulation of antitumor immunity following radiation therapy. Cell Rep. *8*, 818–830.

Engelman, R.M., Rousou, J.A., Flack, J.E., 3rd, Deaton, D.W., Kalfin, R., and Das, D.K. (1995). Influence of steroids on complement and cytokine generation after cardiopulmonary bypass. Ann. Thorac. Surg. *60*, 801–804.

Eriksson, D., and Stigbrand, T. (2010). Radiation-induced cell death mechanisms. Tumour biology: the journal of the International Society for Oncodevelopmental Biology and Medicine *31*, 363–372.

Farrar, C.A., and Sacks, S.H. (2014). Mechanisms of rejection: role of complement. Curr. Opin. Organ Transplant. *19*, 8–13.

Favaudon, V., Caplier, L., Monceau, V., Pouzoulet, F., Sayarath, M., Fouillade, C., Poupon, M.F., Brito, I., Hupe, P., Bourhis, J., et al. (2014). Ultrahigh dose-rate FLASH irradiation increases the differential response between normal and tumor tissue in mice. Science translational medicine *6*, 245ra293.

Formenti, S.C., and Demaria, S. (2012). Radiation therapy to convert the tumor into an in situ vaccine. Int. J. Radiat. Oncol. Biol. Phys. *84*, 879–880.

Fridman, W.H., Galon, J., Pagès, F., Tartour, E., Sautès-Fridman, C., and Kroemer, G. (2011). Prognostic and predictive impact of intra- and peritumoral immune infiltrates. Cancer Res. *71*, 5601–5605.

Fuertes, M.B., Kacha, A.K., Kline, J., Woo, S.R., Kranz, D.M., Murphy, K.M., and Gajewski, T.F. (2011). Host type I IFN signals are required for antitumor CD8+ T cell responses through CD8alpha+ dendritic cells. J. Exp. Med. *208*, 2005–2016.

Fukuoka, Y., Hite, M.R., Dellinger, A.L., and Schwartz, L.B. (2013). Human skin mast cells express complement factors C3 and C5. J. Immunol. *191*, 1827–1834.

Godau, J., Heller, T., Hawlisch, H., Trappe, M., Howells, E., Best, J., Zwirner, J., Verbeek, J.S., Hogarth, P.M., Gerard, C., et al. (2004). C5a initiates the inflammatory cascade in immune complex peritonitis. J. Immunol. *173*, 3437–3445.

Gupta, A., Probst, H.C., Vuong, V., Landshammer, A., Muth, S., Yagita, H., Schwendener, R., Pruschy, M., Knuth, A., and van den Broek, M. (2012). Radiotherapy promotes tumor-specific effector CD8+ T cells via dendritic cell activation. J. Immunol. *189*, 558–566.

Hasegawa, M., Yada, S., Liu, M.Z., Kamada, N., Muñoz-Planillo, R., Do, N., Núñez, G., and Inohara, N. (2014). Interleukin-22 regulates the complement system to promote resistance against pathobionts after pathogen-induced intestinal damage. Immunity *41*, 620–632.

Hempen, C., Weiss, E., and Hess, C.F. (2002). Dexamethasone treatment in patients with brain metastases and primary brain tumors: do the benefits outweigh the side-effects? Support. Care Cancer *10*, 322–328.

Huang, Y., Krein, P.M., Muruve, D.A., and Winston, B.W. (2002). Complement factor B gene regulation: synergistic effects of TNF-alpha and IFN-gamma in macrophages. J. Immunol. *169*, 2627–2635.

Hughes, M.A., Parisi, M., Grossman, S., and Kleinberg, L. (2005). Primary brain tumors treated with steroids and radiotherapy: low CD4 counts and risk of infection. Int. J. Radiat. Oncol. Biol. Phys. *62*, 1423–1426.

Keller, A.M., Schildknecht, A., Xiao, Y., van den Broek, M., and Borst, J. (2008). Expression of costimulatory ligand CD70 on steady-state dendritic cells breaks CD8+ T cell tolerance and permits effective immunity. Immunity *29*, 934–946.

Kemper, C., Mitchell, L.M., Zhang, L., and Hourcade, D.E. (2008). The complement protein properdin binds apoptotic T cells and promotes complement activation and phagocytosis. Proc. Natl. Acad. Sci. USA *105*, 9023–9028.

Koebel, C.M., Vermi, W., Swann, J.B., Zerafa, N., Rodig, S.J., Old, L.J., Smyth, M.J., and Schreiber, R.D. (2007). Adaptive immunity maintains occult cancer in an equilibrium state. Nature *450*, 903–907.

Kolev, M., Towner, L., and Donev, R. (2011). Complement in cancer and cancer immunotherapy. Arch. Immunol. Ther. Exp. (Warsz.) *59*, 407–419.

Kolev, M., Le Friec, G., and Kemper, C. (2014). Complement—tapping into new sites and effector systems. Nat. Rev. Immunol. *14*, 811–820.

Kopf, M., Abel, B., Gallimore, A., Carroll, M., and Bachmann, M.F. (2002). Complement component C3 promotes T-cell priming and lung migration to control acute influenza virus infection. Nat. Med. *8*, 373–378.

Lalli, P.N., Strainic, M.G., Lin, F., Medof, M.E., and Heeger, P.S. (2007). Decay accelerating factor can control T cell differentiation into IFN-gamma-producing effector cells via regulating local C5a-induced IL-12 production. J. Immunol. *179*, 5793–5802.

Li, K., Sacks, S.H., and Zhou, W. (2007). The relative importance of local and systemic complement production in ischaemia, transplantation and other pathologies. Mol. Immunol. *44*, 3866–3874.

Liszewski, M.K., Kolev, M., Le Friec, G., Leung, M., Bertram, P.G., Fara, A.F., Subias, M., Pickering, M.C., Drouet, C., Meri, S., et al. (2013). Intracellular complement activation sustains T cell homeostasis and mediates effector differentiation. Immunity *39*, 1143–1157.

Liu, F., and Whitton, J.L. (2005). Cutting edge: re-evaluating the in vivo cytokine responses of CD8+ T cells during primary and secondary viral infections. J. Immunol. *174*, 5936–5940.

Liu, J., Lin, F., Strainic, M.G., An, F., Miller, R.H., Altuntas, C.Z., Heeger, P.S., Tuohy, V.K., and Medof, M.E. (2008). IFN-gamma and IL-17 production in experimental autoimmune encephalomyelitis depends on local APC-T cell complement production. J. Immunol. *180*, 5882–5889.

Lugade, A.A., Moran, J.P., Gerber, S.A., Rose, R.C., Frelinger, J.G., and Lord, E.M. (2005). Local radiation therapy of B16 melanoma tumors increases the generation of tumor antigen-specific effector cells that traffic to the tumor. J. Immunol. *174*, 7516–7523.

Ma, Y., Kepp, O., Ghiringhelli, F., Apetoh, L., Aymeric, L., Locher, C., Tesniere, A., Martins, I., Ly, A., Haynes, N.M., et al. (2010). Chemotherapy and radiotherapy: cryptic anticancer vaccines. Semin. Immunol. *22*, 113–124.

Markiewski, M.M., and Lambris, J.D. (2007). The role of complement in inflammatory diseases from behind the scenes into the spotlight. Am. J. Pathol. *171*, 715–727.

Markiewski, M.M., and Lambris, J.D. (2009). Is complement good or bad for cancer patients? A new perspective on an old dilemma. Trends Immunol. *30*, 286–292.

Markiewski, M.M., DeAngelis, R.A., Benencia, F., Ricklin-Lichtsteiner, S.K., Koutoulaki, A., Gerard, C., Coukos, G., and Lambris, J.D. (2008). Modulation of the antitumor immune response by complement. Nat. Immunol. *9*, 1225–1235.

Matsumura, S., Wang, B., Kawashima, N., Braunstein, S., Badura, M., Cameron, T.O., Babb, J.S., Schneider, R.J., Formenti, S.C., Dustin, M.L., and Demaria, S. (2008). Radiation-induced CXCL16 release by breast cancer cells attracts effector T cells. J. Immunol. *181*, 3099–3107.

McDermott, D.F., and Atkins, M.B. (2013). PD-1 as a potential target in cancer therapy. Cancer Med *2*, 662–673.

Mellman, I., Coukos, G., and Dranoff, G. (2011). Cancer immunotherapy comes of age. Nature *480*, 480–489.

Merrick, A., Errington, F., Milward, K., O'Donnell, D., Harrington, K., Bateman, A., Pandha, H., Vile, R., Morrison, E., Selby, P., and Melcher, A. (2005). Immunosuppressive effects of radiation on human dendritic cells: reduced IL-12 production on activation and impairment of naive T-cell priming. Br. J. Cancer *92*, 1450–1458.

Packard, B.D., and Weiler, J.M. (1983). Steroids inhibit activation of the alternative-amplification pathway of complement. Infect. Immun. *40*, 1011–1014.

Peng, Q., Li, K., Wang, N., Li, Q., Asgari, E., Lu, B., Woodruff, T.M., Sacks, S.H., and Zhou, W. (2009). Dendritic cell function in allostimulation is modulated by C5aR signaling. J. Immunol. *183*, 6058–6068.

Pio, R., Corrales, L., and Lambris, J.D. (2014). The role of complement in tumor growth. Adv. Exp. Med. Biol. *772*, 229–262.

Postow, M.A., Callahan, M.K., Barker, C.A., Yamada, Y., Yuan, J., Kitano, S., Mu, Z., Rasalan, T., Adamow, M., Ritter, E., et al. (2012). Immunologic

correlates of the abscopal effect in a patient with melanoma. N. Engl. J. Med. *366*, 925–931.

Prise, K.M., and O'Sullivan, J.M. (2009). Radiation-induced bystander signalling in cancer therapy. Nat. Rev. Cancer *9*, 351–360.

Probst, H.C., Lagnel, J., Kollias, G., and van den Broek, M. (2003). Inducible transgenic mice reveal resting dendritic cells as potent inducers of CD8+ T cell tolerance. Immunity *18*, 713–720.

Qing, X., Koo, G.C., and Salmon, J.E. (2012). Complement regulates conventional DC-mediated NK-cell activation by inducing TGF-β1 in Gr-1+ myeloid cells. Eur. J. Immunol. *42*, 1723–1734.

Quartier, P., Potter, P.K., Ehrenstein, M.R., Walport, M.J., and Botto, M. (2005). Predominant role of IgM-dependent activation of the classical pathway in the clearance of dying cells by murine bone marrow-derived macrophages in vitro. Eur. J. Immunol. *35*, 252–260.

Reits, E.A., Hodge, J.W., Herberts, C.A., Groothuis, T.A., Chakraborty, M., Wansley, E.K., Camphausen, K., Luiten, R.M., de Ru, A.H., Neijssen, J., et al. (2006). Radiation modulates the peptide repertoire, enhances MHC class I expression, and induces successful antitumor immunotherapy. J. Exp. Med. *203*, 1259–1271.

Ricklin, D., Hajishengallis, G., Yang, K., and Lambris, J.D. (2010). Complement: a key system for immune surveillance and homeostasis. Nat. Immunol. *11*, 785–797.

Roumenina, L.T., Sène, D., Radanova, M., Blouin, J., Halbwachs-Mecarelli, L., Dragon-Durey, M.A., Fridman, W.H., and Fremeaux-Bacchi, V. (2011). Functional complement C1q abnormality leads to impaired immune complexes and apoptotic cell clearance. J. Immunol. *187*, 4369–4373.

Schmudde, I., Laumonnier, Y., and Köhl, J. (2013). Anaphylatoxins coordinate innate and adaptive immune responses in allergic asthma. Semin. Immunol. *25*, 2–11.

Schonthaler, H.B., Guinea-Viniegra, J., Wculek, S.K., Ruppen, I., Ximénez-Embún, P., Guío-Carrión, A., Navarro, R., Hogg, N., Ashman, K., and Wagner, E.F. (2013). S100A8-S100A9 protein complex mediates psoriasis by regulating the expression of complement factor C3. Immunity *39*, 1171–1181.

Schreiber, R.D., Old, L.J., and Smyth, M.J. (2011). Cancer immunoediting: integrating immunity's roles in cancer suppression and promotion. Science *331*, 1565–1570.

Sharma, A., Bode, B., Studer, G., Moch, H., Okoniewski, M., Knuth, A., von Boehmer, L., and van den Broek, M. (2013). Radiotherapy of human sarcoma promotes an intratumoral immune effector signature. Clinical cancer research: an official journal of the American Association for Cancer Research *19*, 4843–4853.

Strainic, M.G., Liu, J., Huang, D., An, F., Lalli, P.N., Muqim, N., Shapiro, V.S., Dubyak, G.R., Heeger, P.S., and Medof, M.E. (2008). Locally produced complement fragments C5a and C3a provide both costimulatory and survival signals to naive CD4+ T cells. Immunity *28*, 425–435.

Strainic, M.G., Shevach, E.M., An, F., Lin, F., and Medof, M.E. (2013). Absence of signaling into $CD4^+$ cells via C3aR and C5aR enables autoinductive TGF-β1 signaling and induction of $Foxp3^+$ regulatory T cells. Nat. Immunol. *14*, 162–171.

Sun, S., Guo, Y., Zhao, G., Zhou, X., Li, J., Hu, J., Yu, H., Chen, Y., Song, H., Qiao, F., et al. (2011). Complement and the alternative pathway play an important role in LPS/D-GalN-induced fulminant hepatic failure. PLoS ONE *6*, e26838.

Takeshima, T., Chamoto, K., Wakita, D., Ohkuri, T., Togashi, Y., Shirato, H., Kitamura, H., and Nishimura, T. (2010). Local radiation therapy inhibits tumor growth through the generation of tumor-specific CTL: its potentiation by combination with Th1 cell therapy. Cancer Res. *70*, 2697–2706.

Verbrugge, I., Gasparini, A., Haynes, N.M., Hagekyriakou, J., Galli, M., Stewart, T.J., Abrams, S.I., Yagita, H., Verheij, M., Johnstone, R.W., et al. (2014). The curative outcome of radioimmunotherapy in a mouse breast cancer model relies on mTOR signaling. Radiat. Res. *182*, 219–229.

Wang, S. (2008). The promise of cancer therapeutics targeting the TNF-related apoptosis-inducing ligand and TRAIL receptor pathway. Oncogene *27*, 6207–6215.

4 Discussion

4.1 Role of homologous recombination and non-homologous end joining in the repair of proton-induced DNA damages

Radiobiological properties of high energy protons have long been considered to be comparable to the sparsely ionizing radiation properties of X-rays. Both are considered low-LET radiation, thus acting primarily through the induction of indirect damage and only minimally by directly damaging the DNA. The oxygen enhancement ratio is indeed very similar for high-energy protons and photons [1-2], as it is the dependence on the two major pathways, HRR and NHEJ, which repairs DNA damage. Therefore, the main focus has been to better understand the physical properties of proton radiation, like the *Bragg* peak improve physical and technology-related aspects of proton radiation, like dose delivery and conformity, development of IMPT or 4D proton therapy, which takes the organ motion into account, rather than deeply understanding the subtle variations in the biological effect of proton radiation.

It is now widely accepted in the clinic to employ an RBE of 1.1 for proton therapy. It is defined as the ratio of the dose of photons (typically 250 keV x-rays) divided by the dose of protons which is needed to result in the same biological effect. This generic value has derived from several *in vitro* studies with tumor or untransformed cell lines. The reasons behind this value have not been clearly identified yet, as there are probably several factors contributing to the RBE. The main differences may rely on different quality (e.g. structure) and/or on quantity (e.g. amount) of proton-induced damage. Furthermore, there may be a differential involvement of the DNA repair pathways, which may become significant only in specific situations where one of them is dysfunctional, for example in tumors bearing specific mutations.

In this PhD study, I have investigated the molecular and biological endpoints after irradiation with high-energy protons and conventional photons using both genetically defined biological systems and pharmacologically active compounds. A special focus has been put on the involvement of DNA double strand break repair machineries after proton vs. photon irradiation in human cancer cell lines. A panel of cell lines with either wild-type status or harboring specific mutations in the DNA repair machinery was used to unravel possible differential sensitivity toward proton radiation. We further implemented our study by employing pharmacologically active compounds to selectively exploit these differences with regards to the clinical perspective.

As has been demonstrated by our group and others, the present work could corroborate the enhanced efficacy of proton irradiation versus photon irradiation with specific regard to cell killing by the proton spot scanning beam used at the Paul Scherrer Institute (PSI).

The increase in RBE points towards a more severe damage after proton radiation compared to photon radiation, which specifically requires the homologous recombination repair pathway to be properly repaired.

The RBE is usually dependent on the dose or survival level chosen, with a decrease in RBE by increase of dose or at low survival levels, specifically with systems with low α/β-ratio [4]. We therefore analyzed the RBE values at the 10% survival level throughout our study, termed RBE_{10}.

In a first set of experiments, published in the *Int. J. Radiat. Oncol. Biol. Phys.*, we have investigated the differential treatment response of photon and proton irradiation in genetically-defined Chinese hamster ovary cells (CHO cells) [3]. These cells are well known in the field of radiation biology to study the effect of ionizing radiation, especially photon radiation. We have used this defined cell system for our initial studies.

We initially have shown that exponentially growing mutant CHO cells deficient in HRR were significantly more sensitive to proton irradiation than photon irradiation, compared to cells with intact homologous recombination repair (HRR) (relative biological effectiveness, RBE_{10} of 1.44±0.06 vs. 1.24±0.03). When these cells were irradiated in plateau (growth arrested) phase, there was no longer a difference in the RBE of the two cell lines (RBE_{10} of 1.29±0.03 vs. 1.27±0.03). In contrast, exponentially growing non-homologous end joining (NHEJ)-deficient cells did not show a specifically enhanced sensitivity to proton irradiation (RBE_{10} of 1.2±0.05, vs. 1.09±0.10). However, after irradiation in plateau phase, these cells became highly radiosensitive and significantly more sensitive to proton radiation. Cells lacking classical, Ku-dependent NHEJ possess only minor backup repair pathways in plateau phase, which possibly can deal with some photon-induced DNA damages but not with proton-induced DNA damages. We further determined initial DNA DSBs, repair kinetics, cell-cycle distributions, and chromosomal aberrations in CHO cells with different genetic mutations. No quantitative differences in initially induced γH2AX and 53BP1 foci could be determined in response to the two types of ionizing radiation. The repair kinetics of DNA damage in wild type cells were the same after both types of radiation (γH2AX, RAD51, and 53BP1 foci), even though proton irradiation resulted in more residual chromosomal DNA fragments and lethal chromosome aberrations. Interestingly, the repair kinetics in HRR-deficient cells was significantly delayed after proton irradiation, leading to an elevated amount of residual γH2AX-foci 24 h after irradiation (45 % vs. 27 % γH2AX foci after protons vs. photons, respectively). Thus, these data show the same amount of initial DNA DSBs after both types of radiation and rather point to a differential damage pattern.

As all previous experiments have been performed with Chinese hamster ovary cells, we decided to probe if human cancer cells also display the same pattern of differential requirement of the two main DNA DSB repair pathways. For our study we chose the non-small cell lung cancer cell line A549 [5-6]. A549 cells represent a good model for *in vitro* studies. They are a p53 wild-type, but harbor a mutation in the KRAS oncogene [7]. Therefore, they are fast proliferating cells, with a doubling time rate of approximatively 19 hours. Irradiation of A549 cells with high-energy protons resulted in an RBE_{10} of 1±0.04. The reasons behind this small RBE_{10} value may be several, but it is known that NSCLC cells, including A549 typically overexpress several HRR proteins, including RAD51 [8]. Increased levels of HRR may be responsible for an efficient processing of the more complex, proton-induced DNA damage. Therefore, these cells may be more prone to repair proton-induced damages than cells with low HRR levels, in which the RBE may draw to a value of 1. The same pattern was also observed in γH2AX-foci kinetic analysis, namely irradiation of A549 cells with 1Gy of both radiation types resulted in the same foci kinetic profile, e.g. the same amount of initial and residual foci was observed. This was coupled with an identical cell cycle profile after both proton and photon radiation, with approximatively 50% of cells in G_2-arrest after 24 hours. Thus, proton-induced damages in wild-type A549 presumably seem to be repaired in a similar way than photon-induced damage.

To further investigate the two main pathways in detail, we analyzed the repair kinetics for DNA-PKcs at both Ser-2056 and Thr-2609 clusters to investigate NHEJ along with RAD51 and RPA32-foci to investigate HRR. We observed a time-dependent increase of RAD51 and RPA32-foci formation in these cells 1 hour and 4 hour after photon ionizing radiation. Proton irradiation induced similar amount of foci, suggesting HRR is activated in a similar way after both types of ionizing radiation. On the other hand, DNA-PKcs activation was strongly hampered after proton radiation compared to photon radiation, with a reduction of about 40% after 1 hour for both phosphorylation clusters analyzed. Therefore, even if the cell killing in A549 cells appears to be equal, there is a differential involvement of the DNA repair pathways present after proton and photon radiation.

We therefore investigated the role of DNA-PKcs in more detail by selectively inhibiting the catalytic subunit with the novel compound NU7026, which interferes with Ser-2056 auto-phosphorylation, therefore blocking the synaptic resolution process [9].

After DBS induction by ionizing radiation, DNA break recognition by the high-affine Ku70/Ku80 heterodimer takes place, which in turn recruits DNA-PKcs to form the DNA-PK complex. Ku70/Ku80 bound to DNA-PKcs is forming a channel where the DNA fits in and differs from the conformation of unbound DNA-PKcs. The interaction of two DNA-PKcs molecules on adjacent sides of the DSB (a configuration often referred to as a synaptic complex) stimulates the protein kinase activity of DNA-PKcs and causes *trans*-autophosphorylation at both Ser-2056 and Thr-2609 cluster regions, leading to the dissociation of the DNA-PK catalytic subunit from the synaptic complex.

NU7026 is a potent chemo- and radiosensitizing compound, and it is currently in clinical evaluation for several malignancies. Again, we observed potent radiosensitization toward photon, but to a much lesser extent toward proton radiation.

As expected, γH2AX removal was strongly delayed in treated cells after photon radiation, but it was surprisingly only minimally affected after proton radiation. The same pattern was observed in the levels of 53BP1 foci, a marker for DNA DSB repair. Because NU7026 does not affect the phosphorylation at the ABCDE cluster, we analyzed Thr-2609 phosphorylation in response to the DNA-PKcs inhibitor, and observed the same pattern as for γH2AX and 53BP1, in cells treated with NU7026 and in response to photon and proton irradiation. Because NU7026 affects the auto-phosphorylation at the Ser-2056 site, but not at the Thr-2609 site, which is mainly ATM-mediated, we analyzed DNA-PKcs (Thr-2609) phosphorylation kinetics in response to the DNA-PKcs inhibitor NU7026. Again, we observed the same pattern as for γH2AX and 53BP1, suggesting that NU7026 directly blocks the catalytic subunit to the damage site, avoiding its release.

Because of this enzyme blockade, we speculate that HRR would equally be inhibited, thus leading to a strong delay in repair. We therefore analyzed RPA32-foci formation, a known marker for HRR, in the presence of NU726. DNA-PKcs inhibition strongly reduced RPA32-foci formation, with only about 35% of foci detectable 4 hours after photon radiation, whereas almost no reduction was observed after proton radiation.

We then studied the effect of NHEJ deficiency by downregulating the NHEJ-factor DNA-PKcs in A549 cells. Although significantly more radiosensitive than control cells, no statistically significant variation in RBE_{10} value was observed in the DNA-PKcs-transfected cells after both types of irradiation. The Kinetic profile of γH2AX-focus repair was also equal after photon and proton irradiation although it was strongly

delayed. This could be explained by the fact that in NHEJ-deficient cells, HRR is the only active pathway and it is usually slower in repairing damage. Furthermore, ATM kinase is expressed at low levels in DNA-PKcs-null cells, but restored to wild-type level in cells expressing a kinase-death form of DNA-PKcs. Therefore, DNA-PKcs-null cells or where the enzyme has been downregulated by siRNA treatment would show a strongly hampered γH2AX- and RAD51-foci resolution, which is strongly ATM dependent. Indeed, analysis of RPA32 foci resolution showed that siDNA-PKcs-transfected cells had a much slower activation of HRR, compared to control cells.

To confirm differential sensitivity of DNA-PKcs inhibition over DNA-PKcs deficiency, we have investigated cell survival and γH2AX-focus repair in the DNA-PKcs-deficient cells M059J and their proficient, isogenic counterpart M059K. Although M059J were significantly more radiosensitive than their proficient counterpart, once again, we observed no difference between photon and proton radiation at the level of clonogenic survival and γH2AX-focus repair. Pretreatment of the DNA-PKcs-proficient M059K cells with NU7026 resulted in a stronger radiosensitizing effect after photon radiation, compared to proton radiation.

We as well as others have previously demonstrated that there is a specific requirement for homologous recombination repair for DNA repair after particle radiation [3, 10-11]. To confirm the enhanced sensitivity of HRR-mutated cells, we have downregulated the key HRR-recombinase RAD51. A549 cells with siRNA-downregulated RAD51 were markedly hypersensitive to proton radiation, compared to wild-type cells which were equally sensitive to both types of radiation.

To confirm enhanced sensitivity of HRR-mutated cells to proton radiation versus photon radiation, we investigated the BRCA2-deficient cells PEO1 and their wild-type, isogenic counterpart PEO4. Both PEO4 and PEO1 cells were more sensitive to proton than to photon-irradiation, but the BRCA2-deficient cells PEO1 were more sensitive to proton-irradiation. These results are in accordance with data gathered in CHO systems, therefore confirming the enhanced cell killing in HRR-deficient cells after proton radiation in a human cancer cell system. Many open questions still remain to be answered: how the two main pathways, HRR and NHEJ deal with proton-induced DNA damage, compared to photon-induced DNA damage, especially what are the structural differences between proton- and photon-induced DNA damage, and what is exactly generating these presumably differential types of DNA damage.

4.2 Mechanistic insight into the repair after DNA damage induction by high energy proton radiation

In our study, we compared the radiobiological efficacy of high-energy proton radiation versus photon radiation. Proton therapy treatments are based on a proton RBE of 1.1. The use of this generic, spatially invariant RBE within tumors and normal tissues disregards the evidence that proton RBE varies with linear energy transfer (LET), physiological and biological factors, and clinical endpoint. Furthermore, the biological (genetic) background of the cell line analyzed may influence the RBE value [4,14]. Our experiments were primarily performed in A549 cells, and we observed an RBE value of 1. As discussed before, the reasons behind this value may be several, including an overexpression of key components

of the HRR pathway. One of the reasons for the improved cell killing of proton radiation over photon radiation observed in several cell lines could be that proton radiation initially induced more DNA damage, specifically DSBs than photon radiation. Therefore, we analyzed the initial amount of damage by determining at the formation of γH2AX and 53BP1 foci. Both proteins have been shown to localize at the DNA damage site immediately after induction of a breakage site, only to be removed after the damage has been fixed [15-16]. γH2AX and 53BP1 foci formation was identical in both wild-type A549 cells and glioblastoma M059K cells after both types of irradiation. Interestingly, these cells showed the same repair kinetics after 1Gy of both types of ionizing radiation, meaning that cells with properly functional DNA repair machinery can repair both photon- and proton-induced damage equally.

The *quality* of DNA damage in terms of structural complexity cannot be solely identified via markers such as γH2AX or 53BP1. These proteins localize around the DNA damage to form scaffolds of several units together, and a putative increase of small fragments within few helical turns would be so close in space, that the foci scaffold would be completely overlying, which makes complex damages (cluster damages) indistinguishable from classical DSB. Therefore, we approached this challenge in an indirect way, by assessing the involvement of the two main repair pathways, HRR and NHEJ after both types of radiation. Interestingly, analysis of DNA-PKcs autophosphorylation, a marker for NHEJ revealed a stronger activation after photon radiation, compared to proton radiation, whereas RAD51 and RPA32 activation was identical after both types of irradiation. The reason behind the impaired activation of DNA-PKcs after proton radiation may be due to the quality of the DNA damage induced by high-energy protons. Several studies have shown that both the yield and the spatial distribution of DSBs are strongly dependent on the radiation quality [17]. Due to their physical properties, highly energy, low-LET proton particles have different energy deposition around critical structures like DNA [18-23]. The particle energy is usually deposited in a very narrow space, hence the increased LET value, and can generate very complex DNA damage. As a direct consequence, several smaller fragments may be generated (direct DSBs) or proton radiation may produce more oxidative cluster lesions, like abasic and oxybase lesions. These lesions can be then converted to DSBs by early repair processes like the base excision repair (indirect DSBs). Therefore, the overall result of proton radiation may induce a more complex damage, with more small fragments produced. A few studies have been performed to analyze the fragmentation pattern and yield of particle radiation [24-25]. They reported a decreased yield of all damage (both DSBs and base damages) with increasing LET. This is probably due to the more localized deposition of the energy of heavy particles leading to less but highly complex DNA damage. High-energy, low-LET protons were in the same range of damage induction as X-rays [54]. Nevertheless, the frequency of DSBs versus abasic and oxybase clusters was higher for the high-energy protons than for X-rays. Therefore, proton irradiation induces the same amount of complex clusters as photon irradiation but more non-DSB cluster lesions (oxidative cluster lesions). The higher frequency of smaller fragments may be the reason why NHEJ activation is impaired after proton radiation. Detailed crystallographic analysis of the Ku70/Ku80 complex revealed the formation of a ring structure, which accommodates the DNA helix within [26], where the fragment length seems to be a key determinant in the binding efficacy of the heterodimer [11,27]. The detailed molecular aspects for this size-dependent binding between Ku heterodimer and the DNA fragments are not yet clear, but is seems that the cut-off size is around 40 Megabase [10].

Interestingly, a detailed analysis of the Mre11 nuclease binding properties to DNA revealed its ability to bind fragments *independent* of their size [11, 28]. Therefore, the repair through the HRR pathway can take place to repair damages of any complexity, independently on the LET of the radiation beam.

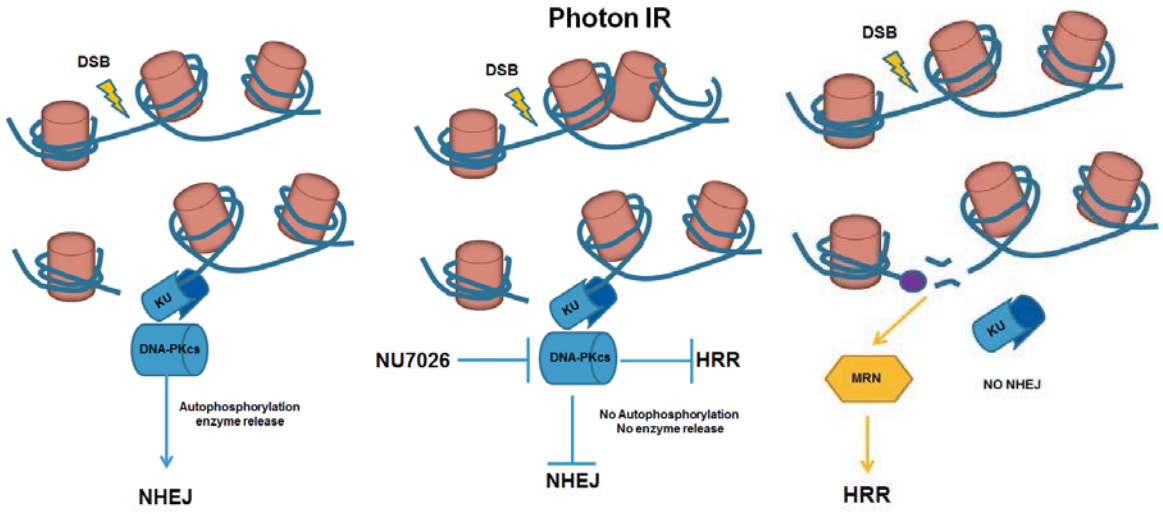

WT **NU7026** **DNA-PK$_{cs}$-/-**

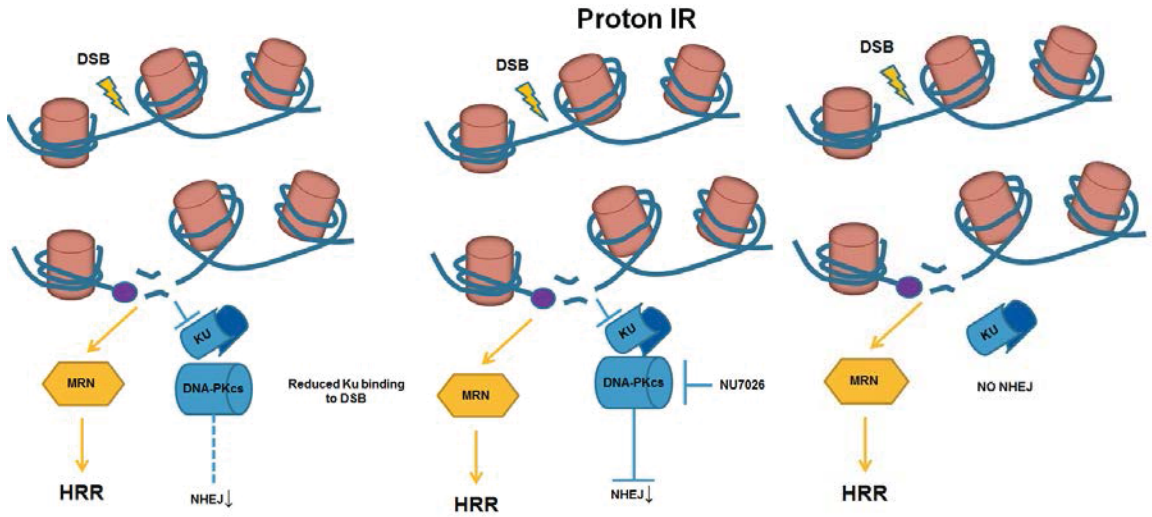

WT **NU7026** **DNA-PK$_{cs}$-/-**

Differential sensitivity to proton and photon irradiation in NU7026-pretreated, DNA-PKcs-inhibited cells in comparison to DNA-PKcs-knockdown cells and wild-type cells.

In wild-type, untreated cells treatment with ionizing radiation activates the DDR machinery to promote DNA repair. DNA damage is primarily repaired by the non-homologous end joining (NHEJ) pathway, which is strongly activated already at low dose and only in a minor way by the homologous recombination repair (HRR). Proton-irradiated cells display a reduced activation of DNA-PKcs, but equal involvement of RAD51. Because A549 have high expression of HRR proteins, proton-induced DNA damages can be properly repaired, leading to an RBE_{10} value of 1 in this cell line. Pretreatment with NU7026 selectively inhibits the DNA-PKcs autophosphorylation at Ser-2056, therefore blocking the

enzyme resolution and the consequent release from the DNA damage site. After photon irradiation, DNA-PKcs gets stuck at the DNA damage site, not allowing further damage processing by either NHEJ or HRR, causing a strong delay in DNA damage repair (as depicted by γH2AX, 53BP1 and pDNA-PKcs-Thr-2609 repair kinetics) (*continues to next page*).
Proton radiation generates a different type of DNA damage (simple and more complex, *cluster* DNA damages), which cannot be properly repaired by the Ku80-dependent NHEJ pathway. Consequently, DNA-PKcs involvement is strongly hampered in repair response to proton-induced DNA damage. Therefore, treatment with NU7026 will only minimally affect the NHEJ repair pathway in combination with proton radiation, and the HRR is the main pathway involved in the repair of proton-induced DNA damage. This lead to a reduced DMF_{10} in combination with proton radiation, compared to photon radiation. An involvement of the error-prone, Ku80-independent alternative end-joining (a-EJ) cannot be excluded. In DNA-PKcs-deficient cells, the NHEJ repair is not available. Therefore, these cells primarily rely on HRR, which is usually slow in DSB repair but can repair photon- and proton-induced damages equally well. This is due to the ability of the Mre11 nuclease to bind and repair DNA fragments independent of their size, whereas the Ku70/Ku80 heterodimer cannot. Therefore, the RBE_{10}-value for DNA-PKcs-deficient cells is around 1.

In our study we observed that HRR-deficient cells were hypersensitive to proton radiation, whereas NHEJ-deficient cells were equally sensitive toward proton and photon radiation. The reason behind this differential sensitivity of HRR-deficient cells is pointing towards an impaired functionality of the NHEJ pathway to repair proton-induced DNA damage. Our experiments are highlighting, although indirectly, that DNA-PK_{cs} activation is strongly hampered after proton radiation, leading to a reduced activation of NHEJ. Therefore, HRR becomes even more important as it is the main pathway involved in the repair of proton-induced damages, which would otherwise not be repaired at all (see graphic representation). In this respect, the alternative end joining pathway may also play an important role. It is known that this process is slow, but error-prone and most importantly does not require Ku70/Ku80 or DNA-PK_{cs} to work properly [13-14]. Therefore, this enhanced cell killing in HRR-compromised cells after proton radiation may be due to either *unrepaired* damage, which would lead to enhanced mutagenesis and cell killing, or alternatively to damage *misrepaired* by the alternative end joining. In this respect, the involvement of the alternate end joining pathway should be investigated in more detail in the near future.

4.3 Combined treatment modalities

Radiotherapy alone is a very potent tool to control and eventually cure cancer. Its combination with chemotherapy further increases the efficacy of radiotherapy via several mechanisms [29]. Several chemotherapeutic compounds have been approved in the past decades to be combined with conventional radiotherapy. However, their combination with proton therapy, although often clinically employed, has not always been investigated in detail at a molecular and cellular level so far. Currently, DNA-PKcs and in general the NHEJ pathway represent a very interesting target in radiation therapy. Autophosphorylation of DNA-PKcs after genotoxic stress is a key step in the activation of the NHEJ pathway [30]. After ionizing radiation, about 90% of the DSBs are repaired by the NHEJ pathway, whereas only minimal involvement of HRR has been described [31]. We therefore investigated the role and effect of DNA-PKcs inhibition by NU7026 in combination with both photon and proton radiation. This

compound selectively blocks Ser-2056 autophosphorylation site, which is necessary to allow the release of the synaptic complex from the damaged site. Indeed, inhibition of DNA-PKcs strongly prolonged γH2AX and DNA-PKcs (Thr-2609) phosphorylation after photon irradiation and potent radiosensitisation was also observed in vitro in both A549 and M059K cells.

We speculated that the strong radiosensitization observed in cells pretreated with NU7026 in combination with photon radiation would be strongly impaired in combination with proton radiation. The reason would be the impaired binding and activation of the DNA-PKcs enzyme, as observed by the diminished Ser-2056 and Thr-2609 activation in response to proton radiation, compared to photon irradiation. Indeed, combination of NU7026 with proton radiation resulted in a much weaker level of radiosensitisation in response to proton radiation, and there was no delay in foci resolution in the presence of the inhibitor. Based on our mechanistic data, we can conclude that the combination of proton therapy with DNA-PKcs inhibitor, and more widely with NHEJ inhibitors does not represent a favorable approach, due to the limited involvement of NHEJ after proton radiation.

Our study highlighted how a compromised HRR cause hypersensitivity toward proton, but not photon radiation. Therefore, combining proton therapy with chemotherapeutic agents targeting HRR would be of great clinical significance.

Pharmacological targeting of the HRR pathway has proved to be unsuccessful in the past years, mostly because of the lack of clearly druggable target proteins. Several chemotherapeutic agents, already widely used in the clinic are known to downregulate RAD51, however through different molecular mechanisms. The broad-range histone deacetylase inhibitor SAHA (Vorinostat) and the selective Bcr-Abl Tyrosine kinase inhibitor Imatinib (Gleevec) lead to downregulation of RAD51 and showed radiosensitizing properties *in vitro* and also *in vivo* [32-35]. Due to broad range of effects, of these substances on the cell, their specificity and efficacy is strongly cell-type dependent. Recently, selective inhibitors of the RAD51 protein have been developed, such as RI-1 and IBR2 [36-38]. However, they did not prove to be highly efficient in our hands. Due to the essential role of the RAD_{51} recombinase and the fact that it is often overexpressed in several cancer types, RAD51 is an attractive target molecule for developing tumor-selective inhibitors.

Our previous results in A549 cells demonstrated that RAD51 is a key factor in repairing proton-induced damages. We therefore decided to test whether the histone deacetylase inhibitor SAHA would lead to an increased efficacy in combination with proton radiation.

Continuous exposure with 2μM SAHA for 24 hours strongly reduced RAD51 protein levels, but without any significant effect on the Ku80 or DNA-PKcs protein levels, thus only affecting the HRR but not the NHEJ pathway. The radiosensitizing effect of SAHA with photon radiation was relatively weak, again highlighting the primary role of the NHEJ pathway in repairing the simple, photon-induced damage [31]. Pretreatment of A549 cells with SAHA in combination with proton radiation produced a much stronger response. The strong radiosensitizing effect was independent of NHEJ, as demonstrated by the strong delay in γH2AX but not pDNA-PKcs (Thr-2609) foci resolution observed in pretreated cells in combination with proton radiation.

Our study further supports the evidence to rationally combine proton radiation with agents directly or indirectly modulating the HRR pathway. This unique and selective combination can further increase the efficacy of proton therapy and broaden the spectrum of combined treatment approaches.

4.4 Insight into the relative biological effectiveness of proton radiation

As discussed above, the RBE, or relative biological effectiveness, is the ratio of the dose of photons (typically 250 keV x-rays) divided by the dose of protons which is needed to result in the same biological effect. It is obtained by dividing the dose necessary to obtain a certain cell survival (for example 10%) with a certain radiation type, to the dose necessary to obtain the same cell survival with a reference radiation, usually X-rays. RBE is usually dependent on the dose or survival level (endpoint) chosen, with a decrease in RBE by increase of dose or at low survival levels [4] and also on the proton beam energy. The concept of RBE is clinically significant only if two basic assumptions hold true, namely that the dose chosen is meant to be the macroscopic dose in a well-defined volume (for example a cell culture sample irradiated) because at the microscopic level (e.g. cellular level) inhomogeneity is generated due to the track structure and the energy deposition profile. Furthermore, a homogeneous dose distribution is assumed in the region of interest (usually an organ or a part of it). Small inhomogeneities in the radiation field can translate into an incorrect RBE prediction [39]. It is widely accepted to use an RBE value of 1.1 for clinical proton therapy, which means protons are 10% more effective than photons (considering a determined endpoint) when a defined dose is applied. On the physico-chemical level, the difference between photon and proton irradiation exposure is still unclear. Although high-energy protons are considered low-LET radiation, thus similar to photon radiation, protons are charged particles, which have different properties than simple photons. It has been demonstrated that the RBE is dependent on the charge other than the energy of the particle [40]. The result is a different track structure and energy deposition profile compared to photon radiation at the microscopical level. Damage induced by protons may result from a direct effect (to the DNA) or indirect effect through generation of secondary electrons and eventually neutrons.

Typically, photons generated from X-rays or γ-rays show the highest dose deposition near the entry site, the depth being directly proportional to the energy, to then steadily decrease. Due to the charge and the size of the proton, protons particles deeply penetrate within the cells and the energy is released during the slowing process in a very limited space, generating the *Bragg peak* and causing an increase in LET. The secondary radiation generated through this process also usually increases, which can cause further damage to the DNA. Furthermore, clinically relevant proton beams are the sum of several monoenergetic beams, and are generated through the actions of collimators to create the SOBP. Nevertheless, there is always a fraction of protons which may have lower energy, altering the profile of the SOBP and thus the LET. All these factors combined contribute to the differential DNA damage complexity observed with proton radiation.

4.5 Translational significance: biology as stratification criteria in the clinic?

Nowadays, proton beam therapy plays a very important role in the treatment of malignancies. For some defined tumors, like chondrosarcomas and uveal melanoma protons represent the primary treatment option. This is due to the physico-chemical properties of particle radiation, namely the different dose-energy distribution profile of protons compared to photons. At the tissue entrance, proton particles deposit a very low dose, whereas the maximal dose deposition occurs within the Bragg peak, whose

tissue depth is dependent upon the beam energy. Upon reaching a certain (threshold) velocity due to particle interactions, protons lose most of their energy. Therefore, no significant dose is deposited behind this region. Several mono-energetic beams of different energies are overlaid to result in a beam able to cover all the desired volume, with the most energetic beams covering the distal part and the less energetic beams the proximal portion. In clinical applications, the resulting *ensemble* of beams is called the spread-out Bragg peak (SOBP).

In contrast, photons deposit their maximum dose close to the entrance surface, usually where the tumor is located (therefore, high-energy beams are used to treat deeply-seated tumors) but also behind this critical structure (see figure 2.4). Therefore, due to their physical properties, protons provide a more localized dose delivery, which is a critical factor for some tumors seated near critical organs. This improved dose can therefore lead to higher dose deliveries without any relevant increase in normal tissue toxicity.

The use of a generic RBE-value of 1.1 is currently widely accepted for clinical proton therapy. Although this value is currently applied for almost every tumor entity treated, variations in the RBE values have been reported [4]. The RBE is strictly dependent on the beam energy used, with high-energy beams being generally considered low-LET radiation. The RBE is also dependent on the biological properties of the cellular system investigated [4, 41]. Some cells line exhibit an RBE close to 1 or even lower, which means they can repair proton-induced damage very well, whereas other cell systems have high RBE values, and they struggle to properly repair proton-induced damage. The reasons for these variations in the RBE are still a matter of debate, but there is more evidence pointing toward a role of the DNA damage response, which is responsible for orchestrating the repair of radiation-induced damage. In our study, we assessed that photons and high-energy protons induce the same amount of initial damage and display identical repair kinetics, with respect to γH2AX and 53BP1 foci. Nevertheless, detailed analysis of the two major pathways involved in the repair of radiation-induced damage revealed a differential involvement of NHEJ, but not of HRR. Therefore, we can conclude that protons do induce differential DNA damage compared to photons. Several proton-radiations DNA repair products are of worse quality, typically misrepaired cluster damages resulting in chromosomal rearrangements; this result in increased mutation rate and cell killing, leading to a superior effectiveness of proton radiation and thus an increased RBE value.

Homologous recombination repair and non-homologous end joining are differentially involved in the repair of complex, proton-induced damage. Cells with compromised HRR repair are highly sensitive toward proton radiation compared to photon radiation, which reveal the essential role of this pathway in repairing proton-induced damage. On the contrary, cells deficient in the NHEJ pathway, although generally very radiosensitive, exhibit the same radiosensitivity toward photon and proton radiation. Thus, these data reveal how photon and proton irradiation can induce differential involvement and activation of these two pathways: simple, photon-induced radiation damages are mainly repaired by the NHEJ pathway, which primarily involves Ku78/Ku80 and DNA-PKcs. Therefore, an intact and functional NHEJ is of major importance to ensure proper repair of photon-radiation induced damage, but less for the repair of more complex, proton-induced damage.

HRR is a very slow but precise process, taking place primarily in S- and G_2-phase cells. Cells lacking HRR are not significantly more sensitive to photon radiation, especially at low radiation doses, probably

because of the efficacy and speed of NHEJ in repairing such damage [42]. On the other hand, deficiency in the HRR apparatus renders cells more sensitive to proton radiation. This is probably due to the incapacity of NHEJ to properly repair the damage, thus the additional deficiency of HRR leaves the cells with no proper functional pathway.

This phenomenon is of great clinical relevance. Nowadays tumors are not stratified based on their biological properties (e.g. mutational status) for radiotherapy treatment. A stratification based on the mutational status of HRR proteins would increase the efficacy of treatment. This is also of great relevance with regard to normal tissue toxicity. Usually, tumors acquire mutations during their development [43-44], so that the normal tissue does not usually harbor specific mutations, or it is only heterozygous for them. Examples are the BRCA genes, namely BRCA1 and BRCA2. These genes are strongly involved in the HRR pathway [45], where they play a role in promoting IR-induced repair. Usually patients harbor a heterozygotic mutation in one of those proteins, but because one copy of the gene is still functional, the cells have a properly active HRR. During tumor development, a second mutation is acquired (loss of heterozygosity) within the tumor, but not in the normal tissue. Thus, the tumor compartment might respond significantly more to proton irradiation, whereas the normal, surrounding tissue would not experiment any additional, toxic radiosensitivity.

The issue of normal tissue toxicity and tumor control becomes important also with regard to combined treatment modalities. Most tumors do not harbor any specific mutation in the DNA repair machinery; therefore a pharmacologically active agent able to target the DNA repair machinery may be employed. We have demonstrated that SAHA (Vorinostat), a non-selective histone deacetylase inhibitor may specifically radiosensitize cells to proton but to a less extent to photon radiation. The radiosensitizing effect is primarily due to the downregulation of the RAD51 nuclease by SAHA. Due to the broad range of effects on gene expression, eventual cell type-specific off-target effects of SAHA cannot be completely excluded.

Still, cell lines with apparently intact repair machinery react very different to proton radiation. Every cell line expresses their proteins at a very specific level, and the process of gene expression and regulation is tightly regulated [46]. Differential gene expression and the subsequent protein levels of DNA damage repair proteins may strongly influence the response to proton radiation. Triple negative breast cancers have reported a diminished expression of DNA repair genes, especially HRR genes [47]. The same pattern has been observed in ovarian cancer [48]. These tumors may clinically be similar to tumors with mutations in the HRR pathway and respond very well to proton radiotherapy.

Other tumor entities are instead overexpressing high levels of HRR proteins, as it is the case of lung cancer [49]. Typically, overexpression of DNA repair proteins is associated with high resistance to chemotherapy, and eventually also to radiotherapy [50-51].

Lung cancer progression is typically associated with increased gene expression of several DNA damage repair (DDR) proteins involved in the homologous recombination repair, like RAD51, BRCA1/2 and FANC proteins [55-56]. Overexpression of these DDR proteins may lead to some sort of protective effect specifically toward proton radiation, as HRR pathway upregulation may allow these cells to repair a considerable amount of the complex, proton-induced damage by reducing process-related misrepair.

Therefore, several HRR proteins like BRCA1 or RAD51 are currently evaluated as possible prognostic markers in NSCLC to predict tumor response to chemotherapy or radiotherapy [52-53].

In our study we have evaluated the response to proton radiation of the non-small cell lung cancer cells A549 and H460 and the Triple-negative breast cancer cells MDA-MB-231 and MDA-MB-436. Interestingly though, A549 cells (p53-positive) did not show any significant sensitivity to protons, with an RBE of about 1. Instead, MDA-MB-231 and MDA-MB-436 cells (both p53-negative) were markedly hypersensitive to proton radiation, with RBE_{10} values of approximatively 1.35. Therefore, stratification in the clinic could be carried out not only on patients with tumors bearing mutations in the DNA repair machinery, as it is the case for BRCA-deficient breast and ovarian cancer, but also on those tumor entities with differential expression levels of selected proteins. Tumors with low HRR protein levels would be more suited to proton therapy, whereas tumors with high HRR protein levels may respond equally to proton and photon therapy. Because nowadays several tumor entities (e.g. lung, breast and prostate cancer) are under evaluation for proton therapy, not only a technical evaluation (e.g. feasibility to irradiate the tumor due to its localization) but also a biological evaluation (gene expression profile) of such tumors may be an important criterion in deciding which tumors may be more suited for clinical proton therapy, and which may not.

5 Outlook

Here we demonstrate that the homologous recombination repair pathway plays a fundamental role in the repair of complex, proton-induced damage. Genetic deficiency in key components of the pathway, like RAD51 or BRCA2, causes hypersensitivity toward proton, but not photon radiation. It is important to consider that the various components of the HRR pathway may play a differential role in the repair of DNA damage, e.g. RAD51-mediated DNA filament processing is an essential step in HRR, whereas XRCC3 or BRCA2 have more of a supportive role. Therefore, a deficiency or low expression level of RAD51 may have a stronger impact in tumor treatment response than BRCA2 deficiency, especially at low doses used as part of fractionated treatment regimen.

A promising strategy to exploit this increased dependence on the HRR would be to use compounds which can selectively target key components of the pathway. Nowadays, only few compounds target HRR, mostly indirectly. We have shown that SAHA (Vorinostat), an histone deacetylase inhibitor currently approved for the clinical treatment of cutaneous T-cell lymphoma. SAHA has been shown to work by modulating the gene expression of several genes, among them RAD51. Due to its broad effect on cellular gene expression, a certain degree of side-effects should be taken into account. Other compounds are known for their (indirect) effect on RAD51, e.g. Imatinib (Gleevec) and Methotrexate, both widely used in the clinic for several malignancies as part of chemotherapy regimens. It is therefore clear that any combined approach currently used for photon radiotherapy should be accurately evaluated for proton therapy, due to possible new interaction mechanisms.

The ultimate experiment to provide proof on clinical relevance of our finding would be to treat HRR-deficient tumor xenografts with proton and photon radiotherapy, or pharmacological agents specifically targeting the HRR. This would have a great impact on tumor treatment planning for patients with HRR-deficient tumors, where the dose delivered could be reduced, thereby diminishing normal tissue toxicity and at the same time achieving better tumor control. Unfortunately, almost no established HRR-deficient tumor models suited for *in vivo* experiments are in place, therefore establishing a proper tumor model will be of highest priority in the future.

In our study we further demonstrated for the first time that a potent and specific DNA-PKcs inhibitor, NU7026 can selectively radiosensitize cells to photon radiation, but to a much lesser extent to proton radiation. This compound is currently under evaluation for several malignancies, including leukemia and glioblastoma, in combination with Topoisomerase inhibitors and radiation. Due to the key role of DNA-PKcs and NHEJ in repairing DSBs, it is expected that clinical indications for this promising compound and other will be broadened. Here we have shown that DNA-PKcs inhibitors may less be suited for the combination with proton radiation therapy, but more so far in combination with photon therapy.

This data also provides precious insight into the mechanism of how proton radiation works. We have shown that pharmacological inhibition of DNA-PKcs has a selective effect by strongly radiosensitization human cancer cells toward photon radiation than toward proton radiation, whereas genetic deficiency of DNA-PKcs renders cells equally sensitive to both radiation types. These results highlight the role of Ku70/Ku80 heterodimer together with DNA-PKcs (the synaptic complex) in recognizing and promoting the repair of photon-induced DNA damage, and how this process is impaired in the recognition of proton-induced DNA damage, probably because of the different structure of the DNA damage induced by proton radiation, compared to photon radiation.

In conclusion, the present work illustrates the unique role of the homologous recombination pathway in repairing proton-induced damage. On one hand, it provides insight on the molecular mechanism of proton radiation, thus helping to better understand its biological and molecular basis, but on the other, our results open the door to new, clinically relevant implications for proton radiation therapy and new combined treatment approaches.

References

1. Raju MR, Robertson JB, *et al.* A heavy particle comparative study. Part III: OER and RBE. *Br J Radiol* 1978*;* **51**:712-719.
2. C. Allen, T. B. Borak, H. Tsujii and J. A. Nickoloff, Heavy charged particle radiobiology: Using enhanced biological effectiveness and improved beam focusing to advance cancer therapy. Mutat Res 2011; **711**:150-157.
3. Grosse N, Fontana AO, Pruschy MN, et al. Deficiency in homologous recombination renders Mammalian cells more sensitive to proton versus photon irradiation. *Int J Radiat Oncol Biol Phys.* 2014; **88**(1):175-81.
4. Paganetti H, Suit HD, *et al.* Relative biological effectiveness (RBE) values for proton beam therapy. Int J Radiat Oncol Biol Phys 2002; **53**:407-421.
5. Giard DJ, Parks WP *et al*. In vitro cultivation of human tumors: Establishment of cell lines derived from a series of solid tumors. *Journal of the National Cancer Institute* 1973; **1**(5):1417–23.
6. Lieber M. A continuous tumor-cell line from a human lung carcinoma with properties of type II alveolar epithelial cells. *Int. J. Cancer* 1976; 17:62-70.
7. Lehman TA, Harris CC, *et al*. p53 Mutations, ras Mutations, and p53-Heat Shock 70 Protein Complexes in Human Lung Carcinoma Cel Lines. *Cancer Research* 1991; **51**:4090-4096.
8. Stuschke M, *et al.* Targeting of Rad51-depen dent homologous recombination: implications for the radiation sensitivity of human lung cancer cell lines. *British Journal of Cancer* 2005; **92**:1089-1097.
9. Hollick JJ, Griffin RJ, *et al*. 2,6-disubstituted pyran-4-one and thiopyran-4-one inhibitors of DNA-Dependent protein kinase (DNA-PK). *Bioorg Med Chem Lett*. 2003; **13**(18):3083-3086.
10. Wang H, Wang Y, *et al.* The Ku-dependent non-homologous end-joining but no other repair pathway is inhibited by high linear energy transfer ionizing radiation *DNA repair* 2008; **8**:725-733.
11. Wang H, Wang Y, *et al.* Characteristics of DNA-binding proteins determine the biological sensitivity to high-linear energy transfer radiation. *Nucleic Acids Research* 2010; **38**(10):3245–3251.
12. Wang H, Iliakis G. *et al.* Biochemical evidence for Ku-independent backup pathways of NHEJ *Nucleic Acid Research* 2003; **31**(18):5377-88.
13. Dahm-Daphi J, et al. The alternative end-joining pathway for repair of DNA double-strand breaks requires PARP1 but is not dependent upon microhomologies. *Nucleic Acids Research* 2010; **38**(18):6065–6077.

14. Calugaru V, *et al.* Radiobiological characterization of two therapeutic proton beams with different initial energy spectra used at the Institut Curie Proton Therapy Center in Orsay. *Int J Radiat Oncol Biol Phys.* 2011; **81**(4): 1136-43.
15. Goutham HK, Sadashiva SRB, *et al.* DNA double-strand break analysis by γH2AX foci: a useful method for determining the overreactors to radiation-induced acute reactions among head-and-neck cancer patients. *Int J Radiat Oncol Biol Phys.* 2012; e607-e612.
16. Schulz LB, Halazonetis TD, *et al.* p53 binding protein 1 (53BP1) is an early participant in the cellular response to DNA double-strand breaks. *The Journal of cell biology*. 2000; **151**(7): 1381-1390.
17. Prise K, *et al.* A Review of Studies of Ionizing Radiation-Induced Double-Strand Break Clustering: A Review of Studies of Ionizing Radiation-Induced Double-Strand Break Clustering. *Radiation Research*. 2001; **156**(5):572-576.
18. Goodhead DT. Energy deposition stochastics and track structure: what about the target? *Radiat. Prot. Dosimetry.* 2006; **122**:3-15.
19. Chapman JD, Gillespie CJ. Radiation-induced events and their time-scale in mammalian cells. *Adv. Radiat. Biol.* 1981; **9**:143-198.
20. Warters RL, Hofer KG. Radionuclide toxicity in cultured mammalian cells. Elucidation of the primary site for radiation damage. *Curr. Top. Radiat. Res.* 1997; **12**:389-407.
21. Goodhead DT. Radiation effects in living cells. *Can. J. Phys*. 1989; **68**:872-886.
22. Ryberg B. Clusters of DNA damage induced by ionizing radiation: Formation of shorts DNA fragments. II. Experimental detection. *Radiat. Res*. 1996: **145**:200-209
23. Ward JF. The complexity of DNA damage: relevance to biological consequences. *Int. J. Radiat. Biol.* 1994; **66**:427-432.
24. Hada M, Sutherland BM. Spectrum of complex DNA damages depends on the incident radiation. *Radiation Research*. 2006; 165:223-230.
25. Sutherland B, Sutherland J, *et al.* Clustered DNA damages induced by high and low LET radiation, including heavy ions. *Physica Medica*. 2001; **31**:202-204.
26. Goldberg J, *et al.* Structure of the Ku heterodimer bound to DNA and its implications for double-strand break repair. *Nature*. 2001; **412**(6847):607-14.
27. Wang H, Wang Y. Heavier ions with a different linear energy transfer spectrum kill more cells due to similar interference with the ku-dependent DNA repair pathway. *Radiation Research*. 2014; **182**(4): 458-461.
28. Stenerlöw B, et al. Focus Formation of DNA Repair Proteins in Normal and Repair-Deficient Cells Irradiated with High-LET Ions Focus Formation of DNA Repair Proteins in Normal and Repair-Deficient Cells Irradiated with High-LET Ions. *Radiation Research*. 2004; **161**(5): 517-527.
29. Bentzen S, Harari PM, Bernier J. Exploitable mechanisms for combining drugs with radiation: concepts, achievements and future directions. *Nature Clinical Practice*. 2006; **4**(3): 172-180.
30. Chen D, Uematsu N, *et al.* Autophosphorylation of DNA-PKCS regulates its dynamics at DNA double-strand breaks. *The Journal of cell biology*. 2007; 177(2):219-229.

31. Lees-Millers SP, *et al.* Repair of ionizing radiation-induced DNA double-strand breaks by non-homologous end-joining. *Biochem J*. 2009; **417**:639–650.
32. Chen X, Wong JY*, et al.* Suberoylanilide hydroxamic acid as a radiosensitizer through modulation of RAD51 protein and inhibition of homology-directed repair in multiple myeloma *Mol. Cancer Res.* 2012; **10**(8):1052-64.
33. Konstantinopoulos PA, Khabele D, *et al.* Suberoylanilide hydroxamic acid (SAHA) enhances olaparib activity by targeting homologous recombination DNA repair in ovarian cancer *Gynecol Oncol.* 2014; **133**(3):599-606.
34. Choudhury A, Bristow RG, *et al.* Targeting homologous recombination using imatinib results in enhanced tumor cell chemosensitivity and radiosensitivity *Mol. Cancer Ther.* 2009; **8**(1):203-13.
35. Quiao B, Kiltie AE, *et al.* Imatinib radiosensitizes bladder cancer by targeting homologous recombination *Cancer Res*. 2013; **73**(5):1611-20.
36. Budke B, Connell PP, *et al*. RI-1: a chemical inhibitor of RAD51 that disrupts homologous recombination in human cells. *Nucleic acid research* 2012; **40**(15):7347-57.
37. Budke B, Connell PP, *et al*. An optimized RAD51 inhibitor that disrupts homologous recombination without requiring Michael acceptor reactivity. *J Med Chem* 2013; **10**;56(1):254-63
38. Zhu J, Lee WH, *et al.* A novel small molecule RAD51 inactivator overcomes imatinib resistance in chronic myeloid leukaemia. *EMBO Medical Journal* 2013; **5**(3):353-65.
39. Paganetti H. Relative biological effectiveness (RBE) values for proton beam therapy. Variations as a function of biological endpoint, dose, and linear energy transfer. *Physics in Medicine and Biology* 2014; **59**(22):419-472.
40. Friedrich T, Scholz M, *et al.* Particle species dependence of cell survival RBE: Evident and not negligible. *Acta Oncol.* 2013; **52**:589-603.
41. Gerweck LE, Kozin SV. Relative biological effectiveness of proton beams in clinical therapy. Radiotherapy and Oncology. 1999; 50(2):135-142.
42. Shrivastav N, Nickoloff J, *et al.* Regulation of DNA double-strand break repair pathway choice. *Cell research*. 2008; 18(1):134-147.
43. Hanahan D, Weinberg RA. The Hallmarks of Cancer. *Cell* 2000; **100**(1):57–70.
44. Hanahan D, Weinberg, RA. Hallmarks of Cancer: The Next Generation. *Cell* 2011 **144**(5):646–674.
45. Deng C, Brodie S. Roles of BRCA1 and its interacting proteins. *BioEssays : news and reviews in molecular, cellular and developmental biology*. 200; **22**(8):728-737.
46. Hernandez-Verdun D, *et al*. Nucleolus: the fascinating nuclear body. *Histochemistry and Cell Biology*. 2008; **129**(1):13-31.
47. Ribeiro E, Andreis D, *et al.* Triple negative breast cancers have a reduced expression of DNA repair genes. *Plos One*. 2013; **8**(6): e66243.¨
48. Damia G, *et al.* Expression of DNA repair genes in ovarian cancer samples: biological and clinical considerations. *Eur J Cancer.* 2011; 47(7):1086-94.
49. Saviozzi S, Scagliotti GV, *et al*. Non-small cell lung cancer exhibits transcript overexpression of genes associated with homologous recombination and DNA replication pathways. *Cancer Research*. 2009; **69**(8):3390-3396.

50. Bosken CH, Spitz MR, *et al.* An analysis of DNA repairs as a determinant of survival in patients with non-small-cell lung cancer. *J Natl Cancer Inst* 2002; **94**:1091–1099.
51. Zeng-Rong N, Alaoui-Jamali MA, *et al.* Elevated DNA repair capacity is associated with intrinsic resistance of lung cancer to chemotherapy. *Cancer Res.* 1995; **55**:4760–4764.
52. Rosell R, Jassem E, *et al.* BRCA1: a novel prognostic factor in resected non-small-cell lung cancer. *PLoS ONE*. 2007; **2**:e1129.
53. Takenaka T, Kouso H*, et al.* Combined evaluation of Rad51 and ERCC1 expressions for sensitivity to platinum agents in non-small cell lung cancer. *Int J Cancer* 2007; **121**:895–900.
54. Hada M and Sutherland BM. Spectrum of complex DNA damages depend on the incident radiation. *Radiat Res.* 2006; **165**:223-230.
55. Nogueira A, Assis J, Catarino R and Medeiros R. DNA repair and cytotoxic drugs: the potential role of RAD51 in clinical outcome of non-small-cell lung cancer patients. *Pharmacogenomics.* 2013; **14**(6):689-700.
56. Nogueira A, Medeiros R, *et al.* Influence of DNA repair RAD51 gene variants in overall survival of non-small cell lung cancer patients treated with first line chemotherapy. *Cancer Chemother Pharmacol.* 2010; **66**(3):501-6.

Andrea O. Fontana

Curriculum Vitae

Personal information

Surname / First names	**Fontana Andrea Orlando**
Current Address	Katzenbachstrasse 213, 8052 Zürich
Telephone	Mobile: +41795472905
E-mail	andrea.o.fontana@gmail.com
Nationality	Swiss / Italian
Date and Place of birth	3th December 1986, in Como, Italy

Education

Graduate

March 11 – Present

PhD Thesis:
Differential Response to Proton versus Photon Radiotherapy: Biological Implications for new Indications and Combined Treatment Concepts
Department of Radiation Oncology, Laboratory for Radiobiology, University Hospital Zürich
In Collaboration with the Paul Scherrer Institut, Villigen
PhD Thesis Supervisor: Prof. Dr. Martin Pruschy

Sept 08 – Feb 10

Masters of science ETH in Medicinal and Industrial Pharmaceutical Sciences MIPS.
Major Subjects: Medicinal Chemistry, Biopharmacy, Pharmacogenomic and Pharmacotherapy, Clinical Trial Management, Business and Marketing, Logistic.
Federal Institute of Technology, Zurich.
Master Thesis Supervisor: Prof. Dr. Jonathan Hall

Undergraduate

Oct 2005 – Dec 2008

Bachelor of science ETH in Pharmaceutical Sciences.
Major Subjects: Medicinal Chemistry, Molecular Pharmacology, Biopharmacy, Drug Delivery Technologies.Subsidiary subjects: Molecular Biology and Biochemistry, Statistics, Organic Chemistry.

Sept 2001 - June 2005

High School in Mendrisio (TI), Switzerland
Major subjects: Biology and Chemistry
Minor Subject: Physics

Distinction (awarded) for results in Biology and Chemistry (best Matura)

Research experience

March 2011 – present	PhD Thesis (4 years, PhD defense in Mai 2015) in Molecular Radiobiology (Prof. Dr. Martin Pruschy): "**Differential Response to Proton versus Photon Radiotherapy: Biological Implications for new Indications and Combined Treatment Concepts** " Department of Radiation Oncology, Laboratory for Radiobiology, University Hospital Zürich
Sept 2009 – Mar 2010	Master Thesis (22 weeks) in Medicinal Chemistry (Prof. Dr. Jonathan Hall): "**Novel ligands binding precursor for high affinity microRNAs against Hepatitis C Virus** " Institute of Pharmaceutical Chemistry, Federal Institute of Technology, Zurich
July 2009 – Aug 2009	Research Project (6 weeks) in Medicinal Chemistry (Prof. Dr. Howard Cottam and Prof Dr. Dennis Carson): "**Design and synthesis of small molecular weight inhibitors of Wnt Pathway for treatment of different forms of Cancer** " Moore Cancer research Center, University of California at San Diego, La Jolla In Collaboration with The Scripps Oceanography Institute at San Diego, La Jolla
Sept 2008 – Dec 2008	Research Project (9 weeks) in Medicinal Chemistry (Prof. Dr. Jonathan Hall): "**Modified nucleoside building blocks for high affinity oligonucleotides** " Institute of Pharmaceutical Chemistry, Federal Institute of Technology, Zurich
Mar 2008 – Apr 2008	Project (6 weeks) in Drug Delivery Technologies (Dr. Bruno Gander): "Development of an aqueous solution of the antiepileptic Drug Carbamazepine" Institute of Pharmaceutical Chemistry, Federal Institute of Technology, Zurich

Research Interests

Human Pharmacology and Medicine, Oncology and Radiation Oncology, Sport and cellular physiology, Business and Management

Personal skills

First language	Italian
Other languages	Swiss German: fluent oral German: fluent oral/written English: fluent oral/written French: fluent oral/good written
Computer	Operative systems: Windows, Mac Software: Word, SPSS, Endnote, Excel, GraphPad, Power Point, Adobe Photoshop, Burkin Top-Spin NMR, LC-MS.

Jobs

Security Service Sept 2010 – Sept 2013	Various Employees (evenings, week-ends) security guard at different events (concerts, sport events) and clubs in Zürich.
Junior Scientist Mai 2010 – Jan 2011	at Pharmacovigilance Center, Department of Clinical Pharmacology and Toxicology, University Hospital Zürich (Prof. Kullak-Ublick): Pharmacovigilance, Rounds and Lab
Research volunteer July 2009 – Aug 2009	at Moore Cancer research Center, UC San Diego, La Jolla: Synthesis and Evaluation of chemical Compounds
Assistance Sept 2007 - Mar 2008	at ETH Zurich, D-AGRL (6h weekly) for a project on dispersal in the oriental fruit moth (*Cydia molesta*)
Teaching 2003 - 2009	Private lessons in Maths, Science and German

Extracurricular Interests

American Football (Zurich Renegades and Swiss National Football Team), weightlifting, Brazilian Jiu-Jitsu, Travelling

Referees

Prof. Dr. Martin Pruschy	Prof. Dr. Jonathan Hall	PD Dr. S. Russmann	Prof. Dr. H. Cottam
Professor of Radiobiology Department of Radiation Oncology Laboratory for molecular Radiobiology University Hospital Zürich CH-8091 Zürich	Departement of Pharmaceutical Chemistry Institute For Pharmaceutical Sciences, ETH Zurich Wolfgang-Pauli Strasse CH-8093 Zürich	Director of Drug Safety and Pharmacovigilance, Institute for clinical Pharmacology and Toxicology University Hospital Zürich CH-8091 Zürich	Director of the Medicinal Chemistry Core Program, Hematologic Malignancies Program, John Moores Cancer Center at the University of California, San Diego
E-mail: martin.pruschy@usz.ch	E-mail: jonathan.hall@pharma.ethz.ch	E-mail: stephan.russmann@usz.ch	E-mail: hcottam@ucsd.edu

Scientific Publications

Fröhlich T, Zorina O, Fontana AO, Kullak-Ublick GA, Vollenweider A, Russmann S.
Evaluation of medication safety in the discharge medication of 509 surgical inpatients using electronic prescription support software and an extended operational interaction classification.
Eur J Clin Pharmacol. 2011; 67(12):1273-82

Grosse N, Fontana AO, Hug EB, Lomax A, Coray A, Augsburger M, Paganetti H, Sartori AA, Pruschy M.
Deficiency in Homologous Recombination Renders Mammalian Cells More Sensitive to Proton versus Photon Irradiation.
Int J Radiat Oncol Biol Phys. 2014; 88(1):175-181.

Laura Surace, Veronika Lysenko, Andrea Orlando Fontana, Virginia Cecconi, Hans Janssen, Antonela Bicvic, Michal Okoniewski, Martin Pruschy, Reinhard Dummer, Jacques Neefjes, Alexander Knuth, Anurag Gupta, Maries van den Broek.
Complement is a central mediator of radiotherapy-induced tumor-specific immunity and clinical response
Submitted to Immunity (Jan 2015).

Conferences/Schools

- **PSI Winter School 2012 on Proton Therapy**
- **ICTR-PHE International Conference 2012, Geneva** – Oral Presentation
- **ASTRO Annual Meeting 2013, Atlanta US** – Poster Presentation
- **Cancer Network Retreat Switzerland 2014, Interlaken** – Oral Presentation
- **MedPhys 2014, Joint Conference on Medical Physics, Zürich** – Oral Presentation

Acknowledgments

First of all, I would like to express my deep gratitude to Prof. Dr. Martin Pruschy, for his initiative and effort to launch and continue this very interesting project, and for trusting me. Without it, I would not have started my PhD in the Laboratory for Molecular Radiobiology at the University Hospital Zurich and the Centre for proton therapy at the Paul Scherrer Institute (PSI) in Villigen.

Furthermore I would like to thank the other members of my PhD thesis committee for their very helpful supervision and support, especially Prof. Dr. Alessandro A. Sartori. Thanks to his huge expertise in the field of DNA repair, his help was very fruitful, and I am grateful to have him in my committee.
I also want to thank my supervisors Prof. Dr. Anthony Lomax from PSI and PD Dr. med. Oliver Riesterer from the University Hospital Zurich.

In addition I would like to thank all current and former members of the Laboratory for Molecular Radiation Biology in Zurich: Dr. Angela Broggini-Tenzer, Sabine Bender, Sabine Bender, Tamara Codilupi, Ivo Grigic, Dr. Katarzyna Nitko-Karouzakis, Dr. Colette Shen, Janosh Ott, Daniel Hug, Katrin Orlowski, Dr. Martina Zimmermann, and Van Vuong.
Another big thank is for Ashish Sharma, for his help during my work, his encouragement and the nice atmosphere in D-NUK 14.

Big thanks go to my favorite master student Marc Augsburger, who really contributed a lot in the project and was a real good friend during all the time.

Thank you very, very much for the nice atmosphere in the lab and for many more things.

Special thanks to Rosanna Branch, Marta Worni and Angela Broggini for proof-reading this thesis!

I would like to thank as well the Department of Radiation Oncology, the physicists, and MTRAs, especially my coach Chris Winter.

A big thanks is also for the proton therapy center at PSI. Dr. Terence Böhringer, Hans-Ueli, Benno Rohrer and Dr. Stefan König were always very patient helping me with the proton irradiation of cell dishes. Often we had fruitful discussions and time just passed by.

Many thanks go to my friends and roommates Pietro, Andrea, Martino and Jack, who supported my trough this journey and in the everyday life, especially at home. I want to thanks also Kevin and all my friends at the renegade family, playing ball with you was really the best.

Infine, vorrei ringraziare la mia famiglia, mia sorella Maddalena, mia mamma Mariarosa e mio papà Alberto ed in particolare Vanessa. Per aver creduto in me fin dall'inizio, e per il vostro sostegno in tutti questi lunghi e faticosi anni. Senza di voi non avrei raggiunto nulla di tutto ciò. Grazie di cuore.